

กำลังการผลิตที่รับได้สูงสุดของเครื่องกำเนิดไฟฟ้าขนาดเล็กโดยคำนึงถึงการประสานสัมพันธ์ของ
ระบบป้องกันและกำลังสูญเสีย

นายทิตติ ศักดิ์ศรีชัย

วิทยานิพนธ์นี้เป็นส่วนหนึ่งของการศึกษาตามหลักสูตรปริญญาวิศวกรรมศาสตรดุษฎีบัณฑิต
สาขาวิชาวิศวกรรมไฟฟ้า ภาควิชาวิศวกรรมไฟฟ้า
คณะวิศวกรรมศาสตร์ จุฬาลงกรณ์มหาวิทยาลัย
ปีการศึกษา 2554
ลิขสิทธิ์ของจุฬาลงกรณ์มหาวิทยาลัย

บทคัดย่อและแฟ้มข้อมูลฉบับเต็มของวิทยานิพนธ์ตั้งแต่ปีการศึกษา 2554 ที่ให้บริการในคลังปัญญาจุฬาฯ (CUIR)
เป็นแฟ้มข้อมูลของนิสิตเจ้าของวิทยานิพนธ์ที่ส่งผ่านทางบัณฑิตวิทยาลัย

The abstract and full text of theses from the academic year 2011 in Chulalongkorn University Intellectual Repository (CUIR)
are the thesis authors' files submitted through the Graduate School.

MAXIMUM ALLOWABLE DISTRIBUTED GENERATION WITH PROTECTION SYSTEM
COORDINATION AND POWER LOSS CONSIDERATIONS

Mr. Titti Saksornchai

A Dissertation Submitted in Partial Fulfillment of the Requirements
for the Degree of Doctor of Philosophy Program in Electrical Engineering

Department of Electrical Engineering

Faculty of Engineering

Chulalongkorn University

Academic year 2011

Copyright of Chulalongkorn University

ทิตติ ศักดิ์ศรีชัย : กำลังการผลิตที่รับได้สูงสุดของเครื่องกำเนิดไฟฟ้าขนาดเล็กโดย
 คำนึงถึงการประสานสัมพันธ์ของระบบป้องกันและกำลังสูญเสีย. (MAXIMUM
 ALLOWABLE DISTRIBUTED GENERATION WITH PROTECTION SYSTEM
 COORDINATION AND POWER LOSS CONSIDERATIONS) อ. ที่ปรึกษา
 วิทยานิพนธ์หลัก: ศ.ดร. บัณฑิต เอื้ออาภรณ์, 146 หน้า.

วิทยานิพนธ์นี้นำเสนอวิธีการหาขนาดกำลังผลิตที่รับได้สูงสุดของเครื่องกำเนิดไฟฟ้า
 ขนาดเล็กที่จะเชื่อมต่อกับระบบจำหน่ายไฟฟ้า โดยคำนึงถึงการประสานสัมพันธ์ของระบบ
 ป้องกันและกำลังสูญเสีย ที่ผ่านมานั้นวิธีการที่ใช้ประเมินหาขนาดสูงสุดของเครื่องกำเนิด
 ไฟฟ้าขนาดเล็กนั้นยังขาดความชัดเจนในกระบวนการวิเคราะห์การทำงานของระบบป้องกัน
 และกำลังสูญเสียของระบบที่เปลี่ยนไป รวมถึงผลกระทบที่จะเกิดขึ้นได้จากการเชื่อมต่อของ
 เครื่องกำเนิดไฟฟ้าขนาดเล็ก ได้แก่ การทำงานผิดพลาดของระบบป้องกัน การเพิ่มขึ้นของกำลัง
 สูญเสีย และการเปลี่ยนแปลงของความเชื่อถือได้ของระบบไฟฟ้า นอกจากนี้วิทยานิพนธ์ฉบับ
 นี้ยังนำเสนอวิธีการปรับปรุงระบบป้องกันเพื่อช่วยให้ระบบไฟฟ้าสามารถรองรับกำลังผลิตที่
 เพิ่มขึ้น และยังสามารถเสนอวิธีประเมินผลกระทบเชิงปริมาณของเครื่องกำเนิดไฟฟ้าที่มีต่อความ
 น่าเชื่อถือได้ของระบบ ทำให้สามารถทราบถึงผลดีและผลเสียที่จะเกิดขึ้นจากการเชื่อมต่อของ
 เครื่องกำเนิดไฟฟ้าขนาดเล็ก ผลการทดสอบกับระบบไฟฟ้า RBTS Bus 2 และ ระบบไฟฟ้า
 จำหน่ายของการไฟฟ้าส่วนภูมิภาค แสดงให้เห็นว่า วิธีการที่นำเสนอมีศักยภาพเพียงพอในการ
 นำไปประยุกต์ใช้สำหรับงานวิเคราะห์หาขนาดกำลังผลิตสูงสุดที่ระบบไฟฟ้าจำหน่ายสามารถ
 รับได้ ตลอดจนสามารถนำไปใช้ประเมินผลกระทบ และการวางแผนเกี่ยวกับการเชื่อมต่อของ
 เครื่องกำเนิดไฟฟ้าขนาดเล็กได้อย่างมีประสิทธิภาพ

ภาควิชาวิศวกรรมไฟฟ้า.....ลายมือชื่อผู้ผลิต.....
 สาขาวิชาวิศวกรรมไฟฟ้า.....ลายมือชื่อ อ.ที่ปรึกษาวิทยานิพนธ์หลัก.....
 ปีการศึกษา2554.....

5171810121 : MAJOR ELECTRICAL ENGINEERING

KEYWORDS : DISTRIBUTED GENERATION / PROTECTION COORDINATION /
POWER LOSS / DISTRIBUTION SYSTEM / SYSTEM SERVICE QUALITY

TITTI SAKSORNCHAI : MAXIMUM ALLOWABLE DISTRIBUTED
GENERATION WITH PROTECTION SYSTEM COORDINATION AND POWER
LOSS CONSIDERATIONS. ADVISOR : PROF. BUNDHIT EUA-ARPORN,
Ph.D., 146 pp.

This thesis proposes a method for determining a maximum allowable distributed generation (DG) with protection system coordination and power loss consideration in a distribution system. Although there are a number of methods for determining a maximum DG penetration in a distribution system, only few works explicitly investigate impact on protection system coordination and power loss. In general, impacts of a DG connection, i.e. protection mis-coordination, power loss increase, and system service quality variation are not taken into account. In this thesis, protection adjustment procedures for increasing the maximum allowable DG are proposed. In addition, a method for evaluating the impact of DG connection on system service quality has been developed. As a result, the advantage and disadvantage of DG connection can be determined quantitatively. The proposed methods have been tested with the RBTS Bus 2 and an actual Provincial Electricity Authority (PEA) distribution systems. The results show the effectiveness of the methods to calculate for maximum allowable DG, system impact evaluation, and planning for DG connection.

Department : Electrical Engineering..... Student's Signature

Field of Study : Electrical Engineering..... Advisor's Signature

Academic Year : 2011.....

Acknowledgements

I would like to express my deepest gratitude to my advisor, Professor Dr. Bundhit Eua-arporn who has given invaluable advice and wisdom in both academic and practical aspects through my doctoral degree. I also express my thankfulness to my thesis committee: Assistant Professor Dr. Naebboon Hoonchareon, Associate Professor Trin Saengsuwan, Assistant Professor Somporn Sirisumrannukul, and Dr. Surachai Chaitusaney, for their helpful comments on this research.

I would like to extend my thankfulness to Mr. Narong Tantichayakorn and all of my supervisors at PEA who provide me invaluable advices and a great opportunity to continue my study in which I have a strong willingness to apply my knowledge from the research for benefits of the organization.

I would like to express my gratitude to Dr. Somphop Asadamongkol for his helpful suggestion to my research and my colleague at PEA for every support.

Lastly, and most importantly, I would like to thank my father, Mr. Chaloe Saksornchai and my mother, Mrs. Kanda Saksornchai for their moral support and undying love.

Contents

	Page
Abstract (Thai)	iv
Abstract (English)	v
Acknowledgements	vi
Contents	vii
List of Tables	xi
List of Figures	xiii
List of Abbreviations	xvi
 Chapter	
I Introduction	1
1.1 Problem Statement.....	1
1.2 Objective.....	8
1.3 Research Scope for DG Impact Investigation.....	9
II Distributed Generation	13
2.1 Basic Types of DG.....	13
2.2 Standards and Practices for DG Connection.....	14
2.3 DG Model.....	15
III Protection Coordination Analysis	18
3.1 Distribution System Protective Devices.....	18
3.1.1 Over-Current Relay.....	19
3.1.2 Recloser.....	20
3.1.3 Fuse.....	21
3.2 Protection Coordination in Distribution System.....	23
3.2.1 Over-Current Protection Coordination.....	23
3.2.2 Fuse Saving Scheme.....	24
3.3 Protection Coordination Example.....	27

Chapter	Page
3.4 DG Impact on Distribution Protection System.....	27
3.5 Summary.....	34
IV Service Quality.....	36
4.1 Reliability Index.....	37
4.2 Voltage Sag Index.....	39
4.3 Service Quality Evaluation Example.....	44
4.4 DG Impact on Distribution System Service Quality.....	48
4.4.1 DG Impact on System Reliability Index.....	50
4.4.2 DG Impact on System Voltage Sag Index.....	53
4.5 Summary.....	55
V Power Loss Analysis.....	56
5.1 Power Loss Calculation.....	56
5.2 Appropriate DG Output with Loss Consideration.....	57
5.3 Impact of System Demand on Feeder Loss.....	58
5.4 Appropriate DG Output Power at Different Load Levels.....	60
5.5 BCDLA Loss Allocation Method.....	62
5.6 Summary.....	64
VI Proposed Methodology.....	65
6.1 Maximum Allowable DG Capacity with Protection Coordination Consideration.....	66
6.1.1 Assumption.....	66
6.1.2 Problem Formulation.....	66
6.1.3 Maximum Allowable Capacity Determination Procedure.....	70
6.1.4 More than One DG Connection Application.....	70
6.2 Protection Adjustment Method for Higher Penetration of DG.....	73
6.2.1 Protective Device Resetting.....	73

Chapter	Page
6.2.2 Directional Recloser Application.....	75
6.2.3 Replacement of Fuse with Recloser.....	76
6.3 System Service Quality Index Evaluation.....	77
6.3.1 System Reliability.....	77
6.3.2 System Voltage Sag.....	80
6.4 Appropriate DG Output with Customer Load Profile Consideration	83
6.4.1 Appropriate DG Output Using Direct Search Method.....	83
6.4.2 The Developed Methodology.....	84
6.4.3 Derivation of Appropriate DG Output and Load Variation Relationship.....	87
6.4.4 General Formula and Calculation Procedure.....	89
6.5 Summary.....	91
VII Simulation Results.....	93
7.1 Maximum Allowable DG Capacity with Protection Consideration ...	93
7.1.1 Simulation Results.....	93
7.1.2 More than One DG Connection Application.....	98
7.1.3 Summary.....	100
7.2 Protection Adjustment Method for Higher Penetration of DG.....	102
7.2.1 Protective Device Resetting.....	102
7.2.2 Directional Recloser Application.....	104
7.2.3 Replacement of Fuse with Recloser.....	105
7.2.4 Summary.....	106
7.3 System Service Quality Index Evaluation.....	108
7.3.1 Results of System Reliability.....	109
7.3.2 Results of System Voltage Sag.....	112
7.3.3 Summary.....	114

Chapter	Page
7.4 Appropriate DG Output Power with Loss and Customer Load	
Profile Consideration.....	114
7.4.1 Simulation Results Using Direct Search Method.....	114
7.4.2 Simulation Results Using Approximation Method.....	116
7.4.3 Summary.....	120
VIII Applications on Actual System.....	121
IX Conclusions.....	129
References.....	131
Appendices.....	136
Biography.....	146

List of Tables

Table	Page
1.1 Existing VSPP in Thailand.....	2
3.1 Fuse Coordination based on fault current magnitude (A).....	25
3.2 Summary of protective device settings.....	28
3.3 Summary of the possible mis-coordination pattern.....	33
4.1 Failure rate and repair time of SAIFI and SAIDI calculation.....	39
4.2 Failure rate and protective device consideration for the calculation of SARFI-X and SARFI-Curve.....	44
4.3 Reliability Indices at each load point of Feeder 3.....	45
4.4 SAIFI and SAIDI calculation of Feeder 3.....	46
4.5 SARFI-X on Feeder 3.....	46
4.6 SARFI-X based on approximation method.....	47
4.7 SARFI-Curve of Modified RBTS Bus 2 from approximation method....	48
4.8 Summary of criteria on PMA calculation.....	53
5.1 Appropriate DG output power at peak load condition.....	58
5.2 Appropriate DG output power at different load levels.....	60
6.1 Summary of protection constraints.....	69
7.1 Maximum allowable DG capacity at each location.....	94
7.2 The maximum allowable DG capacity of the system with a DG connected to location 1A.....	99
7.3 Maximum allowable DG capacity for a multiple DG case.....	100
7.4 Summary of protection resettings.....	104
7.5 Maximum allowable DG capacity after protection resetting.....	105
7.6 Maximum allowable capacity of a DG after directional recloser application.....	105
7.7 Maximum allowable capacity with replacement of fuse by recloser.....	106
7.8 Summary of characteristic of each protection adjustment method.....	108

Table	Page
7.9 Update of λ_i and r_i from PMA for all load point in Feeder 3.....	111
7.10 SAIFI and SAIDI value of Feeder 3 after DG connection.....	112
7.11 SARFI-X improvement after 6 MW DG connection at location 3B.....	113
7.12 SARFI-Curve improvement after 6 MW DG connection at location 3B.	113
7.13 Aggregated feeder load pattern.....	115
7.14 Appropriate output of the DG according to load variation.....	115
7.15 Appropriate output power of a DG at location B.....	118
7.16 Average system bus voltage at different load level when DG of 10.54 MW is connected at location B.....	118
7.17 Power and energy losses.....	119
8.1 Maximum allowable DG capacity of PEA test system.....	122
8.2 SARFI-X improvement after 3 MW DG connection at location B.....	123
8.3 SARFI-Curve improvement after 3 MW DG connection at location B	123
8.4 Feeder load pattern of PEA test system.....	124
8.5 Appropriate output of the DG at location B according to load variation.	124
8.6 Appropriate output power of a DG at location B.....	126
8.7 Power and energy losses.....	127
A.1 Modified RBTS Bus 2 Feeder length data.....	137
A.2 Modified RBTS Bus 2 Feeder impedance (Ohm/km).....	137
A.3 Modified RBTS Bus 2 Load information.....	137
A.4 Modified RBTS Bus 2 Load summary per feeder.....	138
D.1 Failure rate and repair time of the equipment in test system.....	141
D.2 Type and number of customer at each load point.....	142
E.1 Equipment impedance of PEA test system.....	143
E.2 Customer data for PEA test system.....	144
E.3 Protection setting of PEA test system	144

List of Figures

Figure	Page
1.1 Research scope.....	12
2.1 DG model for fault calculation.....	16
3.1 Typical distribution feeder with over-current protective devices.....	19
3.2 IEC time over-current inverse curve.....	20
3.3 Recloser fast and slow curve.....	21
3.4 Fuse 65K operating curve.....	22
3.5 Example of protection coordination and CTI.....	25
3.6 Protection coordination for fuse saving scheme.....	26
3.7 Time coordination curve of protective device in Feeder 1.....	29
3.8 Fault in the lateral located behind recloser when DG is behind recloser.	29
3.9 Fault in the lateral located in front of recloser when DG is behind recloser.....	30
3.10 Fault in the lateral located behind recloser when DG is in front of recloser.....	31
3.11 Fault in the lateral located in front of recloser when DG is in front of recloser.....	31
3.12 Fault in the lateral behind recloser at a nearby feeder.....	32
3.13 Fuse-fuse coordination in presence of a DG.....	34
4.1 ITIC and SEMI F47 voltage envelope curve.....	40
4.2 Model for voltage sag calculation.....	41
4.3 Modified RBTS Bus 2 – Feeder 3.....	45
4.4 Voltage sag magnitude as a function of distance to fault at different system fault level.....	49
4.5 Back-feed problem illustration as a result of DG in the system.....	51
4.6 Fuse saving scheme problem illustration as a result of DG in the system.....	52

Figure	Page
4.7 Improvement on SARFI-Curve due to a presence of DG in the system..	54
5.1 Modified RBTS Bus 2 Feeder 1.....	58
5.2 Feeder loss with and without the presence of DG at location A.....	59
5.3 Appropriate output power at different load levels.....	61
5.4 Illustration for BCDLA loss allocation method.....	62
6.1 Procedure for determining maximum allowable capacity of one DG connection.....	71
6.2 Procedure for determining maximum allowable capacity of more than one DG connection.....	72
6.3 Procedure in evaluating system reliability in the presence of DG.....	81
6.4 Simple three-node feeder.....	85
6.5 Procedure in determining load and DG output power relationship.....	90
7.1 Comparison of maximum allowable DG capacity of Feeder 3 of Case (a) and Case (c).....	95
7.2 Comparison among the maximum allowable capacities of DGs located in front and behind the recloser of each feeder.....	96
7.3 Maximum allowable capacity and its associated % loss reduction.....	97
7.4 Maximum allowable capacity of a DG at each location with protection and losses consideration.....	97
7.5 The maximum allowable DG capacity after DG connections at 1A and 2B of 5 MW and 3C of 2.5 MW.....	101
7.6 Protection coordination after resetting.....	103
7.7 The comparison of all protection adjustment methods.....	107
7.8 $PMA_{back-feed}$ in main and lateral feeders.....	110
7.9 $PMA_{fuse-save}$ in lateral feeders.....	110
7.10 Appropriate DG output at location B and feeder load profile.....	116
8.1 PEA test system and potential locations for DG connection.....	121
8.2 Appropriate DG output at location B and feeder load profile.....	125

Figure	Page
A.1 Test System RBTS Bus 2.....	136
B.1 Load profile of each customer type.....	139
E.1 PEA test system.....	143

List of Abbreviations

Variables

t_{op}	Operating time of protective device; in sec,
TM	time multiplier or time dial of an over-current relay,
I	Magnitude of current; in A,
I_F	Magnitude of fault current; in A,
I_s	Pick-up current setting of protective device; in A,
$I_{R,Pickup}$	Pick-up setting of recloser; in A,
I_R	Fault current passing through recloser; in A,
I_{Fuse}	Fault current passing through fuse; in A,
$I_{Fuse-max}$	The maximum fault current for fuse-fuse coordination, in A,
$I_{F,Sub}$	Fault current contribution from substation; in A,
$I_{F,DG}$	Fault current contribution from DG; in A,
L_{ij}	Power loss in line $i - j$; in MW,
V_i	Complex voltage at bus i ; in V,
I_{ij}	Complex current from bus $i - j$; in A,
P_{DG}	Output power of a DG; in MW,
L	Total system loss; in MW,
L_{base}	Total system loss when there is no DG in the system; in MW,
$T_{Rf}(I_F)$	Recloser fast curve operating time at I_F ; in sec,
$MMT_F(I_F)$	Fuse minimum melting time at I_F ; in sec,
b	Branch number
k	Node number
$I^{(b)}$	Complex current flowing through branch b ; in A,
$\alpha^{(b)}$	Real part current flowing through branch b ; in A,
$\beta^{(b)}$	Imaginary part current flowing through branch b ; in A,
$R^{(b)}$	Resistance parameter of branch b ; in ohm,
$L^{(b)}$	Loss occurred in branch b ; in MW,
I_k	Complex current supplied to node k ; in A,
α_k	Real part current supplied to node k ; in A,

β_k	Imaginary part current supplied to node k ; in A,
S_k	Complex power supplied to node k ; in MVA,
P_k	Real power supplied to node k ; in MW,
Q_k	Reactive power supplied to node k ; in MVAR,
V_k	Complex voltage at node k ; in p.u.,
W_k	Virtual voltage at node k ; in p.u.,
c_k	Real component of a virtual voltage W_k ; in p.u.,
d_k	Imaginary component of a virtual voltage W_k ; in p.u.,
L_k	Loss allocation factor for node k ; in MW,
L_{total}	Total feeder loss; in MW,
λ_{p-n}	Permanent failure rate of equipment n , in times/year/km,
λ_{t-n}	Temporary failure rate of equipment n , in times/year/km,
r_{p-n}	Repair time of equipment n , in minute or hour,
r_{s-n}	Switching time of equipment n , in minute or hour,
λ_i	Average failure rate at load point i for sustained interruption, times/year,
r_i	Average repair/switching time at load point i for sustained interruption, minute or hour,
N_i	Number of customers at load point i ,
V_{sag}	Voltage sag magnitude monitored at a substation, in p.u.,
X	Voltage sag threshold, in p.u.,
Z_F	Impedance between substation and fault location, in p.u.,
Z_S	System source impedance, in p.u.,
z	Line impedance per unit length, in p.u./km
l	Distance from substation to fault location, in km,
l_{crit-X}	Critical distance for a voltage sag threshold X , in km,
Z_{crit-X}	Critical impedance for a voltage sag threshold X , in p.u.,
I_{pickup}	Pick-up current setting of protective device, in A.,
$I_{pickup-down}$	Pick-up current setting of the downstream protective device, in A.,
$I_{pickup-up}$	Pick-up current setting of the upstream protective device, in A.,
K	Safety factor for coordination between pick-up current setting,
I_{spec}	A specified current of which the maximum is equipment rating, in A.,

$T_{up}(I)$	Operating time of upstream device for fault current I , in sec.,
$T_{down}(I)$	Operating time of downstream device for fault current I , in sec.,
I_{down}	Fault current magnitude at the location of downstream device, in A.,
t_{margin}	Required operating time margin, in sec.,
$PMA_{back-feed,m}$	PMA in the main feeder for back-feed problem, in km,
$PMA_{back-feed,l-n}$	PMA in the lateral n for back-feed problem, in km,
$PMA_{fuse-save,l-n}$	PMA in the lateral n for fuse saving scheme problem, in km,
$PMA_{fuse-fuse,l-n}$	PMA in the sub-lateral n for fuse-fuse coordination problem, in km,
PMI_i	PMI for customer load point i ,
l_{sec}	Length of a sectional line, in km,

Sets

B	Set of bus number.
B_k	Set of branches which connect the node k to the root node.
K^(b)	Set of nodes supplied from branch b , i.e. the downstream of branch b .

Abbreviations

BCDLA	Branch Current Decomposition Loss Allocation
CTI	Coordination Time Interval
DG	Distributed Generation
EI	Extremely Inverse time-current characteristic curve
ITIC	Information Technology Industry Council
LP	Load Point
MMT	Minimum Melting Time
MV	Medium Voltage
PCC	Point of Common Coupling
PMA	Protection Mis-coordination Area
PMI	Protection Mis-coordination Index
RE	Renewable Energy
SAIDI	System Average Interruption Duration Index

SAIFI	System Average Interruption Frequency Index
SARFI	System Average RMS variation Frequency Index
SEMI	Semiconductor Equipment and Materials Institute
SI	Standard Inverse time-current characteristic curve
SPP	Small Power Producer
TCC	Time Characteristic Curve
TCT	Total Clearing Time
VI	Very Inverse time-current characteristic curve
VSP	Very Small Power Producer

CHAPTER I

INTRODUCTION

1.1 Problem Statement

The number of distributed generations (DG) connected to a distribution system continually increases, mainly driven by environmental and energy concerns. These DGs are generally fueled by renewable energy resources, e.g. biomass, hydroelectric, photovoltaic, wind being connected to distribution systems. Consequently, generation and transmission facilities should be developed accordingly.

In general, a DG provides several benefits to society and distribution network. Firstly, it can reduce system loss since the DG is generally located close to load center. Secondly, DG can also serve as an emergency unit or operate for load management purposes. Consequently, it can help postpone the investment of new infrastructure. Finally, a DG driven by renewable energy, compared to a conventional power plant, emits low green house gas to the environment [1-2].

In Thailand, there is an increasing activity regarding renewable energy (RE). This is mainly due to the high price of energy. In addition, the security for national energy is of important concerns. To solve and alleviate these issues, the government issued regulation for Small Power Producer (SPP) and Very Small Power Producer (VSPP), for which private sector can sell electricity to utility grids. VSPP is separated from those of SPP based on the capacity in which it is defined to be less than 10 MW. Due to its small size and cost of investment, VSPP is therefore typically connected in a distribution grid.

Regarding regulation issue, the government aims to support the utilization of renewable energy and to make a full use of indigenous resources, e.g. biomass, biogas, solar. It is anticipated that these renewable energy utilization could help country save imported energy cost in a large amount. In addition, VSPP will help reduce emission from power sector which plays an important role on the green house gas emission.

According to existing regulation [3], the VSPP is classified into two groups, i.e. cogeneration and renewable energy. For RE, several resources are listed, comprising biomass, biogas, wastes, wind, hydro, and solar power. The Thai government has provided special extra rate called as “adder” in addition to normal tariff to support such VSPP. It is expected that the proportion of energy produced from RE will account for 20% of the total energy within next 15 years. Current situation of VSPP, as of March 2011, based on types of fuel can be summarized in Table 1.1 [4].

Table 1.1 Existing VSPP in Thailand

Fuel	Contracted			In progress			Total		
	No.	MW	%	No.	MW	%	No.	MW	%
Biomass	61	783.92	79.03	282	2405.31	39.79	343	3189.23	45.32
Biogas	61	91.53	9.23	84	174.53	2.89	145	266.06	3.78
Solar	77	43.62	4.40	664	3140.57	51.95	741	3184.19	45.25
Wastes	13	33.27	3.35	29	153.17	2.53	42	186.44	2.65
Wind	3	0.38	0.04	36	100.77	1.67	39	101.15	1.44
Hydro	5	1.10	0.11	7	6.24	0.10	12	7.34	0.10
Co-gen	4	38.10	3.84	10	64.82	1.07	14	102.92	1.46
Total	224	991.92	100	1112	6045.39	100	1336	7037.31	100

It is anticipated that higher penetration of VSPP will become common for distribution system utilities. It can be seen from the table that biomass represents a large percentage of the VSPP which is typically operated using synchronous machine.

Nevertheless, the presence of a DG has brought several impacts to a distribution system, e.g. increase fault level, network topology change. The increase of fault current may exceed rating of existing equipment, e.g. protective devices. With high penetration of DG, the magnitude and path in which the fault current flows will be altered from that of the original network without DG. As a result, the distribution network is no longer a passive circuit. However, it becomes active due to the

embedded DG sources. An overview of several impacts of DG on the distribution system have been illustrated in [5], i.e. power loss, voltage regulation, harmonics, fault level, and islanding condition. Nevertheless, there is no detailed discussion of impact of DG on distribution protection coordination.

In general, a distribution network operates under radial configuration with application of typical protective devices, i.e. over-current relay, recloser and fuse, most of which are non-directional type. The protection coordination of these devices is usually designed based on time-current coordination, i.e. protective device must not operate under possible maximum load condition and must clear fault in its zone before the operation of upstream protective devices.

Another protection application in a distribution system is the fuse saving scheme. Since most faults occurred in the distribution system are temporary fault types, it can be an advantage for trying to save fuse from unnecessary operation under a temporary fault condition by fast operation of a recloser. This will help reduce an outage time and cost of operation especially when a fuse is located in a rural or inconveniently accessible area. However, there will be a trade-off with the increase number of outage frequency.

Both time-current coordination and fuse saving scheme are generally set up to work properly up to a certain fault level. If the fault current is out of the designed range, the coordination may fail and fuse saving scheme may not work properly. Since the presence of a DG generally increases fault level, it can also cause coordination failure to the existing protection system. Consequently, it may result in negative impact to system reliability.

In classifying the impact of the DG on distribution protection system, Doyle, M.T. [6] demonstrated a few cases of the impact based on location of fault and DG with respect to the recloser, i.e. up-line and down-line of the recloser. First, it is illustrated that the presence of the DG located up-line of the recloser would increase fault current perceived by the protective device, and might result in protection coordination failure. Secondly, it showed that the presence of the DG located down-

line of the recloser could reduce fault current perceived by the protective device and thus reduce sensitivity of the device. Finally, the paper mentioned about possible unnecessary operation of the recloser caused by back feed fault current from the DG. However, the paper did not cover other protection schemes which were widely used in the distribution system, i.e. fuse saving scheme.

More details impact analysis of the DG on protection coordination has been proposed by [7-8]. In the same way, the literatures classify the pattern of protection mis-coordination caused by the DG based on fault and DG location with respect to the recloser. They have taken into account fuse saving scheme application into the problem. In addition, the papers have developed a set of constraint equations based on protection mis-coordination pattern for determining maximum allowable DG capacity which does not result in protection mis-coordination. Nevertheless, they did not mention about fuse-fuse coordination. In this thesis, the impact of DG on protection mis-coordination is further improved in order to cover all the cases. In addition, the protection constraint equations in determining the maximum allowable DG capacity will be revised.

It is also widely understood that high penetration of DGs can possibly increase feeder loss. In addition, it can cause voltage violation which may provide adverse effect to electrical equipment especially during light load conditions [2, 5]. Therefore, the determination of appropriate DG capacity subjected to normal system operating condition, including protection coordination, system loss, and voltage profile, is essential issues to be taken into account.

Another important issue regarding DG problem is an islanding condition which can be developed during a typical reclosing operation. Generally, DG is not allowed to island with any part of utility system since it can lead to safety and power quality problems that may affect utility and customers [6]. Besides, if an auto-reclose blocking or other synchronization facility is not provided, a reconnection in out of phase condition between utility and DG may result in damage to utility, DG, and customer equipment. For that reason, DG is normally prohibited from islanding

operation in most utilities by which its related protection function will be specified [3, 9].

It can be seen that the distribution system is originally designed not to accommodate the entrance of distributed resources. To prevent several problems and safety concerns, there is an established standard for interconnection of the DG [10]. The standard generally defines several rules for the DG to be complied with specified conditions before being connected to the grid, e.g. voltage regulation, synchronization, islanding condition, response to voltage and frequency disturbance.

In evaluating the DG request for connection, there are a number of current practices in specifying maximum allowable DG units which can be connected to a feeder. For example, the DG is limited by feeder maximum capacity which depends on conductor size and circuit length [3]. In the other way, DG capacity may be limited by a percentage of minimum demand in that feeder, or by a percentage increase of fault level at point of common coupling (PCC).

All of the criteria presented above can help provide some guidelines for system operators as rough evaluation of requesting DG for grid connection, before detailed interconnection study is performed. However, these methods only provide rough evaluation and sometimes may hinder high penetration of DG connection. As a result, the system may not be able to utilize full benefit from DGs. More precise determination of allowable DG capacity will be proposed in this thesis with consideration of protection coordination and power loss.

In order to achieve maximum benefits from DG connection, several research works have focused on the methodology for determining the best size and locations of a DG. The main objective generally concerns system loss reduction or cost benefit [11-13]. Most of the proposed methods have been developed using an optimization based technique with a set of appropriate constraints [11-13]. Peak load shaving, voltage regulation, postponement of investment in new infrastructure, and other purposes can also be considered.

Optimal DG allocation and sizing for reliability, power loss, and voltage improvement were proposed in [9], which applies Genetic Algorithm (GA) to solve for a solution. The objective is to determine an optimal DG capacity which provides the best cost benefit in term of power loss consideration. The constraints consist of voltage regulation, reliability indices and a maximum DG capacity which are allowed to be installed in the system. For example, the utility may set the limitation of maximum DG capacity at 10 MW according to [10].

In [12], load model is included in the problem of determining the best capacity and location of the DG using GA method. In addition, it determines the optimal DG based on multiple indices, i.e. power loss, voltage profile, MVA capacity with application of weighting factors. However, with an open and non-discriminatory access to the network, utility generally cannot fully control the entry of a DG regarding its location and capacity. As a result, it is a difficult task for utility officers to plan for an appropriate DG capacity to be connected to their feeders. It is found that this paper did not take into account protection coordination.

A method for determining the maximum allowable penetration of DG with no voltage violations has been proposed in [13]. It aims to identify maximum DG capacity which will not cause system voltage violation by considering minimum and maximum system demand. The consideration of demand variation is necessary since the change in system operating conditions may result in different appropriate DG capacity or output power. The paper also considers different DG operating modes including multiple DG cases. The obtained results ensure that the installed DG capacity will not cause voltage violation to the system. However, this method did not consider protection coordination. Also, the installed DG can possibly increase power loss from the base case where there is no presence of a DG. Therefore, this thesis proposes the method to identify an appropriate DG output power with power loss consideration. In addition, the paper also considers customer load profiles.

From all the above literature review, it can be seen that most of the methods in determining maximum allowable DG capacity only consider possible system operating conditions, i.e. loss and fault level and voltage violation. However they

generally neglect protection coordination [9, 11-16]. Considering only fault level, though preventing damage to electrical equipment in the system, can result in either too large or too small DG capacity. With protection coordination included, this thesis will propose a method in determining maximum DG capacity by which the obtained result can be improved and be more appropriate. In addition, the thesis also proposes the methodology of protection adjustment to allow larger penetration of DG.

Another view of DG impact on distribution system is concerned with Service Quality. The Service Quality of the system can be evaluated using Service Quality Index [2, 17-19]. The index can be grouped as interruption and voltage sag events. For interruption event, the Reliability Index, generally SAIFI (System Average Interruption Frequency Index) and SAIDI (System Average Interruption Duration Index) are applied for system evaluation. On the other hand, the index used for describing voltage sag is called SARFI (System Average RMS variation Frequency Index).

The DG may affect Service Quality of the system in both positive and negative ways. A large DG capacity can present a negative impact on the protection system coordination. If the protection system does not operate as designed, the system reliability can be degraded. On contrary, if a DG capacity is within an allowable range, it will increase system fault level but to a certain acceptable values. As a result, the system is more rigid and a number of voltage sag event in the system is expected to be reduced.

This thesis also proposes the methodology for evaluating system Reliability Index in the case that an installed DG capacity is larger than maximum allowable range. Additionally, the thesis introduces new index for protection mis-coordination event, i.e. PMI (Protection Mis-coordination Index). Furthermore, in case that DG capacity is within a design range, the method for evaluating a number of voltage sag event in the system is developed. The positive impact from a DG can then be perceived and determined quantitatively.

Most of the proposed methods determine an appropriate DG capacity in order to minimize system loss. However, the determination is mostly performed at some specific condition, e.g. peak demand. In practice, system demand varies along the time of day. From this fact, the variations in load may impose some impact and alter the appropriate DG capacity, output power, and location. As a result, the pre-specified DG capacity based on only peak or other specified load condition can become either too large or too small for most time of each day. Accordingly, if appropriate DG output power is determined for each time of day according to load conditions, then the results can be applied in case that DG is treated as dispatchable. This thesis also proposes the methodology to determine appropriate dispatchable DG output level. In addition, the thesis also proposes the approximation method to predict an appropriate DG output power according to demand variations

In summary, this thesis focuses on the analysis of DG impact on protection coordination and distribution system loss. A methodology will be developed to determine the maximum allowable capacity of a DG which will not cause protection coordination failure. In addition, the protection adjustment which can help allow more DG capacity will be presented. Then, the method of evaluating system Service Quality index under a presence of a DG is developed to perceive both positive and negative impacts from a DG. Finally, impact of system load variation to an appropriate DG output power is analyzed. Consequently, the appropriate DG output power at each time of day can be determined. This can help system operator to utilize and dispatch an appropriate output power of the DG.

1.2 Objective

The objectives of this thesis are described below.

- (a) Investigate and suggest all possible failures of protection coordination that may result from a connection of a DG in a distribution system.

- (b) Develop a methodology for determining maximum allowable DG capacity with protection consideration. In addition, the methodology will be capable of taking into account existing DGs
- (c) Propose protection adjustment criteria to increase maximum allowable DG capacity.
- (d) Analyze DG impact on system Service Quality.
- (e) Develop the methodology for appropriately dispatching DG output power taking into account power loss and customer load profiles.

1.3 Research Scope for DG Impact Investigation

This section describes the research scope of this thesis, which mainly focuses on the impact of DG on a distribution system. A methodology will be developed to identify appropriate and maximum allowable DG capacity to be connected to the system. In addition, it also proposes and illustrates the developed method to allow a larger capacity of a DG unit. Furthermore, a method to evaluate reliability impact from penetration of DG will be developed.

Generally, maximum allowable DG capacity can be classified into two stages, i.e. planning and operation stages. The planning stage is directly related to the consideration of protection system coordination and Service Quality (Step 0-2). On the other hand, the operation stage is strongly linked with the consideration of power loss (Step 3-5). The procedure and general concept for each calculation step can be described and summarized below and depicted in Figure 1.1.

Step 0: Review and analyze typical protection coordination in a distribution system. Develop problem formulation and analyze impact of DGs on existing protection coordination. The impact will be categorized based on the location of DG and fault (Section 3.4). Then, methodology for determining maximum allowable DG capacity with protection coordination consideration, e.g. fuse saving scheme will be developed. The impact of DG on protection system will be integrated into an

optimization problem, i.e. (6.5) – (6.9). The objective function is defined as maximum DG capacity with appropriate set of constraints, i.e. Eq. (6.1) – (6.9) (Section 6.1). Simulation results from the proposed methodology will be illustrated (Section 7.1). The original test system is modified by increasing feeder length so that it will be in accordance with a typical distribution system of PEA. Multiple DG case is also investigated. In addition, the proposed method is applied to a PEA distribution system.

Step 1: Develop protection adjustment method to increase maximum allowable DG capacity (Section 6.2). Based on the limitation from protection coordination on the maximum DG capacity, this thesis investigates and proposes protection adjustment process to increase allowable DG capacity. The simulation results from the method will be presented in Section 7.2.

Step 2: Analyze the DG impact on system Service Quality (Section 4.4). Then, develop methodology to evaluate DG's impact on system Service Quality Index comprising of interruption and voltage sag events (Section 6.3). In addition to a typical reliability index, a newly developed index will be proposed to measure the impact of the DG. Simulation results from the proposed method are also provided (Section 7.3).

Step 3: Analyze the impact of load variations on an appropriate DG output power, i.e. Section 5.2-5.4. The objective is to avoid an increase of power loss from having DG in the distribution system. To determine for the appropriate DG output power at a specified load condition, a direct search method can be used to obtain the optimal DG output solution. The system voltage according to each DG output level will also be investigated.

Step 4: Develop the methodology for determining appropriate DG output power with customer load profile consideration (Section 6.4). If demand variation in feeder demands, customer load profile for each load point is aggregated to be a single feeder load profile. Based on that, an appropriate DG output power is determined for each individual demand level. The obtained results are then applied to establish the

DG output power profile. In addition to a direct search method, a method to establish the relationship between appropriate DG output power and customer load profiles is proposed in this thesis. The BCDLA (Branch Current Decomposition Loss Allocation) method [20] is utilized to establish such a relationship. With the obtained equation, a change in appropriate DG output power when load at each point changes can be approximated. Moreover, the method is extended for the application of power loss minimization.

Step 5: Perform the simulation and analyze the obtained results. The results from the developed approximation and direct search method are compared (Section 7.4). System loss is calculated based on obtained DG output profile, then used to evaluate the proposed methodology. In addition, the energy loss for the whole day according to each DG output profile is also presented in order to see the benefit from operating the DG according to the obtained profile.

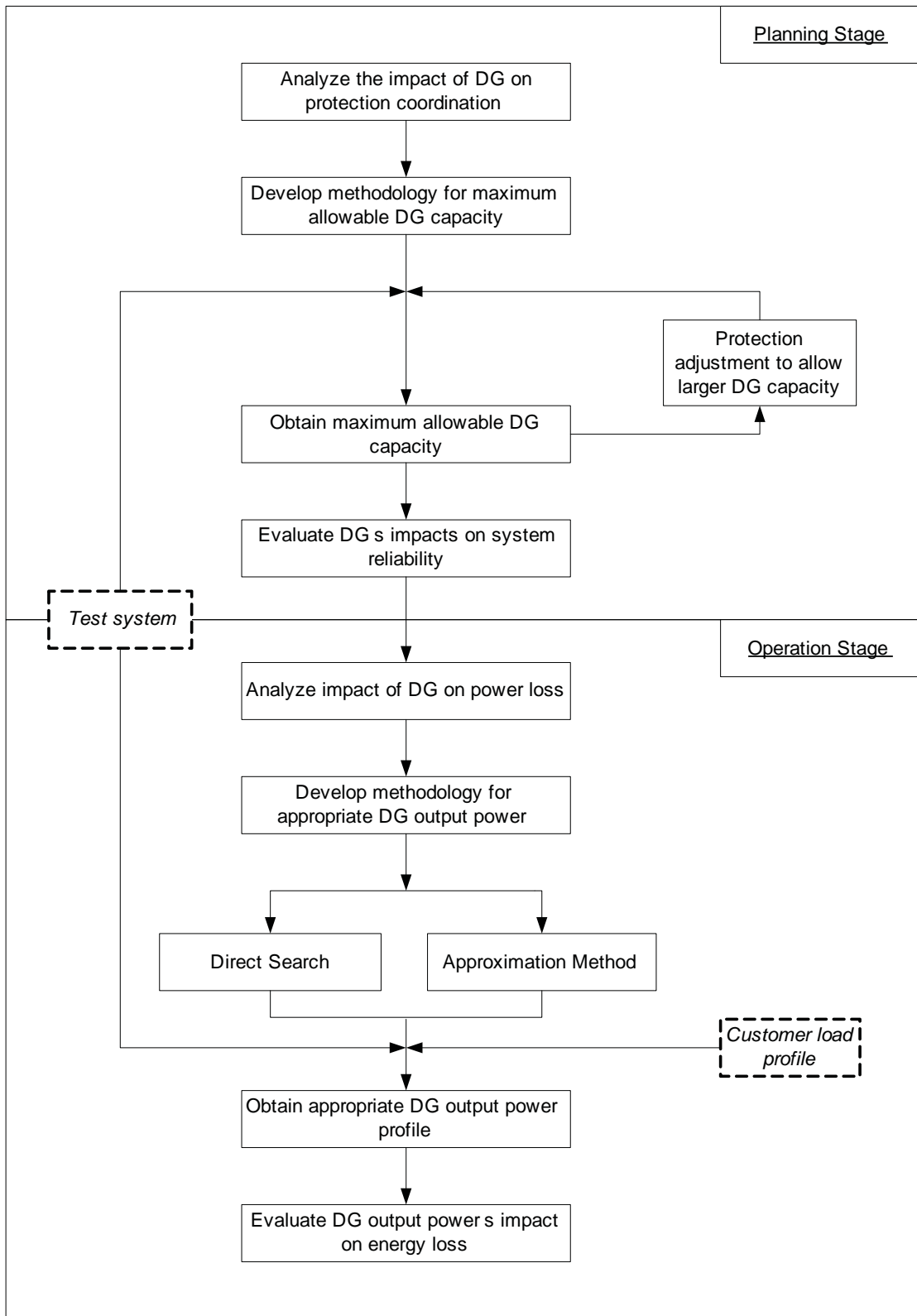


Figure 1.1 Research scope.

CHAPTER II

DISTRIBUTED GENERATION

Distributed Generation (DG) is sometimes called distributed or embedded resources. The definition of DG is a small unit of generation scattering throughout the system to provide electricity in a proximity area to the load either to reduce the purchase power or sell electricity back to the grid and operated in parallel with the grid [1]. The DG can be either renewable or non-renewable type. The renewable energy for electricity generation usually includes biomass, hydroelectric, photovoltaic, wind, etc., whereas the non-renewable energy comprises combined cycle, combustion, fuel cells, etc. In general, the capacity of a DG allowed to connect to a distribution feeder is normally less than 10 MW [10].

In this chapter, the basic types of DG generators are presented. In addition, the standard for interconnection of a DG will be reviewed. Finally, the chapter describes the model of a DG which will be used in this research.

2.1 Basic Type of DG

Based on characteristics and connection type, the DG can be classified into three types, i.e. synchronous, induction, and power electronic converter type [1-2]. The synchronous type contains a dc field winding which provides a source for machine excitation. This type of DG is capable of providing system voltage support by supplying reactive power to the system. In addition, it can supply sustained fault current during fault condition in the power system.

For an induction generator, there is no field winding and its excitation is provided from an external source. As a result, it will absorb reactive power from the system and therefore cannot provide voltage support. Additionally, during fault condition, it can supply fault current for only a few cycles and then become negligible within 10 cycles [2, 5].

As for power electronic converter type, this DG can operate for both lagging and leading power factor similar to that of synchronous type, and thus possible for providing voltage support. However, it contributes only small amount of fault current during system fault condition, and for only short period of time, i.e. less than a cycle [21].

Based on the above fault contribution characteristic of all DG types, it can be seen that a synchronous DG has the biggest impact to the system fault current and is more likely to introduce troubles to existing protection system.

2.2 Standard and Practice for DG Connection

Currently, there are several guidelines and practices in evaluating distributed generation project requesting for connection to the utility distribution system. This subsection provides some examples of the guidelines.

For Con Edison, a total capacity of DG units connected to a distribution feeder is limited to a maximum of 10 MW and 20 MW per network substation. In addition, it is specified that one third of the feeder's all time light load is to be greater than the dispersed generation MW rating [14-15].

Another widely used criterion is California Rule 21 [9]. For simplifying the evaluating process, the capacity of a DG must be less than 15% of line section peak load. This is to ensure that the capacity of a DG remains small compared to the minimum load to prevent reverse power flow which can cause over-voltage conditions and mis-operation to network protector devices. Regarding short circuit current contribution, the ratio should be less than or equal to 10%. This is to prevent an impact to system's short circuit duty, fault detection sensitivity and fuse-saving schemes application. Otherwise, details study before interconnection will be required.

The similar regulation is applied for public utility commission of Texas on DG interconnection manual [16]. For no study fee, the proposed DG must be designed to export power not more than 15% of the total load on feeder. In addition, the DG must

not contribute more than 25% of the maximum potential short circuit current of the feeder. Based on these criteria, one can notice that the allowable capacity of a DG may vary when load and system operating condition changes.

As for Provincial Electricity Authority (PEA), Thailand, the regulation limits aggregated DG capacity per feeder according to circuit loading capability, i.e. 8 MW for 22 kV and 10 MW for 33 kV system voltage levels [3].

Regarding islanding operation, DG is generally not allowed to be islanded with any part of utility system since it can lead to safety and power quality problems that may affect utility and customers. However, this condition may arise from a typical reclosing operation which is designed to auto-clear a temporary fault normally occurred in a circuit [6]. Moreover, a reconnection in out of phase condition between utility and DG can cause damage to utility, DG, and customer equipment. An auto-reclose blocking or other synchronization facility is required to prevent this problem. In addition, to prevent islanding operation from occurring, most utilities generally put a requirement on related protection function of a DG, which is often referred to as anti-islanding protection [3, 9].

Nevertheless, more studies are still being conducted especially on how to determine the practical limits of DG in the network more precisely to reduce evaluation time for the application process. In addition, it is a challenge to include protection coordination consideration when processing for maximum allowable DG capacity for which the DG capacity result will not cause degradation in system reliability.

2.3 DG Model

In this thesis, power flow and fault studies analysis are needed. Fault study is performed in order to calculate fault currents. The obtained results will be used to verify the existing protection coordination and to determine whether protection mis-coordination is occurred. A fault study is performed based on the Z-bus method [22-24]. Since the anticipated results from this thesis concerns distribution system

planning purposes, the DG model of the synchronous type will be used with the reason that it presents the highest impact to the system fault current, compared to induction and converter types. Therefore, the synchronous type DG is most likely to disturb existing protection coordination. Therefore, for fault calculation, the DG will be modeled as a voltage source in series with a reactance (jX) connected to the grid at PCC according to Figure 2.1.

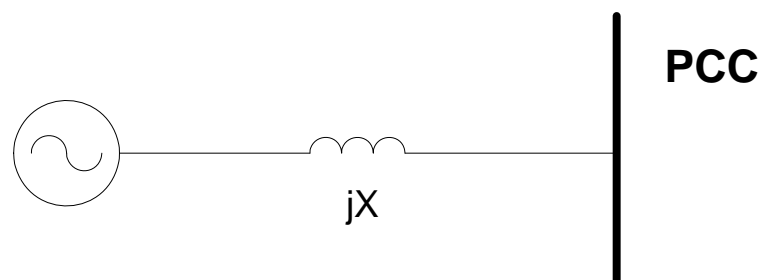


Figure 2.1 DG model for fault calculation [2]

For an operation mode, the DG can be operated under either power factor or voltage control mode. In this research, as DG is fairly small in terms of MW generally less than 10MW, the machine is not aimed for providing voltage support to the system or operating in voltage control mode. Besides, if the DG is to operate in voltage control mode, it may have to supply a varying output of reactive power to the system at some period of day, especially when system demand is rather high. As supplying reactive power, the real output power from the DG can be limited. This is not a desired condition for DG project owners as they can lose some profit from selling of electricity. Therefore, generally, the DG in distribution system will operate under power factor control mode.

As a result, for the required load flow analysis, it is assumed that the DG operates at a unity power factor control mode and therefore injects only real MW power to the system. Without supplying reactive power to the system, the DG can produce a MW output power at full of its capability. Consequently, the DG can be modeled as a PQ bus or negative load with real output power is equal to the DG

capacity limit and reactive output power is equal to zero [2, 23]. Power flow study is performed to study for a change in feeder loss according to the presence of DG.

CHAPTER III

PROTECTION COORDINATION ANALYSIS

This chapter provides an overview of the widely used protection system and discusses about protection coordination. Firstly, protective devices in distribution systems are introduced, followed by protection system coordination. The summary of protective device setting which is applied in this thesis is then presented. This setting of protective devices is important and assumed to be done before further analysis. Finally, the impact of DG on the distribution protection system is analyzed and illustrated.

3.1 Distribution System Protective Devices

Over-current protection is the main and widely used scheme in MV distribution network. This type of protection operates based on the magnitude of fault current with time-inverse characteristic, i.e. higher fault current results in less operating time. Generally, the device operating time depends on the Time Characteristic Curve (TCC).

Though simple and economic, the scheme works very well under radial network configuration in which the system has only a single source and the current flows only in one direction. The over-current protective devices consist of relay and circuit breaker at the substation, recloser, and fuse [25-28]. Figure 3.1 illustrates all the devices located in a distribution feeder.

In general, the protection system is composed of phase and ground protection. The phase protection will respond to a high magnitude of phase current and will detect for phase-to-phase and three-phase fault types. In responding to a phase current, phase protection has to be set above maximum load demand to prevent mis-operation under a normal condition, which may result in low sensitivity in detecting ground fault type. This problem can be solved by the use of ground protection in which it can be set below normal load current. Therefore, it can provide good sensitivity to those of ground fault types.

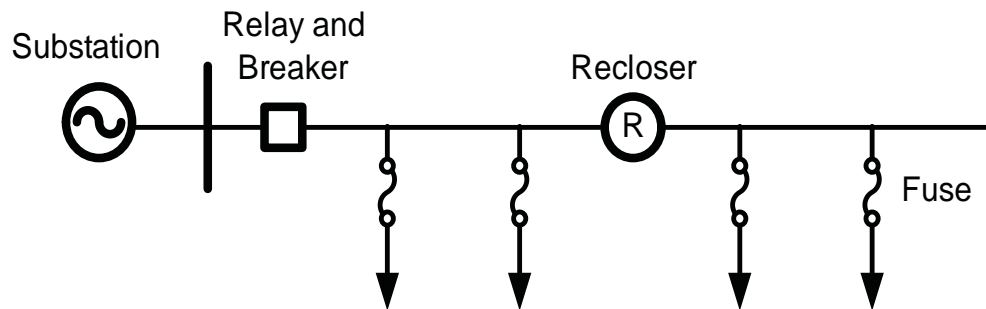


Figure 3.1 Typical distribution feeder with over-current protective devices

With radial characteristic of a typical distribution system, fault current can flow only in one direction. Therefore, non-directional type protective devices are generally used. This implies that the protective devices will respond to the fault current in either direction in the same way.

However, when a DG is presented, the distribution network will lose its radial characteristic. With a passive circuit, the system will now become active. Fault current can flow from either direction. The back-fed fault current from the DG may result in an unnecessary operation of this non-directional protective device.

3.1.1 Over-Current Relay

Over-current relay is a protective device which works with circuit breaker and is normally installed at the beginning of the feeder in the substation. Typically, both phase and ground relay are presented. The setting of the devices consists of pick up current, curve type and time multiplier (TM). Curve type is normally defined according to IEC255 [29]. There are three types widely used which are of Standard Inverse (SI), Very Inverse (VI), and Extremely Inverse (EI). The TCC for each curve can be calculated based on (3.1)-(3.3) and are shown in Figure 3.2.

$$SI: t_{op} = \frac{0.14 \times TMS}{\left(\frac{I}{I_s}\right)^{0.02} - 1} \quad (3.1)$$

$$VI: t_{op} = \frac{13.5 \times TMS}{\left(\frac{I}{I_s}\right)^{-1}} \quad (3.2)$$

$$EI: t_{op} = \frac{80.0 \times TMS}{\left(\frac{I}{I_s}\right)^2 - 1} \quad (3.3)$$

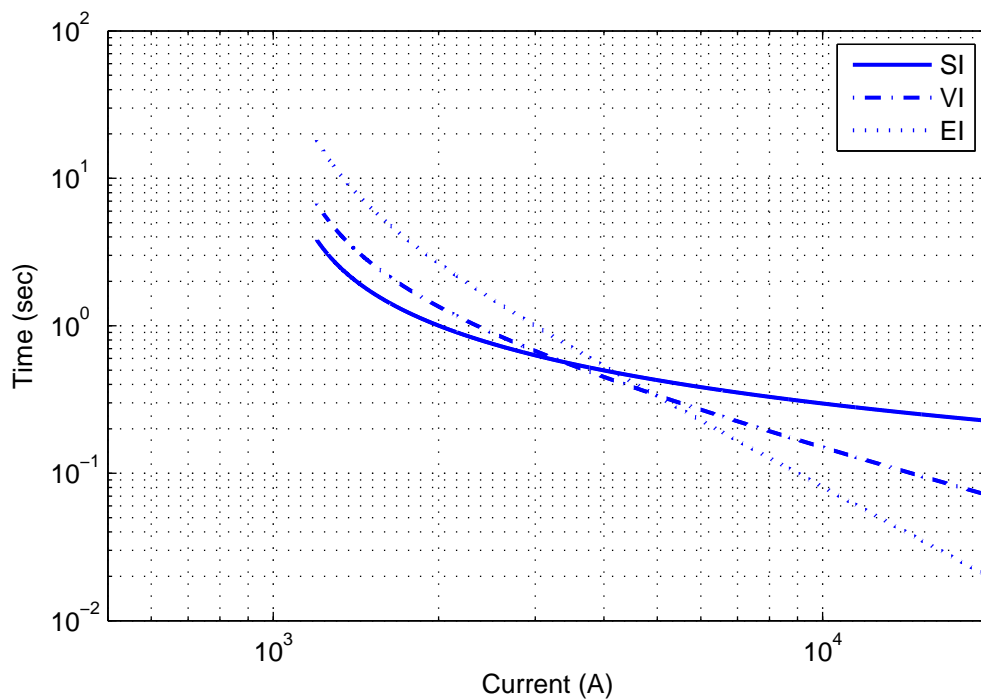


Figure 3.2 IEC time over-current inverse curve

3.1.2 Recloser

Recloser is a device which combines over-current protection and auto-reclose function. This device is normally installed somewhere in the feeder. It is also composed of phase and ground elements. Recloser is widely used in the distribution system since it helps clear temporary faults which are major fault types occurred in the distribution system by reclosing function and automatically restore power back. Consequently, interruption time caused by temporary fault is reduced and thus system

reliability is improved. The setting of the recloser is similar to an over-current relay but the TCC is typically a non-standard curve type [30].

The recloser generally has two operating curves, i.e. fast and slow curves. Fast curve is provided for using in fuse saving scheme application which will be described later in this chapter. The fast curve generally operates much faster than the slow curve and aim to operate before fuse device in response to a temporary fault. Figure 3.3 illustrates fast curve number 101 and slow curve number 116 of the recloser [30].

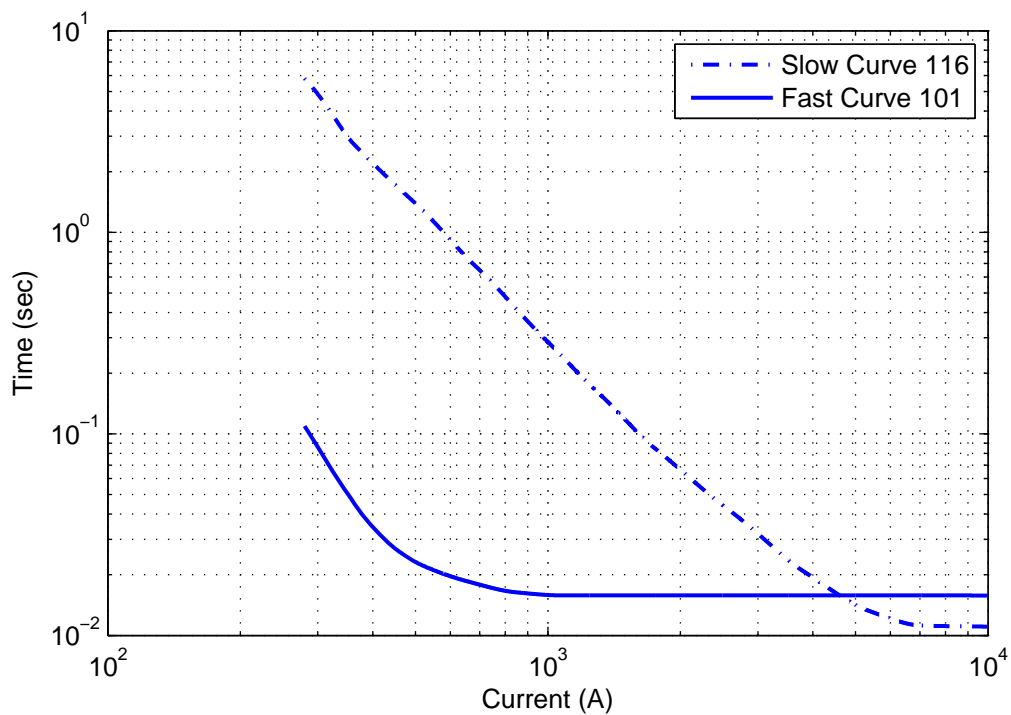


Figure 3.3 Recloser fast and slow curve

3.1.3 Fuse

Fuse is also another type of over-current protection device. Nevertheless, fuse device provides only phase protection. Fuse is simple and reliable, not involving in any electronic component. However, the error in operating time will be more than that of relay and recloser. The error depends on its operating conditions such as pre-load,

pre-damage, ambient temperature, etc. Fuse is normally applied at the lateral line out from the main feeder.

For fuse link selection, its rating must be specified in ampere. In addition, there will be a letter “K” or “T” which indicates the operation speed of the fuse. “K” is the fast type whereas “T” is the slow type. For example, fuse 65K means that fuse rating is equal to 65 A and is a fast type. In this study, fuse type “K” is selected for protection coordination study.

Fault interrupting capability is also another rating of fuse device and indicates the maximum fault current that fuse device can withstand such as 10 kA. The fuse interrupting capability should be selected in accordance with the fault level in the system.

Fuse has two important characteristic curves. First is Minimum Melting Time (MMT), which is the time that fuse is started to be damaged. The later is Total Clearing Time (TCT), which is the time that fuse is already broken. Fuse TCC can be found in [31]. Figure 3.4 shows an example of MMT and TCT curve of fuse device.

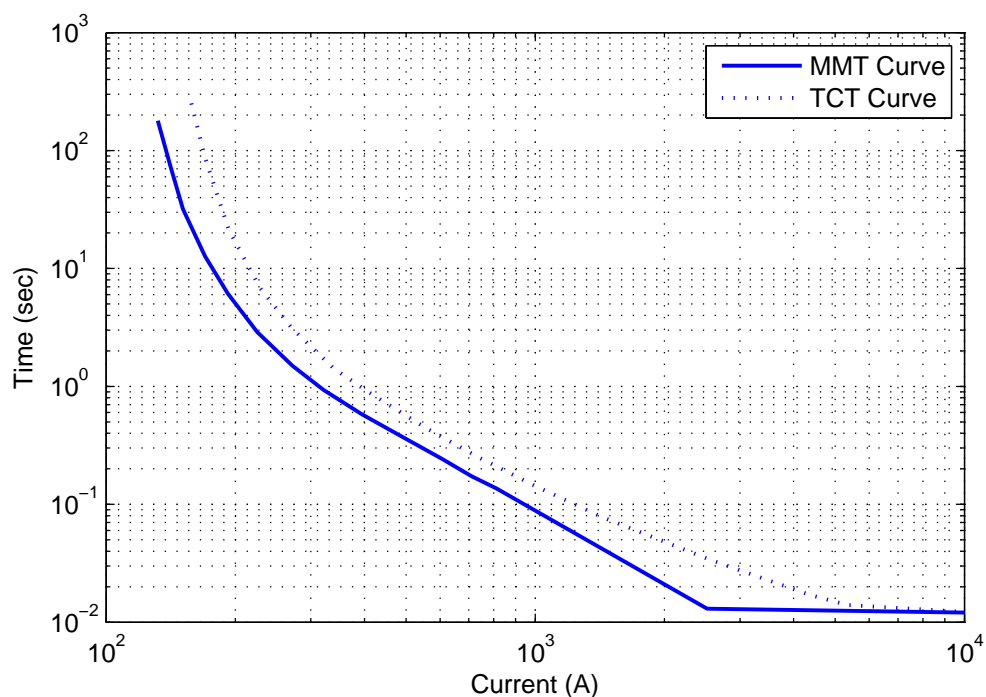


Figure 3.4 Fuse 65K operating curve

In the use of these devices, the selection of the device setting or rating must be done in such a way that it will respond to the fault within its zone of protection and should not operate for fault outside the zone unless providing a back up protection. In addition, when providing a back up protection, to ensure the failure of the downstream device, the operation speed of the upstream device must be slower than that of the downstream device by a proper margin. If satisfying all of the above, it can be said that the devices are well coordinated. The way of doing so is called protection coordination which will be presented in the next section.

3.2 Protection Coordination in Distribution System

Protection coordination is to coordinate protective devices in the system to operate selectively when a fault occurs. Protection coordination is very important. If protective devices in the system are well coordinated, it will respond correctly and selectively to the fault in its protection zone. At the same time, it will provide a back up protection for downstream devices. As a result, the outage area and effected customers will be minimized. The fault location or section can be easily identified and the outage time is reduced accordingly. These all together will have positive impact to the system reliability. In contrast to poor protection coordination, a failure in protection coordination can cause several problems to the utility.

In this subsection, a basic protection coordination applied in the distribution system will be reviewed. The fuse saving scheme application is also described.

3.2.1 Over-Current Protection Coordination

In coordinating protective devices, firstly, the pick-up current of relay and recloser or fuse size must be selected according to the maximum or emergency load current that can pass through the device [25-28]. This is to prevent protective device from mal-operation for all system operating condition especially when load level is high. Relay and recloser may be set above the maximum expected load current by 150-200%. The selection of fuse must also accommodate maximum or emergency load current.

Next, protection coordination can be achieved by selecting different current pick up setting among devices, i.e. downstream device will have a less setting value than that of the upstream device. In addition, time multiplier or time delayed will be set and adjusted in such a way that downstream device will operate faster than that of upstream device for the whole range of minimum and maximum expected fault current.

In judging that the over-current devices are well coordinated, the operating curve or TCC of the devices are typically plotted on log-log scale graph. By looking at the curves, the curve of the upstream device should be above that of downstream device by some appropriate margin called Coordination Time Interval (CTI). The consideration of CTI is generally at the expected maximum fault current that both upstream and downstream devices can see. The typically value of CTI is 0.3-0.4 second [28]. Figure 3.5 illustrates an example of over-current protection coordination.

For coordination between fuse devices, adequate CTI is to consider TCT curve of downstream fuse and MMT curve of upstream fuse. The general practice is to have TCT of downstream fuse divided by MMT of upstream fuse less than 75% in order to achieve protection coordination. Based on that, as fuse device can not be set, the coordination between a pair of selected fuse size will be valid up to a certain fault level. According to the above criteria, fuse coordination table can be established [27]. Table 3.1 shows maximum value of fault current at which type K fuse links will coordinate with each other. Therefore, if maximum fault current is known at the downstream fuse location, the upstream and downstream fuse size can be selected according to the table.

3.2.2 Fuse Saving Scheme [25, 27]

Since most of the fault in distribution system is of temporary type, it can be self-cleared by trying to de-energize the circuit, followed by auto-reclosing. For this kind of fault, utility may not desire to have the protective devices in the system operate especially for fuse device. If fuse is blown in response to the fault, the utility

Based on that, for a fault behind fuse, if the utility has an upstream recloser to operate first with its fast curve characteristic, fuse can be saved from an unnecessary operation to a temporary fault. The operating sequence can be described as shown below. First, the upstream recloser is designed to operate with its fast curve which will respond faster to the fault than the downstream fuse. Then, the recloser will try to energize the circuit back. If the auto-recloser operates successfully which means fault is a temporary fault, and fuse saving scheme operates successfully. In contrast, if the recloser reenergizes the circuit and fault is still there, it means that fault is a permanent fault. At this time, recloser will change to operate with its slow curve and allow the downstream fuse to clear fault in its zone of protection [25, 27].

To coordinate fuse and upstream recloser for fuse saving scheme, fuse TCT curve must lie underneath or operate faster than that of recloser slow curve. In addition, the fuse MMT curve must line above or operate slower than that of recloser fast curve. However, this condition will be well coordinated up to a certain fault level, i.e. where fuse MMT curve and recloser fast curve are intersected. An example of fuse saving scheme coordination is shown in Figure 3.6.

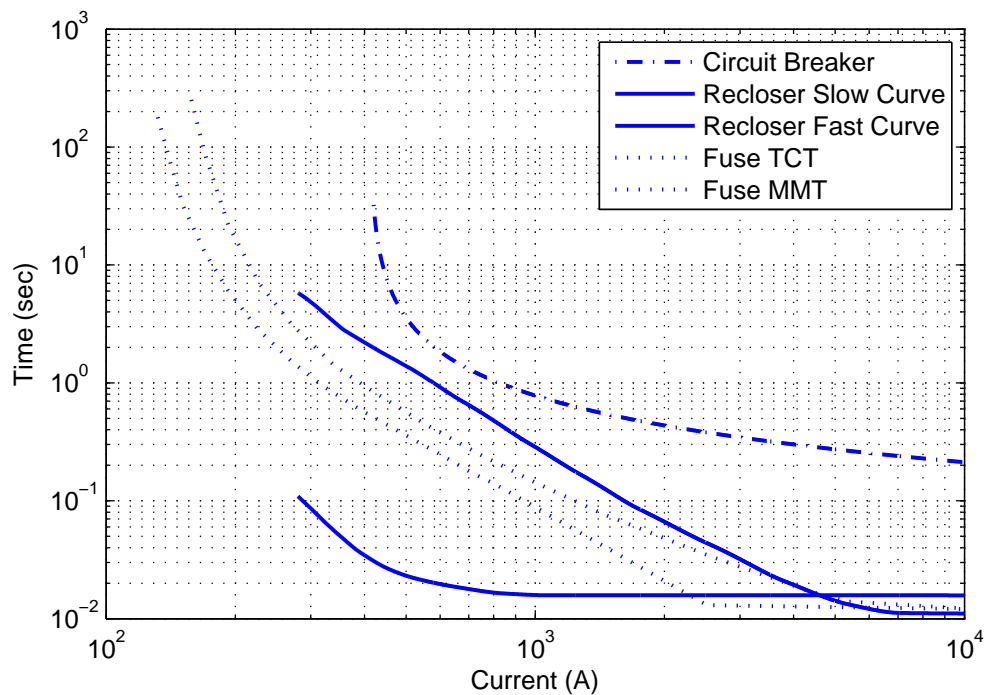


Figure 3.6 Protection coordination for fuse saving scheme

From the figure, it can be seen that for this case upstream recloser can provide fuse saving up to around 2,200 A. Consequently, if fault level at fuse location is raised by the DG to be above this value, fuse may operate faster than that of fast curve of recloser. As a result, fuse saving scheme will be failed. By increasing system fault level, it can be seen now that the DG can have some impact on the protection coordination.

3.3 Protection Coordination Example

In this thesis, a test system based on RBTS Bus 2 [32], of which the details are shown in Appendix A, will be used to illustrate the protective device setting. The system will then be used as an example for further analysis. There are two key types of protective devices, comprising recloser and fuse. It is assumed that relays and circuit breakers are installed at the beginning of each feeder and well coordinated with other protective devices. A non-directional type recloser with application of fuse saving scheme, is placed by the middle of each feeder except for Feeder 2. Fuse link is assumed to be of type K, i.e. fast type.

Protection coordination is set according to a general practice [25-28]. In this thesis, only three-phase faults are considered, since it is the most severe fault type which is basically used for protection coordination settings. The phase setting and selected operating curve of the protective devices can be summarized in Table 3.2. The pick up current setting shown in the table is in the primary value. An example of time-over current coordination of Feeder 1 is presented in Figure 3.7 which shows that fuse saving scheme is valid up to the fault level as of the intersection point between “Recloser 1 fast” curve and “Fuse 65K MMT”, i.e. approximately 2.5×10^3 Ampere.

3.4 DG Impact on Distribution Protection System

The presence of a DG in an MV distribution network generally changes its radial configuration, for which the protection system coordination has been originally set up. Consequently, when a fault occurs, it may cause mis-coordination in the

existing protection system. In this section, the thesis investigates the possibility of the mis-coordination between fuse and recloser due to the DG. It has been shown in [6-8, 33] that investigation of the protection coordination can be classified into two cases according to the DG locations, i.e. behind and in front of the recloser.

Table 3.2 Summary of protective device settings

Feeder	Circuit Breaker	Recloser	Fuse Type K (Branch)		
			40A	65A	100A
1	Curve=SI $I_{pickup}=411A$, $TM=0.1$	Fast curve=101 Slow curve=116 $I_{R,Pickup}=260A$	2, 3, 5, 6	8, 9, 11	-
2	Curve=EI $I_{pickup}=300A$, $TM=0.2$	None	-	-	13, 15
3	Curve=SI $I_{pickup}=349A$, $TM=0.15$	Fast curve=101 Slow curve=116 $I_{R,Pickup}=270A$	17, 19, 20	22, 23, 25	-
4	Curve=SI $I_{pickup}=383A$, $TM=0.1$	Fast curve=101 Slow curve=116 $I_{R,Pickup}=270A$	27, 28, 30, 31	33, 35, 36	-

A. DG behind recloser

A.1 Fault in the lateral located behind recloser

Regarding a fuse saving scheme application, the fast curve of a recloser must operate before fuse minimum melting time (MMT) curve for the fuse close-in fault [25, 27]. This scheme will save fuse from unnecessary operation under the condition of a temporary fault, which is self cleared by de-energizing the circuit by the recloser's fast curve operation.

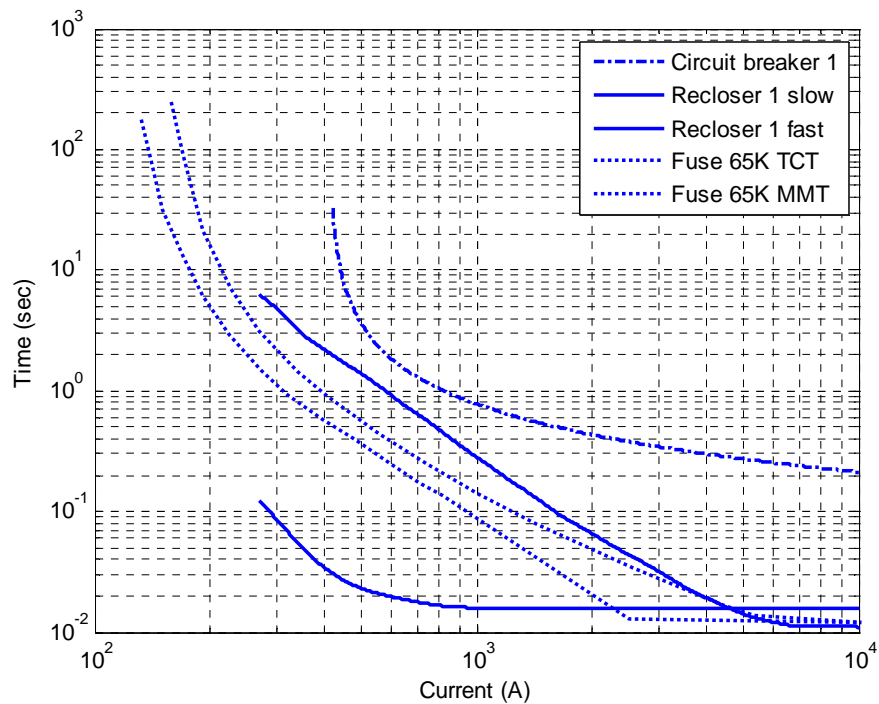


Figure 3.7 Time coordination curve of protective device in Feeder 1

If a DG is installed behind a recloser and a fault occurs in the lateral located behind the recloser, as shown in Figure 3.8, the recloser and fuse will perceive different fault currents. The fuse will perceive a higher fault current, as a combination of fault currents from the system and the DG. In this case, there is a chance that the fuse will operate before the operating time defined by the fast curve of the recloser. Consequently a temporary fault may result in the same impact to the system as a permanent fault, for which fuse operating curve is generally well coordinated with the slow curve of the recloser.

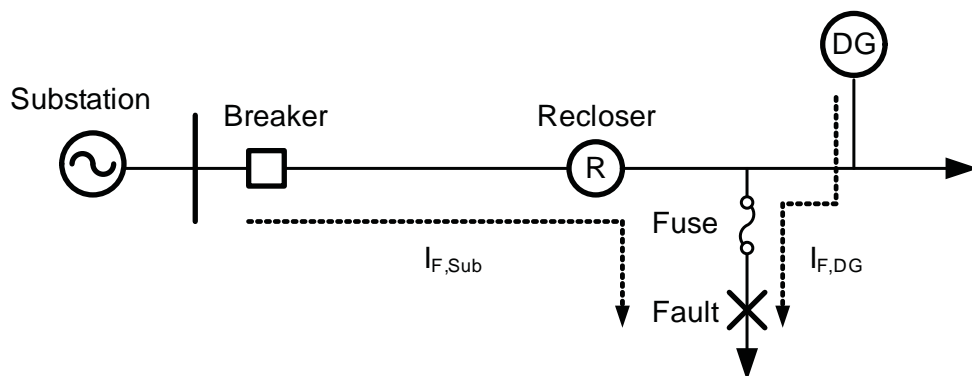


Figure 3.8 Fault in the lateral located behind recloser when DG is behind recloser

A.2 Fault in the lateral located in front of recloser

If a DG is installed behind a recloser and a fault occurs in the lateral located in front of the recloser, as shown in Figure 3.9, there will be a fault current feeding from the DG passing through the recloser in the back-flow direction. This back-feed situation is also occurred for fault in other feeders. If the recloser is a non-directional type, there is a chance that the fast curve of the recloser may operate before the lateral fuse can clear out the fault. This will result in unnecessary momentary interruption to all customers behind the recloser, which reduces system reliability.

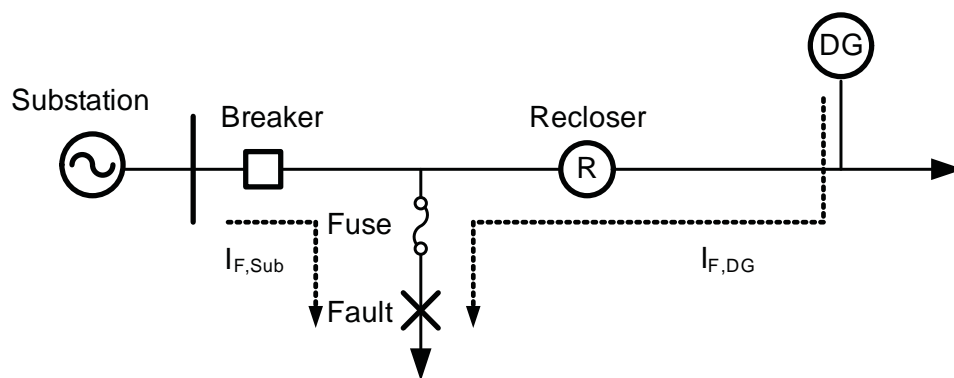


Figure 3.9 Fault in the lateral located in front of recloser when DG is behind recloser

Furthermore, in the situation that fault is occurred in the main line and in front of the recloser, typically the Breaker is responsible for clearing the fault. However, with back-feed problem, the recloser may also operate. As a result, an islanding condition may occur for those areas behind the recloser, which is not a desired condition for a utility. Additionally, if both protective devices equip with an auto-recloser function, the DG may be reconnected to the grid out of synchronization which can cause unintentionally a damaging condition to the DG.

B. DG in front of recloser

B.1 Fault in the lateral located behind recloser

If a DG is installed in front of the recloser and a fault occurs in the lateral placed behind the recloser, as shown in Figure 3.10, the recloser and fuse will

perceive the same fault current. However the fault current is higher compared to the case of with no connected DG. Due to the fact that the fuse saving scheme is generally designed to work to a certain fault level, there is a chance that additional fault current from the DG may cause mis-coordination between fuse and recloser. Again, it has impact only in case of a temporary fault.

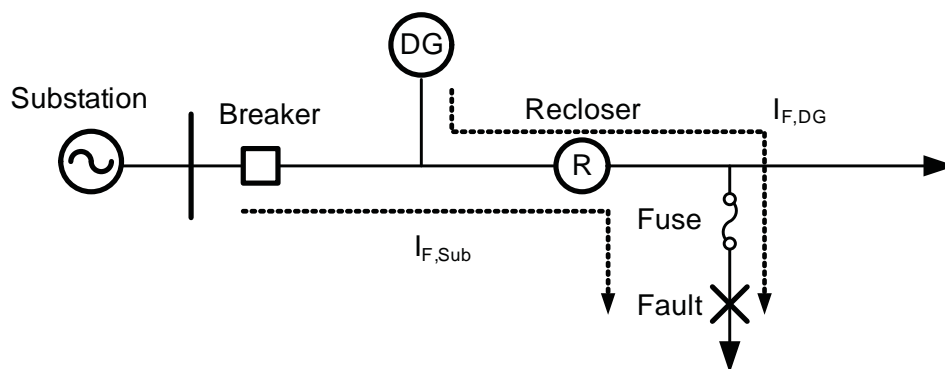


Figure 3.10 Fault in the lateral located behind recloser when DG is in front of recloser

B.2 Fault in the lateral located in front of recloser

If a DG is installed in front of the recloser and a fault occurs on the lateral located in front of the recloser, as shown in Figure 3.11, protection mis-coordination is unlikely. In this case, primary concern is the fuse interruption capacity, as there is additional fault current fed through from the DG.

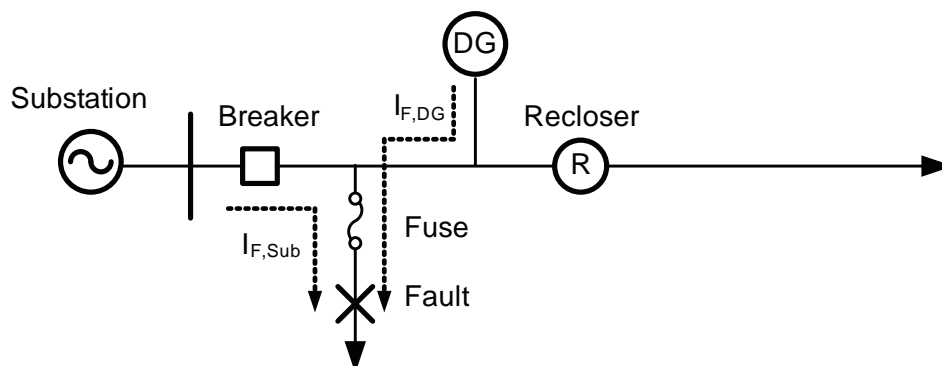


Figure 3.11 Fault in the lateral located in front of recloser when DG is in front of recloser

B.3 Fault in the lateral behind recloser at a nearby feeder

If a DG is installed in front of a recloser and there is a fault on a lateral behind the recloser on a nearby feeder, as shown in Figure 3.12, both recloser and fuse will perceive a higher fault current compared to the case with no DG. If this incremental fault current is large enough, the designed fuse saving scheme may not be achieved, which is similar to Case B.1.

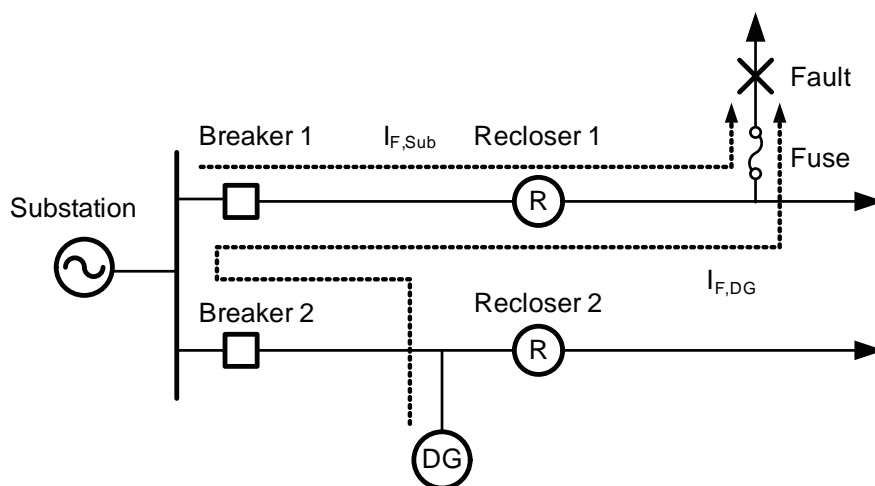


Figure 3.12 Fault in the lateral behind recloser at a nearby feeder

From all the above investigation, the impact from a DG to protection coordination between fuse and recloser can be summarized in Table 3.3.

In fact, a DG installed in front of the recloser can also cause protection miscoordination for a fault on a lateral in front of the recloser on a nearby feeder. For this case, there is an additional fault current feeding from the DG through the circuit breaker at the substation in back flow direction. If the relay at the substation is a non-directional type, the circuit breaker may unnecessary operate with this back flow fault current. Nonetheless, the above problem is almost impossible to occur. The fault current feeding from the DG is typically small compared to the fault current from the substation. As a result, with time characteristic of over current relay, it will take a fairly long time for the circuit breaker to operate. In addition, the lateral fuse with a higher fault current contributing from both substation and DG will operate even

faster. Therefore, the lateral fuse in front of the recloser on a nearby feeder always clear faults before the circuit breaker at substation. Therefore, the installed DG generally has no impact in this case.

Table 3.3 Summary of the possible mis-coordination pattern

Case	DG position	Fault location	Fault current
A.1	Behind recloser	Behind recloser	$I_R = I_{F,Sub}$ $I_{Fuse} = I_{F,Sub} + I_{F,DG}$
A.2	Behind recloser	In front of recloser	$I_R = I_{F,DG}$ $I_{Fuse} = I_{F,Sub} + I_{F,DG}$
B.1	In front of recloser	Behind recloser	$I_R = I_{F,Sub} + I_{F,DG}$ $I_{Fuse} = I_{F,Sub} + I_{F,DG}$
B.2	In front of recloser	In front of recloser	$I_R = 0$ $I_{Fuse} = I_{F,Sub} + I_{F,DG}$
B.3	In front of recloser	Behind recloser (Nearby feeder)	$I_R = I_{F,Sub} + I_{F,DG}$ $I_{Fuse} = I_{F,Sub} + I_{F,DG}$

Another protection coordination which can be affected by a DG is a fuse-fuse coordination. In a typical distribution network, there exists a configuration that the lateral fuse out of the main feeder can be an upstream device for a smaller fuse, as shown in Figure 3.13. This smaller fuse provides a protection to the sub-lateral. Table 3.1 can be applied to achieve a proper coordination between these two fuses by which Fuse 1 is protected link and Fuse 2 is protecting link. The fuse size will be selected in accordance with the maximum fault current design shown in the table. Consequently, in case that the DG increases fault current above the design value, the coordination between these two fuses will be failed.

According to the above impacts, the maximum allowable DG capacity at each location should be analyzed and controlled such that it will not create problems to the existing protection system and reduce system reliability. Accordingly, this thesis will propose the method for determining the maximum allowable capacity of the DG at

each location. Moreover, in case that the DG is larger than the maximum allowable, this thesis proposes a newly developed index to quantify a protection mis-coordination. The method for reevaluating the system reliability, i.e. SAIFI and SAIDI is also illustrated. Finally, to accept a higher penetration of DG, this thesis proposes the protection adjustment methods to increase the maximum allowable DG capacity.

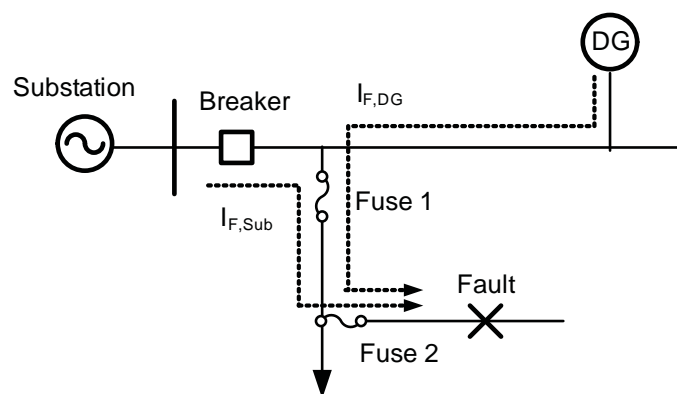


Figure 3.13 Fuse-fuse coordination in presence of a DG

3.5 Summary

In distribution system, protection scheme is generally designed based on time over-current principle. Typical protective devices are consisted of circuit breaker with relay, recloser, and fuse. TCC of an over-current relay is defined according to IEC standard, i.e. (3.1) – (3.3) whereas non-standard curve is normally applied for recloser, both fast and slow of its operating sequence. Fuse TCC comprises MMT and TCT characteristic.

Protection coordination is necessary for selectivity of each protective device. For time over-current protection, the pick-up current setting is set above maximum load level providing that the value is in between its upstream and downstream protective devices. TM is a time multiplier for TCC to achieve a desired CTI among devices. For fuse-fuse coordination, protected fuse can be selected based on maximum fault current at protecting fuse as shown in Table 3.1. Another widely used

scheme in distribution system is fuse saving by which the fast operation of recloser will save downstream lateral fuse from a temporary fault.

From all above, an example of protection setting of modified RBTS Bus 2 is shown in Table 3.2.

From the analysis, the DG impact on protection system coordination can be classified based on DG and fault locations as presented in Table 3.3. The resulting protection mis-coordination can be listed as back feed fault current, fuse saving scheme, and equipment rating. In addition, increase in fault level can cause problems to the existing design of fuse-fuse coordination.

CHAPTER IV

SERVICE QUALITY

Service quality can be used to describe system performance. Nowadays, the issue becomes increasingly important and is a major concern for customers. Service quality is consisted of interruption and voltage sag events [17-18]. Interruption occurs when the voltage goes down to zero, either sustained or momentary. Voltage sag or dip event is when the supplied voltage decreases to a certain value during system abnormal conditions or faults.

The system service quality is evaluated by using service quality index. Both interruption and voltage sag events have their own indices, which are called reliability and voltage sag index respectively. The methods to determine such an index are also essential.

In general, a protection system has strong impact on system service quality. Therefore, the service quality can be improved through a proper design of the protection system. Nevertheless, the protection mis-coordination, if occurred, can considerably degrade service quality. Therefore, it can be seen that high penetration of the DG which may result in a negative impact on the protection system, can also degrade service quality.

On the other hand, it is widely understood that an important factor to the number of voltage sag events is system fault level [18]. When fault level is high, the number of voltage sag events tends to decrease. As DG capacity increases system fault level to a certain acceptable level, it may also help the system to face less the number of voltage sag event. Therefore, a connected DG in distribution system, if properly sized, can improve system service quality.

This chapter provides a review of Service Quality index comprising reliability and voltage sag index. The calculation procedure for the index is also described. Then, an example of Service Quality index determination is illustrated using a

modified RBTS Bus 2 [32]. Finally, the impact of a DG on system Service Quality is examined in this chapter.

4.1 Reliability Index

Reliability index is an index to measure system performance in term of a number and duration of interruptions. Each interruption event can be classified as sustained or momentary type [17-18]. The sustained interruption results from a permanent fault. This type of events generally requires time for repairing equipment or performing manual switching. The momentary interruption is generally occurred from a temporary fault together with an automatic switching of network devices in restoring the circuit. The duration time of the event or restoration time is typically less than 5 minutes.

This thesis will firstly focus on the simplest and commonly used reliability indices, i.e. SAIFI and SAIDI [19]. Based on the IEEE 1366-2003, these distribution reliability indices are defined as follows.

SAIFI – System average interruption frequency index: SAIFI determines how often the average customer experiences a sustained interruption over a period of time.

SAIDI- System average interruption duration index: SAIDI determines the total duration of sustained interruption for the average customer during a pre-defined period of time. It is commonly measured in customer minutes or hours of interruption.

In calculating the above indices, two types of equipment information are required. The first is the average failure rate, i.e. permanent failure rate λ_p (resulting in sustained interruptions) and temporary failure rate λ_t (resulting in momentary interruptions). The parameters are generally defined in times per year. The second is the restoration time of service, i.e. repair time r_p or switching time r_s (for resolving a permanent fault and also temporary fault in the case that there is no automatic operation of switching device).

Accordingly, the reliability indices can be calculated based on the below equations.

$$SAIFI = \frac{\text{total number of customer interruptions}}{\text{total number of costumers served}} = \frac{\sum \lambda_i N_i}{\sum N_i} \quad (4.1)$$

$$SAIDI = \frac{\text{sum of customer interruption durations}}{\text{total number of customers}} = \frac{\sum \lambda_i r_i N_i}{\sum N_i} \quad (4.2)$$

Where, λ_i is the average failure rate for sustained interruption, r_i is average repair/switching time for sustained interruption, N_i is the number of customers, and i represents the customer load point.

The average failure rate and average repair/switching time at each customer load point i are determined as follows.

$$\lambda_i = \sum_i \lambda_{p-n} \quad (4.3)$$

$$r_i = \frac{\sum_i \lambda_{p-n} r_{p-n}}{\sum_i \lambda_{p-n}} \quad (4.4)$$

Where λ_{p-n} is permanent failure rate of equipment n and r_{p-n} Repair time of equipment n .

Since only sustained interruption is considered for SAIFI and SAIDI calculation, the failure rate for permanent faults λ_p will be applied to all line sections together with a repair time r_p . The failure rate for temporary faults λ_t is not included where the fault is clear automatically, i.e. on main feeder and lateral line behind the recloser. The main feeder is automatically reenergized by an auto-recloser function of the circuit breaker and the recloser. The lateral line is automatically restored by the recloser providing fuse saving scheme application. Nevertheless, for those laterals in front of the recloser, the failure rate for a temporary fault is taken into account with a

repair time r_s , since after each event, the fuse has to be replaced manually by system crews before restoration of the line. The above explanation can be summarized in Table 4.1.

Table 4.1 Failure rate and repair time of SAIFI and SAIDI calculation

Line Type	Fault type	Applied Failure rate	Applied Repair time
Main	Permanent	λ_{p-n}	r_p
	Temporary	-	-
Lateral in front of recloser	Permanent	λ_{p-n}	r_p
	Temporary	λ_{t-n}	r_s
Lateral behind recloser	Permanent	λ_{p-n}	r_p
	Temporary	-	-

4.2 Voltage Sag Index

Voltage Sag index is one of the power quality indices that provides a count of voltage sag events occurred in the system during system abnormal or fault conditions [17-18]. The event is counted if the voltage goes below a threshold or envelope. The index is called SARFI (System average RMS variation frequency index).

In evaluating service quality index at a particular location, the voltage sag index at a substation location is considered as a good representation of the voltage sag performance which will be experienced by customers supplied by the system [17]. Therefore, in this thesis, the voltage sag will be monitored at the substation bus. Only three phase fault event will be illustrated as it results in most severe voltage sag events for a solidly ground system.

There are two types of SARFI indices based on their voltage criteria which are SARFI-X and SARFI-Curve. SARFI-X is a count of event when the voltage goes down below a threshold value of X. For example, SARFI-70 considers voltage sags event that are below 0.7 per unit, or 70% of the reference voltage. On the other hand,

SARFI-Curve is a count of event if voltage and its duration lie within the voltage envelope curve. Accordingly, for SARFI-Curve, the operating time of protective devices has to be considered as its fault clearing time determines duration of the event.

Voltage envelope or voltage tolerance curve is a guideline or standard for examining voltage sag immunity of equipment. The equipment is capable of riding through the voltage sag events if the sag magnitude and its associated duration are outside the voltage envelope. The two most recognized curves are the ITIC curve [34] and the SEMI F47 curve [35] which are shown in Figure 4.1. The ITIC curve is generally applied for examining typical equipment ability to ride through voltage sag conditions. The SEMI F47 is a developed curve for semiconductor industry.

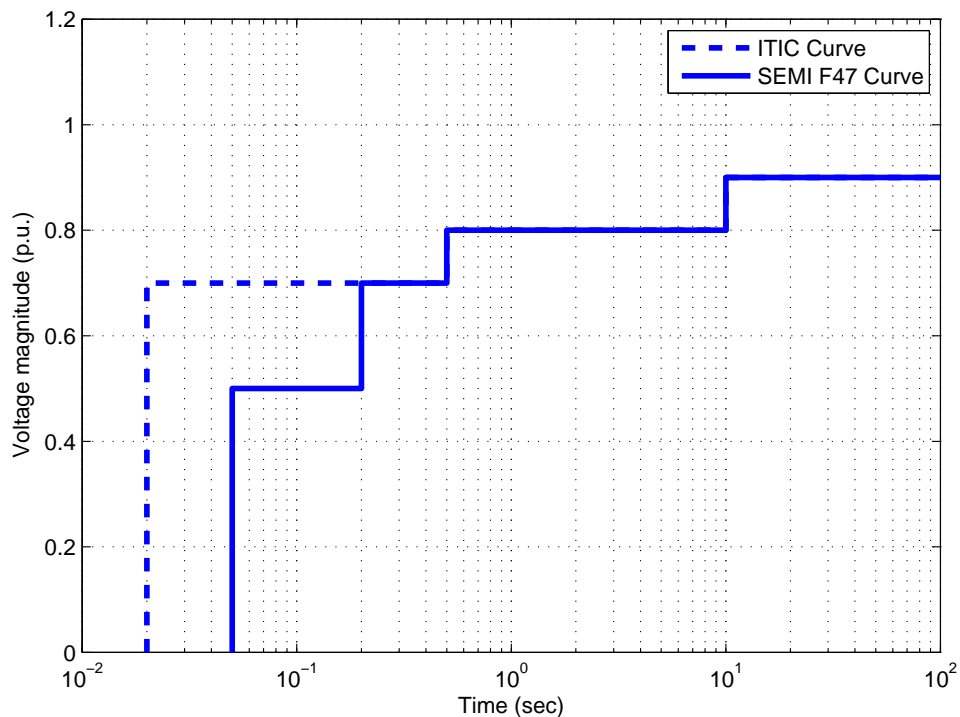


Figure 4.1 ITIC and SEMI F47 voltage envelope curve

From the figure, it can be seen that SEMI F47 curve lies under ITIC curve. As a result, the equipment that meets the SEMI F47 curve requirement will have higher

probability of riding through voltage sag events than that of ITIC curve. In other word, when counting for voltage sag events, SARFI-SEMI F47 will be less than SARFI-ITIC index.

SARFI-X is calculated using critical distance method [18, 36]. The critical distance for SARFI-X is a distance from substation by which when fault is occurred, the voltage will go down below voltage X threshold. The method can be explained using Figure 4.2.

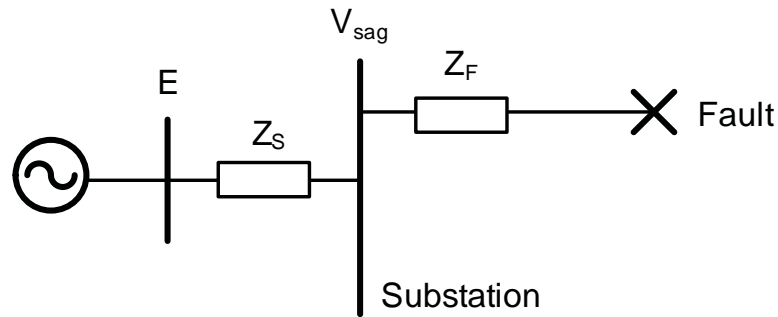


Figure 4.2 Model for voltage sag calculation

From the figure, the voltage sag (V_{sag}) at a substation in per unit (p.u.), neglecting pre-fault current, can be written as follows.

$$V_{sag} = \frac{Z_F}{Z_F + Z_S} \quad (4.5)$$

Where Z_F is the impedance between substation and the fault, Z_S is the system source impedance. By having $Z_F = z \times l$ with z is the line impedance per unit length and l is the distance from the substation to the fault, (4.5) can be written as

$$V_{sag} = \frac{z l}{z l + Z_S} \quad (4.6)$$

At this point the critical distance, l_{crit-X} and critical impedance Z_{crit-X} are introduced by rearranging (4.6). The critical distance and impedance for a voltage sag threshold X can be obtained from the following equations.

$$L_{crit-X} = \frac{Z_S}{z} \times \frac{X}{1-X} \quad (4.7)$$

$$Z_{crit-X} = z \times L_{crit-X} \quad (4.8)$$

Nevertheless, the above express is neglected the angle between real and imaginary part of line impedance. It applies only the absolute value of the impedance z . In [18], it is shown that the error occurred will be significant if the impedance angle is larger than 30° . It is also proposed that an exact expression can be calculated according to the following equation.

$$L_{crit-X} = \frac{Z_S}{z} \times \frac{X}{1-X} \left[\frac{X \cos \alpha + \sqrt{1 - X^2 \sin^2 \alpha}}{X + 1} \right] \quad (4.9)$$

Where

$$\alpha = \arctan\left(\frac{X_S}{R_S}\right) - \arctan\left(\frac{x}{r}\right) \quad (4.10)$$

and $Z_S = |R_S + jX_S|$, $z = |r + jx|$.

Another view of critical distance is an exposed area to the fault that causes an event of voltage sag under X . Therefore, by multiplying the critical distance with the line failure rate or fault occurrence rate information, the frequency of the event for voltage sag threshold X can be easily obtained according to the below equation.

$$\text{SARFI-X} = L_{crit-X} \times (\lambda_{p-n} + \lambda_{t-n}) \quad (4.11)$$

Nevertheless, when a DG is presented in the system, the derivation of a simplified equation as in the case of a typical distribution system is not possible. However, applying the same concept of critical distance and exposed area, the approximation search method can be developed for the calculation of SARFI-X index in a presence of DG. The procedure can be explained in the following steps.

Step 0: The distribution line is sectionalized into small sections.

Step 1: A single event occurred in the sectional line is considered as a representative for every point on the line. Each small section is approximately considered as a single node.

Step 2: From Step 1, a fault calculation is applied to each small section of the line to search for the section which results in a specified voltage sag, starting from the substation into the feeder.

Step 3: From Step 2, the approximated critical distance can be obtained.

Step 4: Multiplying the obtained critical distance with line failure rate.

The thesis proposes an approximation search method in addition to the critical distance method in evaluating Voltage sag indices.

In addition, this method can be extended for the calculation on SARFI-Curve by including fault clearing time of primary protective device. By applying fault in every line section, the obtained voltage sag magnitude and its associated duration of occurrences can be recorded. These two values can then be evaluated using the voltage envelope curves in Figure 4.1. Then, the frequency of occurrence for each individual point is obtained by multiplying with the failure rate of the line. The above explanation for SARFI calculation can be summarized in Table 4.2. The example of the above method is illustrated in the next subsection

Table 4.2 Failure rate and protective device consideration for the calculation of SARFI-X and SARFI-Curve

Line Type	Fault type	Applied Failure rate	Primary protective device
Main in front of recloser	Permanent	λ_{p-n}	Circuit breaker
	Temporary	λ_{t-n}	Circuit breaker
Main behind recloser	Permanent	λ_{p-n}	Recloser (Slow)
	Temporary	λ_{t-n}	Recloser (Fast)
Lateral in front of recloser	Permanent	λ_{p-n}	Fuse
	Temporary	λ_{t-n}	Fuse
Lateral behind recloser	Permanent	λ_{p-n}	Fuse
	Temporary	λ_{t-n}	Recloser (Fast)

4.3 Service Quality Evaluation Example

This section provides an example of the application of the method presented in the previous section to evaluate system service quality. The method will be applied to the Modified RBTS Bus 2 system (Appendix A) using reliability data shown in Appendix D).

First, system reliability, i.e. SAIFI and SAIDI is evaluated for Feeder 3 presented in Figure 4.3. In the figure, the number below the load point (LP) indicates number of customers. The circuit breaker is installed at the substation. At the beginning of each lateral, a fuse is applied. A mid-line recloser is located at point B providing fuse saving scheme application for the lateral lines serving LP 13-15 (See Section 3.3).

From the above information, the reliability indices are calculated for each load point using (4.3) – (4.4). The obtained results are presented in Table 4.3. Then, SAIFI and SAIDI are determined by applying (4.1) – (4.2) and are shown in Table 4.4.

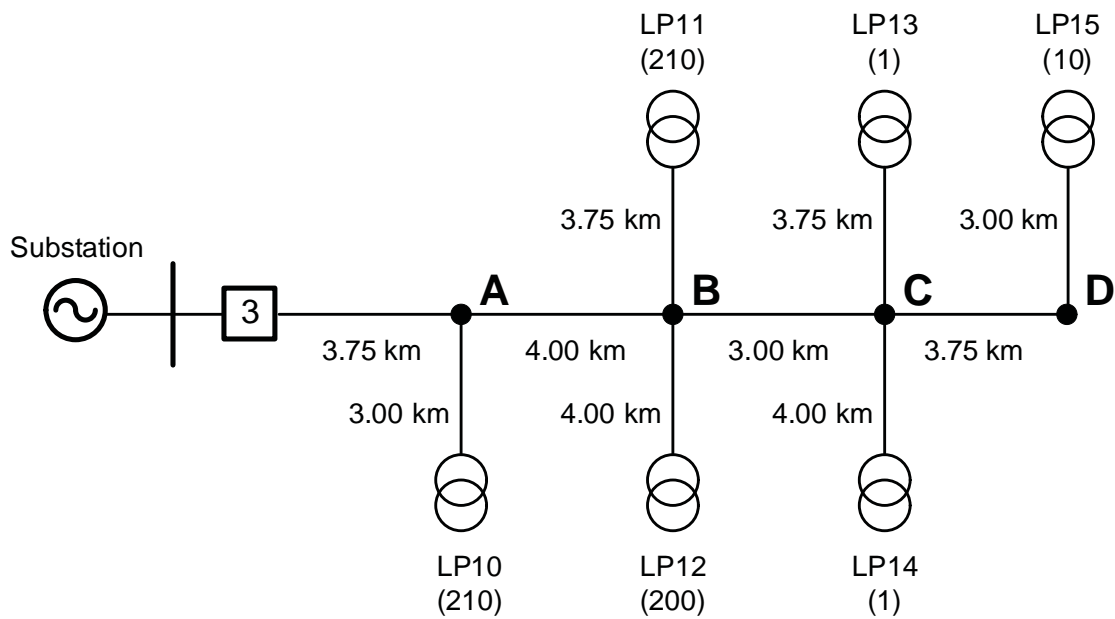


Figure 4.3 Modified RBTS Bus 2 – Feeder 3

Table 4.3 Reliability Indices at each load point of Feeder 3

LP	λ (times/year)			r (minute)		
	λ_{p-i}	λ_{t-i}	λ_i	r_p	r_s	r_i
LP10	0.4945	0.1800	0.6745	480.00	120.00	383.93
LP11	0.5290	0.2250	0.7540	480.00	120.00	372.57
LP12	0.5405	0.2400	0.7805	480.00	120.00	369.30
LP13	0.6670	0.0000	0.6670	480.00	120.00	480.00
LP14	0.6785	0.0000	0.6785	480.00	120.00	480.00
LP15	0.8050	0.0000	0.8050	480.00	120.00	480.00

Next, Voltage Sag indices, i.e. SARFI-X and SARFI-Curve, will be evaluated. Firstly, SARFI-X of the test system will be determined using the critical distance method, i.e. (4.7) – (4.11). A simple equation (4.7) and exact equation (4.9) for critical distance are both applied. Then, SARFI-X index is also evaluated using the

presented approximation search method. In this example, the distribution line is sectionalized to 50 meters each. The results are shown and compared in Table 4.5.

Table 4.4 SAIFI and SAIDI calculation of Feeder 3

LP	Number of customer (N_i)	$\lambda_i N_i$	$\lambda_i r_i N_i$
LP10	210	141.6450	54381.60
LP11	210	158.3400	58993.20
LP12	200	156.1000	57648.00
LP13	1	0.6670	320.16
LP14	1	0.6785	325.68
LP15	10	8.0500	3864.00
Total	632	465.4805	175532.64
SAIFI (times/year)			0.7365
SAIDI (minute)			277.74

Table 4.5 SARFI-X on Feeder 3

Voltage sag (p.u.)	SARFI-X (times/year)		
	Simple Equation	Exact Equation	Search Method
0.9	3.8160	3.8160	3.8107
0.8	3.8160	3.8160	3.8107
0.7	2.6078	2.1941	2.1576
0.6	1.1553	1.0820	1.0674
0.5	0.6776	0.6238	0.6196
0.4	0.3678	0.3520	0.3519
0.3	0.2364	0.2288	0.2284
0.2	0.1379	0.1349	0.1346
0.1	0.0613	0.0606	0.0604

From the Table, it can be seen that the results obtained from the simple equations are significantly different if it is compared to the results from exact equations. The error is high because of the characteristic of distribution system where the line impedance angle is generally large. Nevertheless, the results obtained from the approximation search method are quite similar to those of exact equations, i.e. more accurate than a simple equation. As a result, this method will further utilize for the analysis of SARFI-Curve and the DG impact on system Service quality index. Table 4.6 presents SARFI-X from events in all feeders using the approximate search method.

Table 4.6 SARFI-X based on approximation method

Voltage sag (p.u.)	SARFI-X (times/year)
0.9	13.8405
0.8	13.7265
0.7	8.6841
0.6	4.8039
0.5	2.6332
0.4	1.4076
0.3	0.9136
0.2	0.5384
0.1	0.2416

In calculating SARFI-Curve, both frequency and operating time of protective device are considered according to Table 4.2. SARFI-Curve, ITIC and SEMI F47 of the Modified RBTS Bus 2 are calculated using the approximation method as shown in Table 4.7.

From the table, it can be seen SARFI-ITIC is greater than SARFI-SEMI F47. This can be expected because the ITIC curve is more stringent than that of SEMI F47 curve as illustrated in Figure 4.1. This also implies that there is a higher probability of

riding through the voltage sag events if the equipment can meet the requirement of SEMI F47 standard.

Table 4.7 SARFI-Curve of Modified RBTS Bus 2 from approximation method

Curve	SARFI-Curve (times/year)
SEMI F47	3.0257
ITIC	6.7519

In [17], it is stated that SARFI-70 is usually almost the same as SARFI-ITIC because the voltage sag event is generally shorter than 0.5s. As a result, for simplicity, both indices may be used interchangeably. The SARFI-70 is more convenient for calculation because it only considers voltage magnitude information. This statement is also in line with the results from the Modified RBTS Bus 2.

4.4 DG Impact on Distribution System Service Quality

DG Impact on distribution system service quality has been investigated in many literatures. In [2], the case is classified into two situations, i.e. islanding condition is either allowed or not for the DG to continue supplying the load. If the islanding condition is allowed, it is shown that outage time or SAIDI can be reduced, since after an appropriate switching, the demand can be supplied from the DG instead of waiting for repairing. However, SAIFI remains unchanged since if a fault occurs, protective devices have to operate to clear the fault, thereby resulting in an interruption. In case of the islanding condition is not allowed, the reliability of the system is evaluated based on availability of intermittent resources such as wind and solar.

The above statement is also in line with the study in [37] that shows the improvement in SAIDI in the presence of DG while SAIFI remains unchanged. Another study [38] evaluates reliability of distribution system with wind energy

distributed generation for islanded mode of operation. It also concludes that SAIDI can be improved as a number of wind generation increases.

It is widely understood that the voltage sag situation is better in the system having higher fault levels. In [18], the impact of DG on voltage sag in the system is analyzed. It is illustrated that as presence of DG in the system tends to increase system fault level, the DG thus provides a benefit to an improvement on voltage sag indices. Figure 4.4 demonstrates voltage sag magnitude versus fault location based on several system fault level using (4.6).

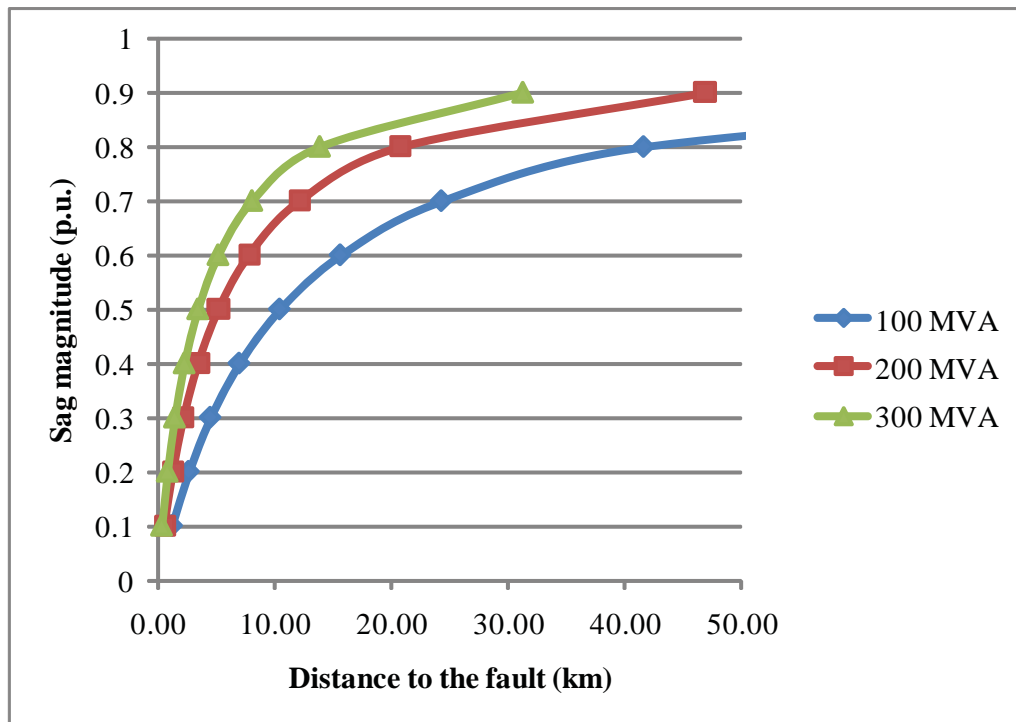


Figure 4.4 Voltage sag magnitude as a function of distance to fault at different system fault level

Nevertheless, few studies have been made on system reliability for a normal condition where islanding operation is not allowed. Moreover, as reliability indices are strongly related to protection system, the impact of DG on the protection coordination can thus affect the system reliability in a negative manner. Accordingly, this thesis will propose a method to evaluate system reliability in the presence of DG

during normal operation. The thesis also introduces a newly developed index to measure the impact of DG on protection coordination, which will be presented in Section 6.3. In addition, this thesis also proposes a methodology to evaluate the voltage sag indices both SARFI-X and SARFI-Curve, in presence of a DG, whereas simulation results are provided in Section 7.3.

Consequently, this subsection presents the impact of a DG on the system. The impact of a DG on system voltage sag is also described. The content in this subsection will help understand the proposed methodology of system service quality evaluation and the index for measuring protection mis-coordination.

4.4.1 DG Impact on System Reliability Index

Impact of DG on protection system coordination is investigated in Section 3.4. A method for determining maximum allowable DG capacity which did not result in protection mis-coordination was proposed. It can be concluded that a DG with capacity less than the maximum allowable will not result in degradation of system reliability or implies that SAIFI and SAIDI remains unaffected.

However, if a capacity of a DG is larger than the maximum allowable, it is likely to create protection mis-coordination. Therefore, it is expected to have an impact on SAIFI and SAIDI. In the same way of protection mis-coordination analysis, the impact on System Reliability occurs from three main causes, i.e. back-feed fault current, fuse saving scheme application and fuse-fuse coordination. Detailed analyses of these three causes are presented below.

The first problem is the back-feed fault current from a DG which can cause mis-operation of the mid-line recloser. The impact can be analyzed using Figure 4.5.

Considering Fault 1, the back-feed fault current of a large DG capacity will cause the mid-line recloser to operate with its fast curve. Nevertheless, since it is on the main feeder and if it is a permanent, the interruption occurs to all the load points in the feeder. As a result, it can be concluded that in the case of fault on the main

feeder, the presence of DG has no impact on system reliability for both frequency and duration of the interruption.

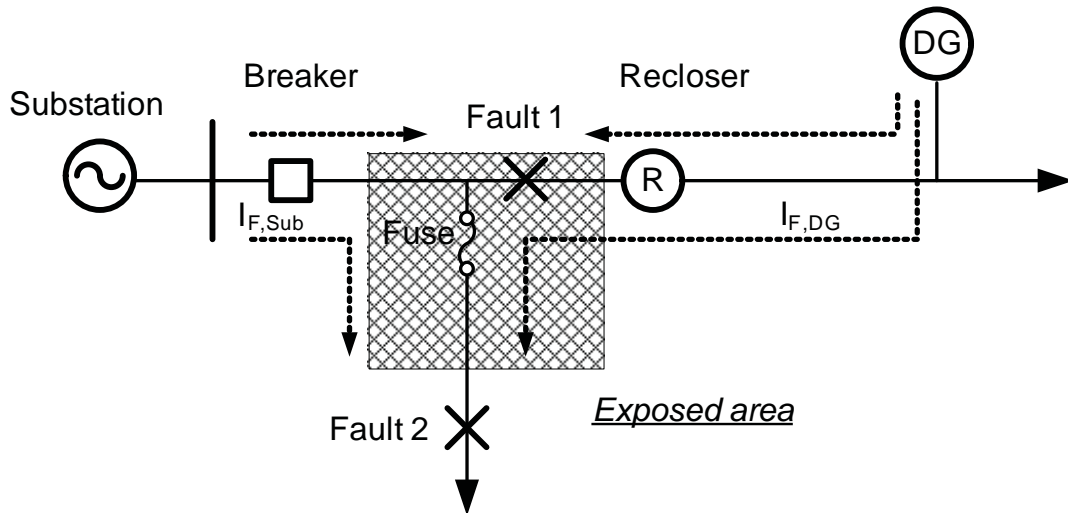


Figure 4.5 Back-feed problem illustration as a result of DG in the system

On the other hand, in case of Fault 2, the fuse will operate to clear the fault and result in an outage on the later line. However, the back-feed fault current will cause unnecessary interruption to all the load point behind the recloser. In the worst case, the recloser may not be able to auto-reclose the portion of the circuit back to the grid because of a large difference between the voltage and frequency on both sides. Together with a trip of DG unit initiated from the anti-islanding protection, a long interruption will be resulted to the load point behind the recloser. This situation is also likely to occur for a temporary fault at Fault 1. Therefore, for both permanent and temporary faults on the lateral in front of the mid-line recloser and the temporary fault on the main feeder, the presence of a DG can have a negative impact on both SAIFI and SAIDI.

Nevertheless, as the distance from the DG goes up, the back-feed fault current will decrease. Consequently, not all the fault event in the lateral will result in a negative impact on system reliability. At this point, the same concept of critical distance or exposed area which is shown in the shaded area of the Figure 4.5 can be applied. This area is named as Protection Mis-coordination Area (PMA), which is the

area of the fault resulting in protection mis-coordination. From this concept, if PMA is known, the frequency of protection mis-coordination can be determined in the same way as (4.11).

However, if the anti-islanding protection of DG can perform perfectly and is well coordinated with the auto-reclose function of recloser, the circuit can always be restored automatically from the interruption. As a result, there will be no PMA and SAIFI and SAIDI remain unchanged.

Regarding the second cause as mentioned earlier, it is related to the fuse saving scheme application. The explanation of the situation in the same way as the back-feed fault current problem is described by using Figure 4.6.

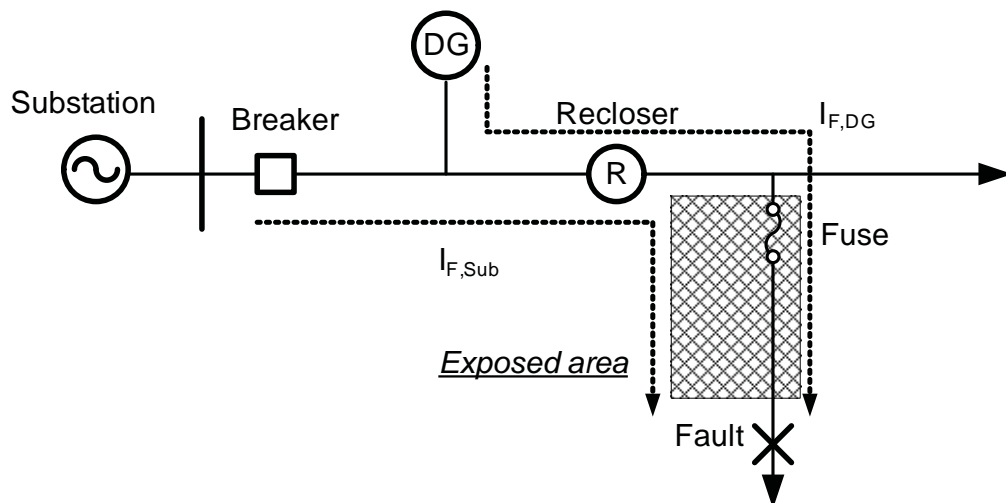


Figure 4.6 Fuse saving scheme problem illustration as a result of DG in the system

From the figure, a large DG unit can cause failure to the fuse saving scheme application by increasing the fault current passing through the fuse to exceed the designed limit. As a result, a temporary fault on the lateral can result in a long interruption. This is expected to increase the value of SAIDI. The same idea of PMA can also be applied in this situation. At some distance from the DG unit, the fault current will drop below the designed limit and the fuse saving scheme will work

properly again. Similarly, with determined PMA, the frequency of the failure to fuse saving scheme can be calculated.

In addition, it should be noticed that the PMA in front of the mid-line recloser is related to the protection mis-coordination due to back-feed fault currents, while the PMA behind the mid-line recloser is the area that the fuse saving scheme problem is occurred.

Lastly, regarding fuse-fuse coordination, the same analysis of fuse saving scheme can be applied. Nevertheless, the PMA of fuse-fuse coordination can occur in both laterals in front of and behind the mid-line recloser.

From all above analyses, the PMA for system reliability evaluation can be summarized below.

Table 4.8 Summary of criteria on PMA calculation

PMA Type	Possible Location	Applied Failure rate	Affected Customer
Back-feed	Main feeder	λ_{r-n}	ΣN_i behind recloser
	Lateral in front of recloser	$\lambda_{r-n} + \lambda_{p-n}$	ΣN_i behind recloser
Fuse-save	Lateral behind recloser	λ_{r-n}	ΣN_i attached to lateral n
Fuse-fuse ¹	All sub-laterals	$\lambda_{r-n} + \lambda_{p-n}$	ΣN_i attached to lateral excluding those in sub-lateral n

4.4.2 DG Impact on System Voltage Sag Index

As previously mentioned, an increase in system fault level due to a DG in the system can provide a benefit to system performance in terms of voltage sag. By considering (4.7), when system fault level is increased, the system source impedance Z_S as shown in Figure 4.2 will decrease. Based on (4.7), the critical distance for any

voltage sag magnitude will also be reduced. Consequently, the frequency of voltage sag event or SARFI-X is reduced based on (4.11). Therefore, the presence of DG in the system can provide benefit to the system by reducing the number of occurrence of voltage sag event.

As for SARFI-Curve, the same idea of increased fault level can also be applied. The frequency of voltage sag event is reduced in the presence of a DG. In general, the fault contribution from a DG will increase the magnitude of the fault current which passes through protective devices. As a result, the devices operate faster. This will help reduce the duration time of voltage sag event. Thus, the DG is beneficial to the SARFI-Curve index in both increasing voltage sag magnitude and reducing its time duration. This can be illustrated by using Figure 4.7.

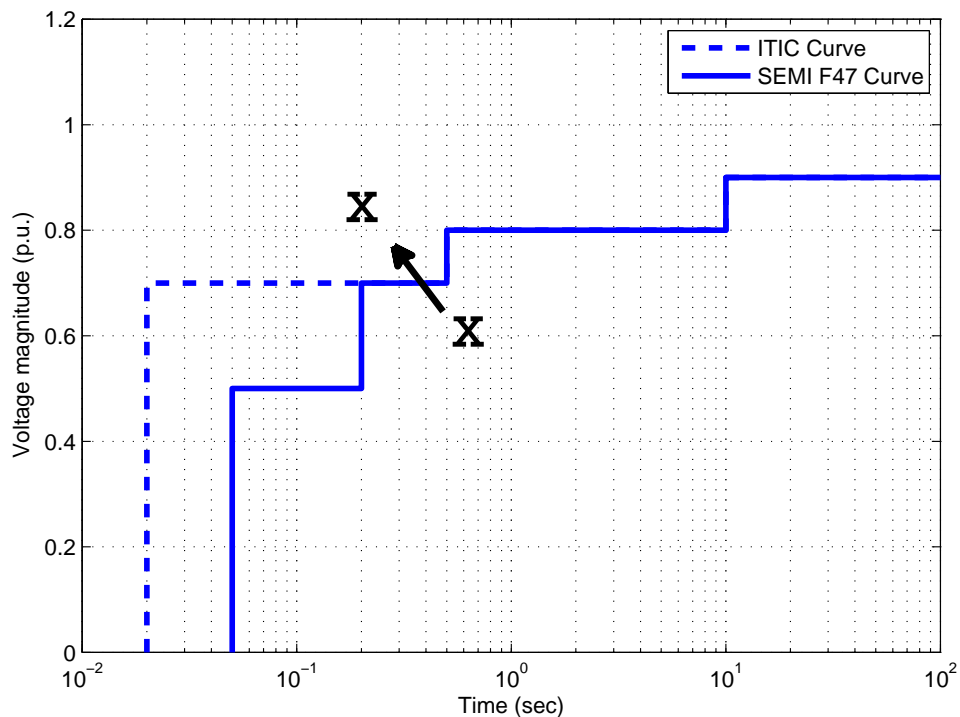


Figure 4.7 Improvement on SARFI-Curve due to a presence of DG in the system

4.5 Summary

Service quality of the system can be measured using reliability and voltage sag indices. Commonly used reliability indices are SAIFI and SAIDI which describe system average frequency and duration for sustained interruptions. The input for calculation on reliability indices are failure rate and repair time of electrical equipment.

There are two types of voltage sag indices, i.e. SARFI-X and SARFI-Curve. SARFI-X describes a number of events for voltage sag X occurred in the system. It can be calculated using a critical distance method, which is determined from a simple or exact equation. In addition, this thesis proposes an approximation search method which provides comparable results to those from the exact equation. SARFI-Curve is the evaluation of an event for both sag magnitude and duration using voltage envelope by which two most recognized are ITIC and SEMI F47. The index can be obtained from the proposed approximation search method by including the operating time of a primary protective device.

An example of service quality evaluation is illustrated on the modified RBTS Bus 2 Section 4.3.

DG impact on system service quality is analyzed in two situations. Firstly, a larger DG capacity than the maximum allowable will result in system reliability degradation since it creates protection mis-coordination. It is proposed that the area of which when fault occurs will create the problem is called Protection Mis-coordination Area (PMA). There are three types of PMA based on resulted protection mis-coordination, i.e. for back-feed current, fuse saving scheme and fuse-fuse coordination problem. Secondly, a DG capacity within the maximum allowable will provide benefit of reduction of number of voltage sag events since it increases system fault level. In addition, it is advantageous to SARFI-Curve since the operating time of protective device will be faster for a higher fault current.

CHAPTER V

POWER LOSS ANALYSIS

In this chapter, the impact of DG output power on distribution feeder loss is investigated. It is assumed that the objective of the system operator is to manage appropriate DG output such that feeder loss will not be increased. Based on this condition, the maximum allowable DG output power will be searched for. The first subsection provides review of power loss calculation. In the second subsection, the maximum allowable DG output power at peak load is presented. The impact of DG on the feeder loss, taking into account demand variation is illustrated in the following subsection. Then, an appropriate DG output power is determined at other different load levels. Finally, the chapter ends with a review of loss allocation technique called Branch Current Decomposition Loss Allocation (BCDLA), which will be further developed to estimate appropriate DG output in this thesis.

5.1 Power Loss Calculation

It is widely proven that the power loss depends on the current magnitude flowing through impedance of the conductor. The greater current magnitude and line impedance, the more system loss will be. Power loss can be determined from the following equation.

$$L_{ij} = \Re \left[(V_i - V_j) I_{ij}^* \right] \quad (5.1)$$

There are several methods to minimize power loss, e.g. power factor improvement, network reconfiguration. Recently, DG can be another alternative way for power loss reduction.

Since power loss is resulted from system demand, therefore it may be allocated among system customers. This process is called loss allocation. At present, several methods for loss allocation have been reported, e.g. [39-41]. When DG is presented, it can either reduce or increase system depending on its output power and

system demand. To account for this, loss allocation must be done for both consumers and suppliers, i.e. load and DG respectively.

5.2 Appropriate DG Output with Loss Consideration

It is widely known that DG can reduce system loss up to a certain level of its output power [2]. The loss will be increased if the DG generates power more than that of output level, which will be considered as appropriate DG output power. In this section, appropriate DG output power will be determined at a specific load condition, i.e. at maximum load level. This problem can be considered as an optimization problem subjected to an appropriate set of constraints [33].

In solving an optimization problem, there are several methods to search for the optimal solution. In this thesis, a direct search method is applied for searching the optimal or appropriate DG output solution. This can be achieved since the solution domain of the problem is not very large.

The objective function is to determine the appropriate output power of a DG, which can be written as

$$\text{Max}(P_{DG}) \quad (5.2)$$

The condition for an appropriate DG output power which will not increase loss of the feeder can be defined as

$$L - L_{base} \leq 0 \quad (5.3)$$

This thesis applies MATPOWER [42] as a tool for calculating loss from power flow solution, from which an appropriate DG output power for a specified location can be searched directly.

For illustration, the above method will be applied to Feeder 1 of the test system, as shown in Figure 5.1, of which the capital letter indicates possible DG locations, based on an assumption that the DG will be connected only to the main

feeder. The obtained results of appropriate output power of the DG at each location are presented in Table 5.1. Similar results can be expected for other feeders. Therefore only the results from Feeder 1 will be presented hereafter.

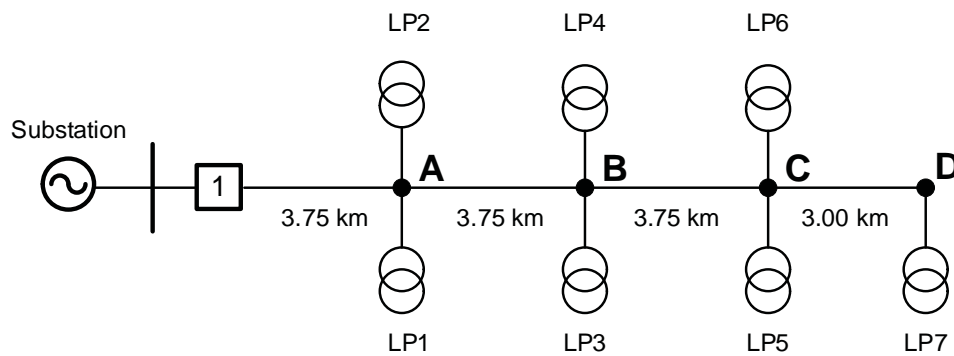


Figure 5.1 Modified RBTS Bus 2 Feeder 1

Table 5.1 Appropriate DG output power at peak load condition

DG Location	Output power of a DG (MW)
A	12.47
B	10.54
C	8.63
D	7.10

According to the results in Table 5.1, it is implied that the appropriate DG output power at location B is equal to 10.54 MW. If the DG output level is greater than this value, the feeder loss will be increased. In contrast, if DG output level is lower than the calculated value, the DG will help decrease feeder loss. Nevertheless, it should be noted at this point that this result is determined only from the maximum load condition.

5.3 Impact of System Demand on Feeder Loss

In actual operation, system load varies along the time of day. To consider the

feeder loss impact from load variation, the amount of load at each point is assumed to be varied at the same proportion. The DG output power at point A of 12.47 MW, as shown in Table 5.1, is used as an example to analyze the feeder loss with load variation from 10%-100% of the peak demand. The impact of the feeder loss in case of having no DG connected to the system is also compared and shown in Figure 5.2.

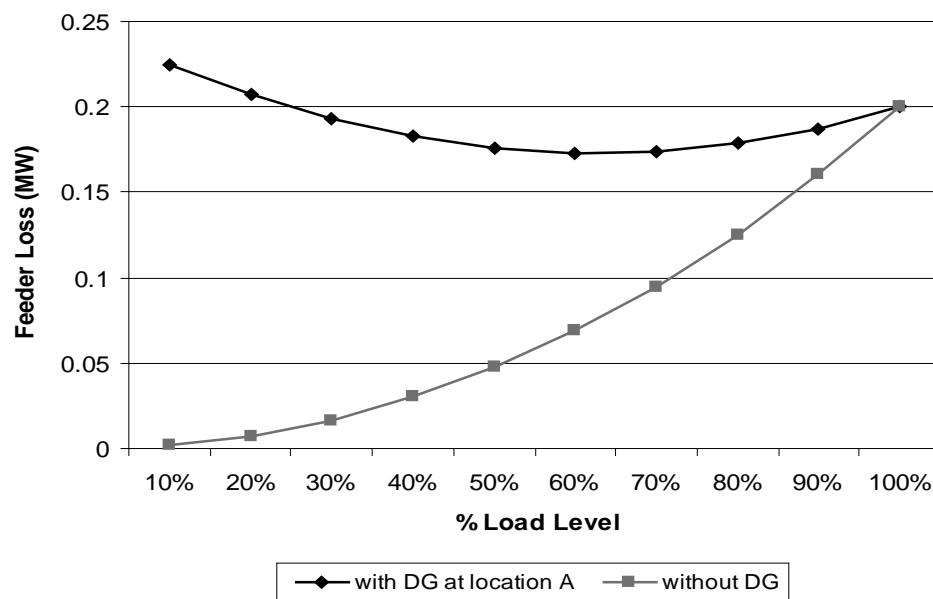


Figure 5.2 Feeder loss with and without the presence of DG at location A

It can be clearly seen from the figure that at the peak demand, 100% load level, feeder loss from both cases are the same, i.e. the presence of DG does not increase the feeder loss compared to the base case as defined by (5.3). It is also clearly seen that in case of having no DG, the feeder loss varies according to load level. However, with the presence of the DG with the fixed output of 12.47 MW, the feeder loss is higher for all other load levels, compared to the base case.

This implies that the obtained appropriate DG output power at peak demand is too large and not suitable for the lower system demand which actually occurs most of the time. As a result, the presence of such a DG can considerably increase the feeder loss from the base case if not properly operated. This result emphasizes the importance of having an appropriate output power from a DG, taking into account

system loss. Therefore, this thesis will propose the methodology for establishing an appropriate DG output power profile which will not result in power loss increase. Besides, the thesis develops an approximation method to reduce computational time and can be applied for a near real-time application for controlling on DG output power.

5.4 Appropriate DG Output Power at Different Load Levels

It has been previously shown that the appropriate DG output power determined at the peak demand may not be suitable for other load conditions. Consequently, it may result in feeder loss increase. To take into account the impact of load variation, the appropriate DG output power is recalculated for different load levels, i.e. 20%, 40%, 60% and 80% of the peak load, using the direct search method as presented in Section 5.2. The obtained results are presented in Table 5.2 and Figure 5.3.

Table 5.2 Appropriate DG output power at different load levels

Load level	Appropriate DG output power (MW)			
	Location A	Location B	Location C	Location D
20%	2.40	2.04	1.68	1.39
40%	4.84	4.11	3.39	2.80
60%	7.33	6.22	5.11	4.22
80%	9.87	8.36	6.86	5.65
100%	12.47	10.54	8.63	7.10

The results from Table 5.2 show that the appropriate DG output power is different at each load level. The DG output power tends to be decreased with the decrease of load. In addition, Figure 5.3 illustrates that the appropriate DG output power is approximately varied with load level in a linear trend.

Based on the above analysis, it is clearly seen that the appropriate DG output

should be determined according to system demand in order to effectively manage the system loss. Such the DG output power can be repeatedly calculated using the calculation process as presented in Section 5.2 for each time of the day. However, it is widely understood that the system demand characteristics depends on its customer load profiles. Therefore, the appropriated DG output power also depends on customer load profiles. If the relationship between the customer load profile at each load point and the appropriate DG output power can be formulated taking into account loss constraint, the allowable DG output power could be directly determined.

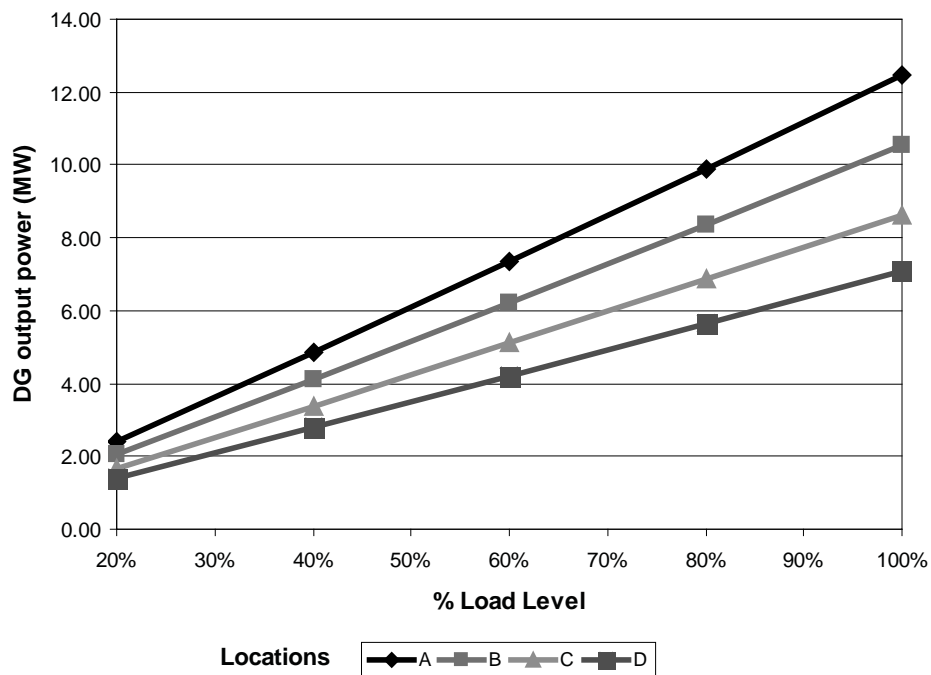


Figure 5.3 Appropriate DG output power at different load levels

To formulate the relationship between the system loss and the variations of supply and demand in the system, the BCDLA [20] is further developed in this thesis, which will be presented in Section 6.4. The review of BCDLA method will be presented in the next subsection.

5.5 BCDLA Loss Allocation Method

The BCDLA is one of the loss allocation methods suitable for distribution system with radial configuration [20]. The advantage of the method is that it provides the meaningful loss allocation factor and is applicable to our problem. First, consider a simple system as shown in Figure. 5.4.

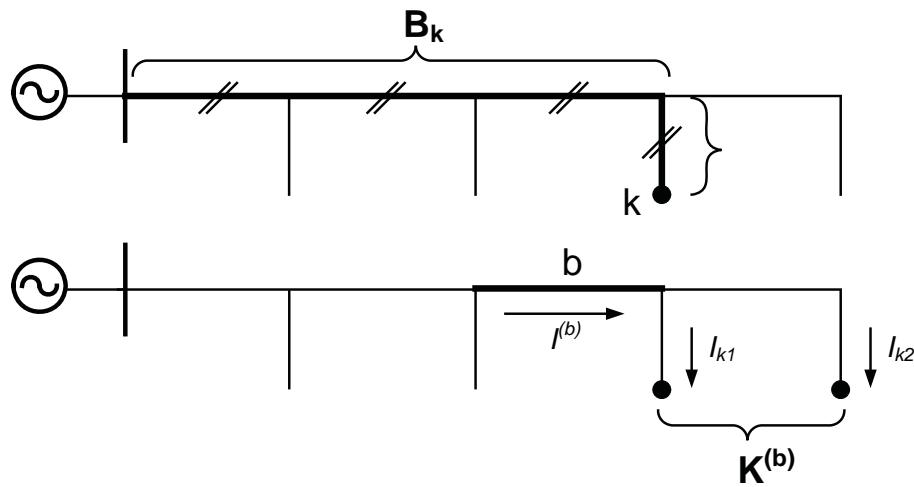


Figure 5.4 Illustration for BCDLA loss allocation method

From Figure 5.4, the current flowing through branch b is

$$\bar{I}^{(b)} = \alpha^{(b)} + j\beta^{(b)} \quad (5.4)$$

The current supplied to node k is

$$\bar{I}_k = \alpha_k + j\beta_k \quad (5.5)$$

which can be expressed in terms of the net active and reactive output power at node k as

$$\bar{I}_k = \alpha_k + j\beta_k = \frac{\bar{S}_k^*}{\bar{V}_k^*} = \frac{P_k - jQ_k}{\bar{V}_k^*} \quad (5.6)$$

Therefore, the injected current to node k can be determined after obtaining voltage V_k from power flow solution.

The branch loss can then be expressed as

$$\begin{aligned}
 L^{(b)} &= R^{(b)} |I^{(b)}|^2 \\
 &= R^{(b)} \left[(\alpha^{(b)})^2 + (\beta^{(b)})^2 \right] \\
 &= (R^{(b)} \alpha^{(b)}) \alpha^{(b)} + (R^{(b)} \beta^{(b)}) \beta^{(b)} \\
 &= (R^{(b)} \alpha^{(b)}) \sum_{k \in \mathbf{K}^{(b)}} \alpha_k + (R^{(b)} \beta^{(b)}) \sum_{k \in \mathbf{K}^{(b)}} \beta_k
 \end{aligned} \tag{5.7}$$

From (5.7), the losses associated to branch b are assigned to the node k located in the path from branch b to the root as follows:

$$L_k^{(b)} = R^{(b)} \alpha^{(b)} \alpha_k + R^{(b)} \beta^{(b)} \beta_k \tag{5.8}$$

The total loss is then allocated for each node k by using the relationship

$$\begin{aligned}
 L_k &= \sum_{b=1}^{B_k} L_k^{(b)} \\
 &= \alpha_k \sum_{b \in \mathbf{B}_k} (R^{(b)} \alpha^{(b)}) + \beta_k \sum_{b \in \mathbf{B}_k} (R^{(b)} \beta^{(b)}) \\
 &= c_k \alpha_k + d_k \beta_k
 \end{aligned} \tag{5.9}$$

where the terms c_k and d_k can be seen as the real and imaginary components of a “virtual” voltage $W_k = c_k + jd_k$ at node k .

$$\begin{aligned}
W_k &= c_k + jd_k \\
&= \sum_{b \in B_k} (R^{(b)} \alpha^{(b)}) + j \sum_{b \in B_k} (R^{(b)} \beta^{(b)})
\end{aligned} \tag{5.10}$$

As previously mentioned, an advantage of BCDLA method is that the summation of L_k at every node k will result in the total system loss, i.e.

$$L_{total} = \sum L_k \tag{5.11}$$

According to (5.9) and (5.11), it can be seen that total system loss composes of two major components independently, i.e. from real and imaginary part of the current at each load or generation point.

5.6 Summary

Power loss is resulted from current flowing through impedance of the line. There are several methods for loss reduction, e.g. power factor improvement, network reconfiguration. More recently, DG is considered as another alternative.

In this thesis, appropriate DG output power is defined as the level that will not increase system power loss. It is generally determined at a specific load condition, i.e. peak load. However, at other load levels, it can increase power loss significantly. In addition, it is shown that as demand varies, appropriate DG output power also varies.

BCDLA is one loss allocation method for allocating power loss to all loads and generations in a distribution system. The main advantage that it provides a meaningful loss allocation factor as the summation is equal to power loss according to (5.11). The method will be further developed in Section 6.4 for determining appropriate DG output power taking into account of load variations.

CHAPTER VI

PROPOSED METHODOLOGY

As previously illustrated, the DG may present negative impact on the existing protection coordination, and may result in an increase of system loss at some light load condition. It has been shown in chapter 3 that too large DG can result in protection coordination failure. An increase in fault current can cause a failure of existing fuse saving scheme application. Additional fault current may exceed protective device interrupting rate. Also, if a DG unit is located behind the mid-line recloser, it can cause unnecessary operation of the recloser for fault upstream and results in outage for the customer behind recloser. Therefore, maximum allowable DG capacity should be determined in the first place. Otherwise, the connected DG can cause problem and decrease system reliability. The obtained results can also be used as a guideline for utility to investigate if the existing protection requires some modifications.

In addition to system reliability, maintaining power loss in the distribution system within an acceptable range is also essential. It has been shown in chapter 5 that too large output power from a DG can increase power loss. In order to manage the power loss, an appropriate DG output power should be determined. The obtained results can be applied for a dispatchable DG unit for loss management.

Accordingly, this chapter proposes a methodology for determining an allowable DG capacity with protection and loss consideration. In the first Section 6.1, the method for determining a maximum allowable DG capacity with protection consideration is proposed. Additionally, as protection system coordination limits the maximum allowable capacity of a DG, a method of protection adjustment to allow higher penetration of a DG will be developed and presented in Section 6.2. Then, in accordance with an impact of DG on system service quality, the methodology for evaluating System Service Quality indices in a presence of DG will be described in Section 6.3. Finally, the methods for determining an appropriate DG output power with loss and customer load profiles consideration are proposed in Section 6.4.

6.1 Maximum Allowable DG Capacity with Protection Coordination Consideration

In chapter 3, possible impact of a DG on the existing protection coordination of distribution system is analyzed. It can be seen that too large DG capacity may lead to protection coordination failure and reduce overall system reliability. In this section, this thesis proposes the methodology in determining maximum allowable DG capacity which will not cause failure to existing protection coordination.

The section starts with general assumption. Next, the problem formulation is described. Then, the procedure in determining maximum allowable DG capacity is illustrated. Finally, the application in the case that there is more than one DG connection is presented.

6.1.1 Assumption

The problem in determining maximum allowable DG capacity is mainly related to fault calculation or incremental fault in the system. The DG in this study is modeled according to Section 2.3, with limited capacity of 10 MW [10], which is applied as the upper limit for the solution. In addition, for simplicity the number of DG is limited to one per feeder.

6.1.2 Problem Formulation

The objective of this study is to identify the maximum allowable capacity of a DG which does not cause protection coordination failure. In addition, the proposed method also takes into account system operating conditions, i.e. the installed DG should not increase feeder loss or violate the required voltage level. Therefore, the problem is formulated as a minimization problem to obtain the maximum allowable capacity of a DG.

A. Objective function and constraints

The objective is to determine the maximum allowable capacity of a DG, which can be written as

$$\text{Max}(P_{DG}) = -\text{Min}(-P_{DG}) \quad (6.1)$$

The constraints are classified into three categories, i.e. system voltage, feeder loss, and protection coordination. The constraint equations can be presented below.

B. Voltage constraints

The voltage at each load point should be within an acceptable range, which is defined to be 0.95-1.05 p.u. in this paper. The conditions can be written as

$$V_i - 1.05 \leq 0, \quad \forall i \in B \quad (6.2)$$

$$0.95 - V_i \leq 0, \quad \forall i \in B \quad (6.3)$$

C. Loss constraints

In this paper, the DG capacity allowed to be connected to the feeder will not increase loss of the feeder. The condition can be defined as

$$L - L_{base} \leq 0 \quad (6.4)$$

D. Protection coordination constraints

Protection constraints are developed to cope with the coordination failure based on the investigation described in Section 3.4.

Referred to Case A.1, the coordination failure may occur if the lateral fuse perceives more fault current than the recloser does. In general the fuse saving scheme will be fail if the fault current is higher than a certain value. Therefore, the condition

for not losing coordination of the fuse saving scheme is to have the recloser fast curve operating time less than the minimum melting time of the fuse. This constraint is applied when the DG and fault location is as shown in Figure 3.8, which can be written as (6.5).

$$T_{Rf}(I_{F,Sub}) - MMT_F(I_{F,Sub} + I_{F,DG}) \leq 0 \quad (6.5)$$

In Case B.1, the problem is similar to that of Case A.1, however the recloser and fuse will perceive the same fault current. Therefore, to keep the fuse saving scheme coordinated, the constraint below is required.

$$T_{Rf}(I_{F,Sub} + I_{F,DG}) - MMT_F(I_{F,Sub} + I_{F,DG}) \leq 0 \quad (6.6)$$

For Case B.2, the concern is about the fuse interruption rating. Since the DG can lead to a higher fault current, the interrupting current should be taken into account. In this paper, the fuse interrupting capacity is chosen to be 10 kA, from which the constraint according to Figure 3.11 will be as shown in (6.7).

$$I_{Fuse} - 10,000 \leq 0 \quad (6.7)$$

It should be noted that (6.7) is also a constraint for all cases described in Section 3.4.

For Case A.2, the problem occurs due to the DG's fault current passing through recloser in the back flow direction. If the DG's fault current is sufficiently high due to its capacity and the recloser is a non-directional type, the recloser may operate with its fast curve before the fuse can clear the fault. This will cause unnecessary momentary interruption to all customers in the feeder behind the recloser. Therefore, fault contribution from the DG should not cause recloser to operate in the case of back flow direction. Thus, for the condition in Figure 3.9, the constraint can be written as (6.8).

$$I_R - I_{R, Pickup} \leq 0 \quad (6.8)$$

As for the last case of B.3, the DG located close to a substation can also interfere with the fuse saving scheme of the nearby feeder. This situation is similar to Case B.1 but only the DG is connected to the other feeder. Similar to the DG in front of a recloser, this DG can also increase fault currents to a nearby feeder perceived by recloser and fuse. As a result, the fuse saving scheme may be violated.

Therefore, for a connected DG in front of the recloser and a fault occurs at lateral behind the recloser of the other feeder, (6.6) must be considered.

Based on all the above analysis, the protection constraints to maintain the protection coordination can be summarized in Table 6.1.

Table 6.1 Summary of protection constraints

Case	DG position	Fault location	Equation
A.1	Behind recloser	Behind recloser	(6.5)
A.2	Behind recloser	In front of recloser	(6.8)
B.1	In front of recloser	Behind recloser	(6.6)
B.2	In front of recloser	In front of recloser	(6.7)
B.3	In front of recloser	Behind recloser (Nearby feeder)	(6.6)

For fuse-fuse coordination, the maximum designed fault current, $I_{Fuse-max}$ must be first specified from Table 3.1. Then, the fault current at the protecting fuse or Fuse 2 in Figure 3.13 is checked with the following constraints.

$$I_{Fuse} - I_{Fuse-max} \leq 0 \quad (6.9)$$

6.1.3 Maximum Allowable Capacity Determination Procedure

This section presents a proposed procedure to identify the maximum allowable capacity of the DG at each location along the distribution feeder subjected to the above mentioned constraints. The procedure is illustrated by Figure 6.1, and can be described below.

Step 0: Run a based case power flow of the existing system and store the results.

Step 1: Select DG connected at bus i and a defined fault location at bus j , then select a proper protection constraint according to Table 6.1 and (6.9) for fuse-fuse coordination checking.

Step 2: Apply a direct search method to the objective function in (6.1) and constraints defined from Step 1 to search for maximum allowable DG capacity at bus i with respect to a fault at bus j . Store the result.

Step 3: Repeat Step 1 – 2 by fixing the DG connected to bus i and change a defined fault location at bus j to every bus in the system.

Step 4: Based on the obtained results from Step 2 – 3, select the minimum value as the solution for the maximum allowable DG capacity connected at bus i .

Step 5: Repeat Step 1 – 4 for all possible DG locations.

6.1.4 More than One DG Connection Application

When dealing with more than one DG connection on the same substation, the above method and procedure can also be adapted to evaluate the maximum allowable DG capacity. However, the request for DG connection will be considered on the basis of first-come-first-serve. Therefore, every time there is a new DG connected to the system, the maximum allowable DG capacity for each location has to be re-evaluated.

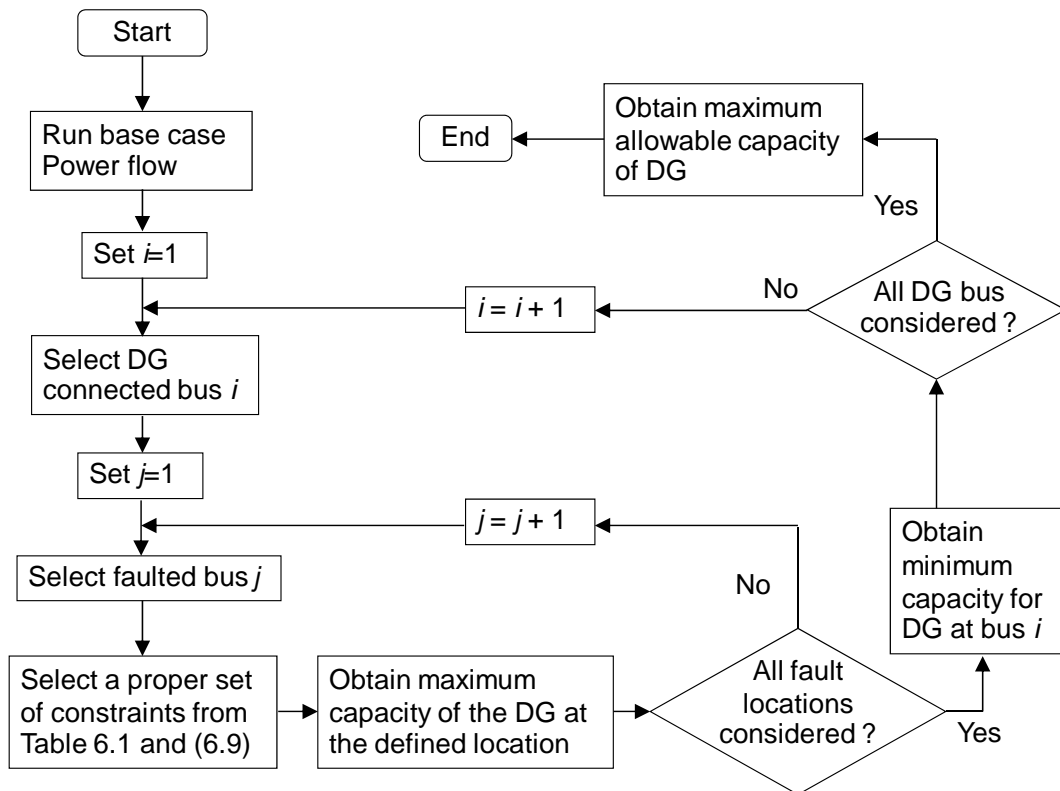


Figure 6.1 Procedure for determining maximum allowable capacity of one DG connection

The existing DG unit does introduce some additional concerns to the methodology. The installed DG unit has to be included in the base case prior to the calculation. In addition, when the distribution network already holds some capacity of DG, the total system loss and voltage is changed from that of the base case.

When DG is presented in the system with appropriate capacity, the total system loss tends to decrease. In fact, the existing DG units help decrease losses only in their feeder where the power flow is modified. Therefore, if the total system loss is considered in (6.4), the loss in other feeders can be greater than that of the base case. As a result, the maximum allowable DG capacity in other feeders can be larger. Nevertheless, if the existing DG unit goes offline, this larger DG unit will result in an increase in total system loss. Therefore, to consider for the worst case, it can be concluded that only loss in the feeder where a DG capacity will be determined should be considered in (6.4).

In contrast to protection coordination, the worst case is when all existing DG units in the system are online by which it will result in the highest fault level that can cause problems to the protection coordination. Therefore, protection coordination constraint remains unchanged.

Based on the above modifications, the proposed method can now be applied to determine the remaining maximum allowable DG capacity in the system where there is more than one DG connection. The procedure can be explained in the following diagram.

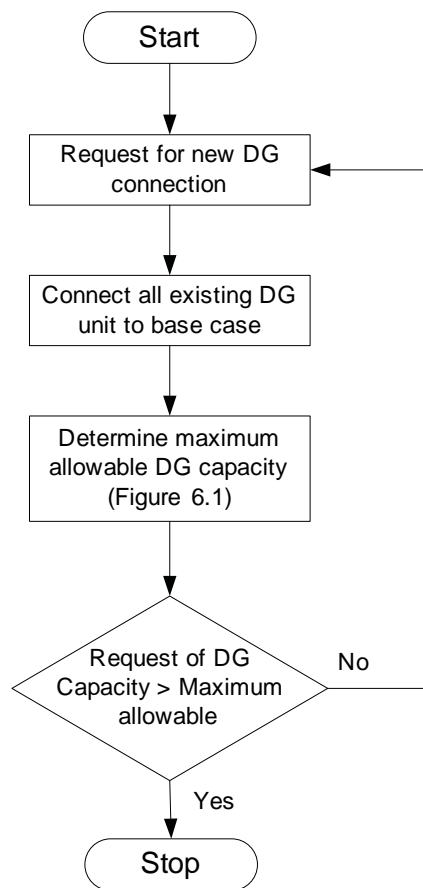


Figure 6.2 Procedure for determining maximum allowable capacity of more than one DG connection

6.2 Protection Adjustment Method for Higher Penetration of DG

In Section 6.1, the method for determining maximum allowable DG capacity taking into account protection system coordination is presented. In this section, a methodology of protection adjustment to allow larger DG capacity, i.e. increase the maximum allowable capacity obtained from the previous section, will be presented. The methods are consisted of protection resetting, application of directional recloser, and fuse replacing by recloser. The first method will help the system cope with a larger DG unit located behind recloser without any hardware change. The second method relieves the problem occurred from back-feed fault current of the DG, where as the final method will be mainly used for coping with high fault current for fuse saving scheme.

It is necessary to emphasize that the cause of protection failure due to the presence of DGs can be classified into two cases based on their locations, i.e.,

- DG in front of recloser – Impact on fuse saving scheme,
- DG behind recloser – Impact on fuse saving scheme and mis-operation of recloser due to back-feed fault current.

In the case that fault level exceeds interrupting rate of equipment, the only solution to the problem is to upgrade the effected devices. The same goes for fuse-fuse coordination by which the upstream fuse has to be upgraded. Therefore, they will not be brought up for discussion in this section.

6.2.1 Protective Device Resetting

It is shown by (6.8) that the maximum allowable capacity of a DG located behind a mid-line recloser is primarily limited by the pick-up current setting of the recloser. Hence, raising recloser pick-up current setting can help allow larger DG capacity. Nevertheless, existing protection coordination also needs to be reset accordingly. It should be reminded that the pick-up current resetting must not be

raised beyond equipment rating, e.g. line capacity by which this thesis will apply as the criteria when resetting protective devices.

With typical over-current protection coordination [25], three constraints are proposed for resetting protective devices. The first constraint is equipment rating. The setting of protective devices must cover an overload condition of the equipment. Therefore, the equipment rating is set as the limit for the pick-up current.

$$I_{pickup} \leq I_{spec} \quad (6.10)$$

where I_{pickup} is pick-up current setting and I_{spec} is a specified current of which the maximum is equipment rating.

Secondly, current setting of the downstream devices should be less than that of the upstream by some safety factor. This is to ensure a proper coordination between the two protective devices.

$$I_{pickup-down} \leq K \cdot I_{pickup-up} \quad (6.11)$$

Where $I_{pickup-up}$, $I_{pickup-down}$ is pick-up current setting of upstream and downstream devices, and K is a safety factor with a value of less than 1.

Finally, operating time of the downstream device must be faster than that of the upstream by an appropriate margin. The previous statement can be written in an equation form as

$$T_{up}(I_{down}) - T_{down}(I_{down}) \geq t_{margin} \quad (6.12)$$

where $T_{up}(I)$ and $T_{down}(I)$ is operating time of upstream and downstream device for fault current I , I_{down} is fault current magnitude at the location of downstream devices, and t_{margin} is a required operating time margin.

From all the above constraints, i.e. (6.10) – (6.12), the pick-up current setting of the recloser can be raised up. The maximum setting which can be raised depends on the setting of circuit breaker. In typical distribution substation, an incoming circuit breaker is normally installed as an upstream device of the feeder circuit breaker to provide a backup protection [25-26]. Consequently, if the pick-up current and time multiplier setting of the circuit breaker are to be adjusted, the coordination between these two circuit breakers must be checked using (6.12). Accordingly, the procedure for resetting the protective devices can then be developed and described below.

Step 0: Calculate fault current at circuit breaker and recloser location.

Step 1: Raise pick-up current setting of the circuit breaker to that of the feeder or of a specified capacity, i.e. (6.10).

Step 2: Determine operating time of incoming circuit breaker based on fault from Step 0.

Step 3: Adjust time multiplier of circuit breaker using (6.12).

Step 4: Raise pick-up setting of recloser using (6.11).

Step 5: Verify coordination between circuit breaker and recloser using (6.12). If not valid, reduce the value in Step 4.

Step 6: Verify coordination between recloser fast operating sequence and fuse MMT. If not valid, reduce the value in Step 4.

6.2.2 Directional Recloser Application

Another protection adjustment is to replace the existing mid-line recloser with a directional type which allows the recloser to distinguish between fault in forward and backward directions. This capability can help utility solve the problem of mis-operation of the mid-line recloser caused by the DG back feed fault current. This is achieved through the setting of recloser to operate for the fault in the forward

direction only. Therefore, the setting adjustment of other protective devices is not required.

Correspondingly, in determining the maximum allowable DG capacity, (6.8) can be discarded by which the result of a larger DG capacity can be expected.

6.2.3 Replacement of Fuse with Recloser

If the DG capacity is sufficiently large, it can increase the fault level to exceed that of the design for fuse saving scheme. As a result, the mid-line recloser will not be able to save a lateral fuse from unnecessary operation due to a temporary fault. Consequently, those temporary faults will result in a permanent outage to the lateral feeder. None of the two previously mentioned methods can help solve this problem.

In order to maintain benefits from the self-clear of a temporary fault with an auto-reclose function, replacement of fuse with recloser may be considered. Once the lateral fuse is replaced by a recloser, the fast operation of the mid-line recloser can be turned off and transferred to the replaced lateral recloser. In this way, instead of using the mid-line recloser to restore the circuit from a temporary fault, the lateral recloser will perform this function. This replacement is applied to all the lateral fuses located behind the mid-line recloser.

At present, newly developed equipment, e.g. dropout recloser [43] has emerged. These devices can also be installed in place of the lateral fuse to resolve the above problem in almost the same way but with lower cost.

In addition, since the fast operation of mid-line recloser can be turn-off, the problem from a large back-feed fault current due to a DG is also disappeared. Consequently, (6.5), (6.6) and (6.8) can be removed during the search process for the maximum allowable DG capacity. Hence, it should result in a larger allowable DG capacity.

6.3 System Service Quality Index Evaluation

The impact of a DG on system service quality has been described in Section 4.4. It is clearly seen that large DG capacity can result in negative impact on protection system coordination and therefore reducing system reliability (SAIFI and SAIDI). Nevertheless, a DG by which its capacity is less than the maximum allowable can provide a benefit to the improvement on system voltage sag by increasing system fault level (SARFI-X and SARFI-Curve).

To realize the impact and benefit of the DG on the system service quality, this section proposes a methodology to evaluate system service quality index in the presence of DG. The method can be divided into two parts, i.e. system reliability and voltage sag evaluations.

6.3.1 System Reliability

It has been shown in Section 4.4 that a DG with capacity less than the maximum allowable does not cause problems to protection system coordination. As a result, system reliability remains unchanged. Consequently, SAIFI and SAIDI will be the same as the original system without DG.

Nevertheless, a capacity of DG exceeding the maximum allowable will result in protection mis-coordination, which is likely to occur if a fault occurs in the Protection Mis-coordination Area (PMA) as described in Section 4.4. The PMA can be classified into three types based on the results of protection mis-coordination events. Firstly, the PMA for the back-feed fault current problem covers areas in front of the recloser and will be determined only if the DG is installed behind the recloser. Secondly, the PMA for the fuse saving scheme problem are those areas on the lateral behind the recloser and will be determined for all DG locations. Finally, the PMA for fuse-fuse coordination are those areas on the sub-laterals which is also determined for all DG location. The procedure in determining the PMA can be described below.

A. Determination of PMA for back-feed fault current ($PMA_{back-feed}$)

Step 0: Starting from recloser moving toward substation, search on the main feeder location where fault current contribution from DG is equal to the recloser pick-up setting. Record the distance from the recloser to the fault location.

Step 1: For all laterals within the range of the distance in Step 0, search on the lateral the location where fault current contribution from DG is equal to the recloser pick-up setting. Record the distance from the main line to the fault location.

Step 2: The distance in Step 0 is $PMA_{back-feed,m}$ and the distance in Step 1 is $PMA_{back-feed,l-n}$. The subscription “ m ” indicates PMA on the mainline while “ l ” indicates PMA on the lateral “ n ”.

B. Determination of PMA for fuse saving scheme problem ($PMA_{fuse-save}$)

Step 0: Determine the maximum fault current design of fuse saving scheme from coordination graph.

Step 1: For all laterals behind the mid-line recloser, search on the lateral location where fault current passing through the fuse is equal to the fault current in Step 0. Record the distance from the main line to the fault location.

Step 2: The distance in Step 1 is $PMA_{fuse-save,l-n}$

C. Determination of PMA for fuse-fuse coordination problem ($PMA_{fuse-fuse}$)

Step 0: Determine the maximum fault current design of fuse-fuse coordination from Table 3.1.

Step 1: For all sub-laterals, search on the sub-lateral the location where fault current passing through the protecting fuse is equal to the fault current in Step 0. Record the distance from the protecting fuse to the fault location.

Step 2: The distance in Step 1 is $PMA_{fuse-fuse,l-n}$

Next, this thesis introduces Protection Mis-coordination Index (PMI) to measure the level of impact of a DG on protection mis-coordination. PMI is defined as the frequency of occurrence of protection mis-coordination events in the system. The index can be calculated from PMA according to the following equation.

$$PMI = PMA_{back-feed,m}(\lambda_t) + \sum_n PMA_{back-feed,l-n}(\lambda_t + \lambda_p) + \sum_n PMA_{fuse-save,l-n}(\lambda_t) + \sum_n PMA_{fuse-fuse,l-n}(\lambda_t + \lambda_p) \quad (6.13)$$

If PMI at each load point i is of interest, it can be determined using below equation.

$$PMI_i = PMA_{back-feed,m}(\lambda_t) + \sum_n PMA_{back-feed,l-n}(\lambda_t + \lambda_p) + PMA_{fuse-save,l-n}(\lambda_t) + PMA_{fuse-fuse,l-n}(\lambda_t + \lambda_p) \quad (6.14)$$

In summary, (6.13) is system index whereas (6.14) is load point index. The difference between (6.13) and (6.14) is the summation sign of $PMA_{fuse-save}$ and $PMA_{fuse-fuse}$. When each load point is considered individually, the $PMA_{fuse-save}$ and $PMA_{fuse-fuse}$ which can have an impact on the customer is only in its supplied lateral. This affected customer can be referred from the analysis in Section 4.4 and the conclusion drawn in Table 4.8.

By using PMI, the impact of DG on protection mis-coordination can be quantified. The comparison between two DG projects is also possible. Also, it is noted that if the DG capacity is within the maximum allowable, the PMI of the DG will be equal to zero, as the DG does not create protection mis-coordination and PMA has a zero value.

Finally, the change in SAIFI and SAIDI after the presence of DG is also calculated by using PMA. The affected load points for each type of PMA are

presented in Table 4.8. Consequently, λ_i and r_i in (4.3) – (4.4) for each affected load point “ i ” will be updated using the following equation.

$$\lambda_i = \sum_i \lambda_{p-n} + PMA_{back-feed,m}(\lambda_i) + \sum_n PMA_{back-feed,l-n}(\lambda_i + \lambda_p) + PMA_{fuse-save,l-n}(\lambda_i) + PMA_{fuse-fuse,l-n}(\lambda_i + \lambda_p) \quad (6.15)$$

$$\lambda_i = \sum_i \lambda_{p-n} + PMI_i \quad (6.16)$$

$$r_i = \frac{\sum_i \lambda_{p-n} r_{p-n} + PMI_i r_{s-n}}{\sum_i \lambda_{p-n} + PMI_i} \quad (6.17)$$

In the above equation, it is assumed that the switching time (r_{s-n}) for restoring the circuit for all protection mis-coordination events are equal. However, different switching time can be applied according to each event. It can be noticed from the above equation that when protection mis-coordination is occurred, the temporary fault failure rate will be included in the calculation since it results in a long interruption.

After obtaining new values of λ_i and r_i for all the load points, (4.1) and (4.2) can then be applied to recalculate for the new SAIFI and SAIDI. In summary, the system reliability in the presence of DG can be evaluated with the procedure shown in Figure 6.3.

6.3.2 System Voltage Sag

As illustrated in Section 4.2, an important concept in calculating System Voltage Sag indices, i.e. SARFI-X and SARFI-Curve, is the critical distance. If the distribution system configuration is simple and there is no DG connection, an explicit equation for critical distance can be easily obtained, as expressed in (4.7) and (4.9). However, if the system is more complicated, or there is a DG connection in the system, it may be a difficult task on deriving such an expression and the equation can

be varied depending on the network configuration and DG location. Additionally, this concept cannot be applied to SARFI-Curve calculation as it does not include the operating time of the protective devices.

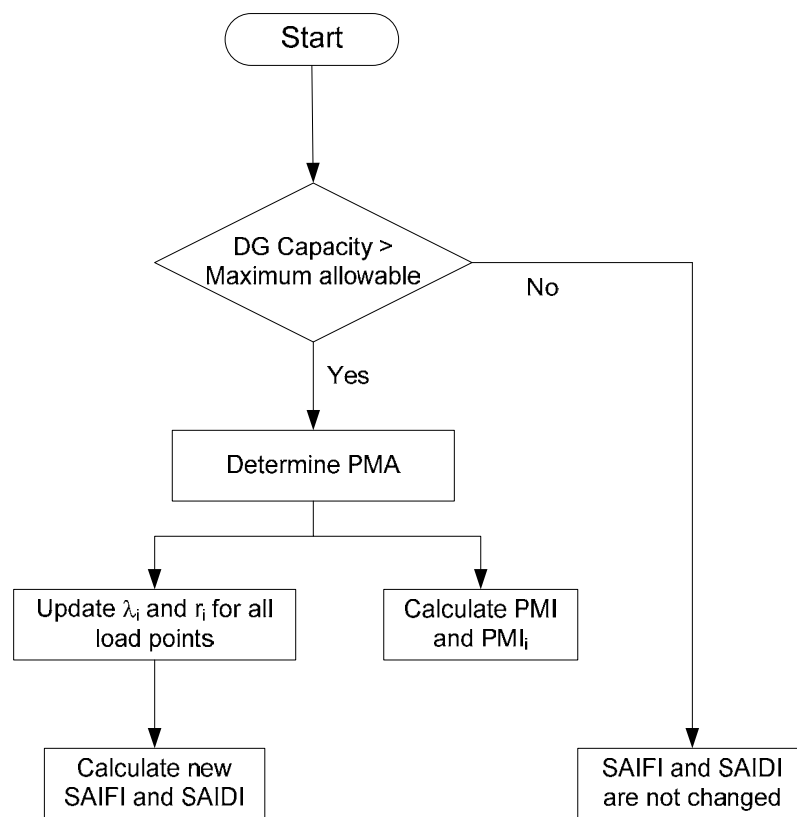


Figure 6.3 Procedure in evaluating system reliability in the presence of DG

From the above mentioned problems, this thesis therefore proposes the methodology presented in Section 4.2 to approximate Voltage Sag indices. The method takes into account both frequency and duration of voltage sage events. Therefore, it can be applied to calculate results on SARFI-Curve. The accuracy of the method can be compared to an exact equation proposed by [18] as shown in Section 4.3. As a result, this thesis will apply the method to analyze SARFI-X and SARFI-Curve in the presence of DG.

The calculation procedure for SARFI-X can be presented by the below process.

Step 0: Specify the length of sectional line (l_{sec}).

Step 1: Set SARFI-X value to zero.

Step 2: Apply fault at the middle of the line section.

Step 3: Verify the voltage at the substation during fault. If the value is under “X” threshold, increase SARFI-X index by the following equation.

$$\text{SARFI-X}_{new} = \text{SARFI-X}_{old} + l_{sec} (\lambda_{p-n} + \lambda_{r-n}) \quad (6.18)$$

Step 4: Repeat steps 2 and 3 for every line section.

Step 5: Obtain SARFI-X value.

The calculation procedure for SARFI-Curve is explained by the following steps.

Step 0: Specify the length of sectional line (l_{sec}).

Step 1: Set SARFI-Curve value to zero.

Step 2: Apply fault at the middle of the line section.

Step 3: Verify the voltage at the substation during fault and the operating time of the primary protective device. Since fuse saving scheme is applied, a careful consideration should be made on the determination of the operating time for which Table 4.2 can be used as a guideline.

After voltage sag magnitude and protection operating time are identified, increase SARFI-Curve index by (6.19) if the coordinate lies within the voltage envelope “Curve”

$$\text{SARFI-Curve}_{new} = \text{SARFI-Curve}_{old} + l_{sec} (\lambda) \quad (6.19)$$

Where λ corresponds to types of fault, i.e. permanent or temporary.

Step 4: Repeat steps 2 and 3 for every line section.

Step 5: Obtain SARFI-Curve value.

From the above process, SARFI-X and SARFI-Curve can be evaluated. As a result, the impact of DG on system service quality can be evaluated, as will be shown in Section 7.3.

6.4 Appropriate DG Output with Customer Load Profile Consideration

As mentioned in the introduction, the size and location of a DG is typically determined at some specific load condition for loss minimization. When system condition moves to a new operating point, the optimal DG size and location will change. The surplus output power during the light load condition can lead to an excessive increase in feeder loss. Therefore, it is important to determine appropriate DG output power to control the loss in feeder.

In this section, the method in determining an appropriate DG output which does not increase feeder loss is presented, taking into account customer load profile. Approximation technique which establishes the relationship between appropriate DG output and load variation from the loss allocation technique, i.e. BCDLA is proposed. The simulation results are also provided.

6.4.1 Appropriate DG Output Using Direct Search Method

It has been shown in Section 5.2 that the appropriate DG output with loss consideration can be determined using a Direct Search Method. In addition, Section 5.4 shows that load variation has impact on the appropriate DG output. Consequently, to take into account system demand variation, the following procedure will be applied.

Step 0: Aggregate each individual customer load along the feeder to obtain a

single load profile of the feeder.

Step 1: Based on the feeder load profile, using the direct search method to determine appropriate DG output for each time of day.

Step 2: From the obtained results, establish appropriate DG output profile for that feeder.

Nevertheless, this method though providing an exact solution, requires a run of optimization search including power flow solutions for every different load level. Therefore, a computational time can be great and the simulation software is of necessary.

6.4.2 The Developed Methodology

In order to simplify the problems on determining an appropriate DG output power taken into account customer load profile, this section proposes and applies the BCDLA loss allocation technique to establish an approximate relationship between appropriate DG output and load variations in that feeder. Based on this relationship, if the amount of load change is known, the new appropriate DG output power can be calculated accordingly. Therefore, this method requires less computational time than that of the direct search method. In addition, it requires only a simple calculation.

Firstly, a three node feeder will be used for demonstration. Then, a general formula and calculation procedure to determine appropriate DG output will be presented in the following subsection.

Let us consider a simple three-node feeder with two load points and one DG as shown in Figure 6.4.

From the figure, R_b represents resistance of branch b , LP_k represents power consumption at load point k , and $\alpha_k + j\beta_k$ represents supplied current to node k . DG_k is the real power injected from the DG at node k . For simplicity, DG in this study is assumed to operate at a unity power factor.

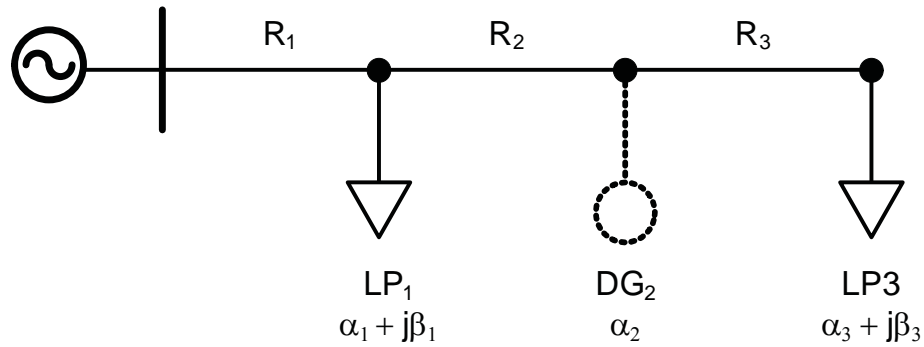


Figure 6.4 Simple three-node feeder

According to (5.6), $\alpha_k + j\beta_k$ can be calculated from $P_k + jQ_k$ after obtaining voltage V_k from a power flow solution. With proper voltage regulation on the feeder, V_k can be approximately set at 1.0 per unit. As a result, the supplied current $\alpha_k + j\beta_k$ is approximately equal to $P_k + jQ_k$ in term of per unit value.

$$\alpha_k + j\beta_k \approx P_k + jQ_k \quad (6.20)$$

Next, let us consider the system in Figure 6.4 when DG is not connected. From (5.9), considering only real power, L_1 and L_3 can be written as

$$L_1 = \alpha_1 [R_1(\alpha_1 + \alpha_3)]$$

$$L_3 = \alpha_3 [R_1(\alpha_1 + \alpha_3) + R_2\alpha_3 + R_3\alpha_3]$$

Therefore, from (5.11), the total system loss before having DG connected to the system is

$$L_{total-noDG} = \alpha_1 [R_1(\alpha_1 + \alpha_3)] + \alpha_3 [R_1(\alpha_1 + \alpha_3) + R_2\alpha_3 + R_3\alpha_3] \quad (6.21)$$

After the installation of the DG at node 2, the loss allocation factor according

to (5.9) has to be recalculated since a certain amount of loss can be allocated to the DG. Accordingly, L_1 , L_2 and L_3 can be written as

$$L_1 = \alpha_1 [R_1(\alpha_1 + \alpha_2 + \alpha_3)]$$

$$L_2 = \alpha_2 [R_1(\alpha_1 + \alpha_2 + \alpha_3) + R_2(\alpha_2 + \alpha_3)]$$

$$L_3 = \alpha_3 [R_1(\alpha_1 + \alpha_2 + \alpha_3) + R_2(\alpha_2 + \alpha_3) + R_3\alpha_3]$$

Therefore, the new total loss with a connected DG will be as follows.

$$\begin{aligned} L_{total-withDG} = & \alpha_1 [R_1(\alpha_1 + \alpha_2 + \alpha_3)] + \\ & \alpha_2 [R_1(\alpha_1 + \alpha_2 + \alpha_3) + R_2(\alpha_2 + \alpha_3)] + \\ & \alpha_3 [R_1(\alpha_1 + \alpha_2 + \alpha_3) + R_2(\alpha_2 + \alpha_3) + R_3\alpha_3] \end{aligned} \quad (6.22)$$

With the requirement that the connected DG should not increase the total system loss, the maximum allowable DG output power has to be calculated in such a way that (6.21) and (6.22) are equal. Having (6.21) equal to (6.22), the equation can then be written as

$$(R_1 + R_2)\alpha_2^2 + 2R_1\alpha_1\alpha_2 + 2R_1\alpha_2\alpha_3 + 2R_2\alpha_2\alpha_3 = 0 \quad (6.23)$$

The reactive power can be included into the equation with a variable similar to that of real power with only α replaced by β . However, as the DG in this study is assumed to operate at a unity power factor, the loss components from reactive power therefore remains unchanged for both with and without DG cases. As a result, this component will cancel out each other at the stage of having (6.21) equal to (6.22). Therefore, when considering a unity power factor DG, the loss component from reactive power can be neglected.

As the impact of load variation to the appropriate DG output power is of interest, differentiating (6.23) and rearranging the obtained equation will result in the following formula.

$$\begin{aligned} [R_1(\alpha_1 + \alpha_2 + \alpha_3) + R_2(\alpha_2 + \alpha_3)]\Delta\alpha_2 &= -[R_1\Delta\alpha_1 + (R_1 + R_2)\Delta\alpha_3]\alpha_2 \\ \Delta\alpha_2 &= -[R_1\Delta\alpha_1 + (R_1 + R_2)\Delta\alpha_3]\frac{\alpha_2}{W_2} \end{aligned} \quad (6.24)$$

From (6.24), the relationship between load variation and an appropriate DG output power is established. It can be seen that the change of appropriate DG output power can be directly calculated from the appropriate DG output power determined at peak load, and the virtual voltage at node 2 defined by (5.10), i.e. α_2 and W_2 respectively.

6.4.3 Derivation of Appropriate DG Output and Load Variation Relationship

Start with (5.9), the total system loss can be expressed as

$$\begin{aligned} L_{total} &= \sum_{k=1}^n L_k \\ &= \sum_{k=1}^n \left\{ \alpha_k \sum_{b \in \mathbf{B}_k} R^{(b)} \alpha^{(b)} \right\} + \sum_{k=1}^n \left\{ \beta_k \sum_{b \in \mathbf{B}_k} R^{(b)} \beta^{(b)} \right\} \end{aligned} \quad (6.25)$$

If a DG is connected to the system, the new total system loss will be as shown in (6.26)

$$L'_{total} = \sum_{k=1}^n \left\{ \alpha_k \sum_{b \in \mathbf{B}_k} R^{(b)} \alpha^{(b)*} \right\} + \alpha_{DG} \sum_{b \in \mathbf{B}_{DG}} R^{(b)} \alpha^{(b)} + \sum_{k=1}^n \left\{ \beta_k \sum_{b \in \mathbf{B}_k} R^{(b)} \beta^{(b)*} \right\} \quad (6.26)$$

where

$$\alpha^{(b)*} = \begin{cases} \alpha^{(b)} + \alpha_{DG} & \text{when } \mathbf{B}_k \subset \mathbf{B}_{DG} \\ \alpha^{(b)} & \text{else} \end{cases}$$

Assuming that after connecting DG to the system, total system loss is the same, subtracting (6.26) from (6.25) will obtain (6.27).

$$\begin{aligned} \sum_{k=1}^n \alpha_k \sum_{b \in \mathbf{B}_k} R^{(b)} \alpha_{DG} + \alpha_{DG} \sum_{b \in \mathbf{B}_{DG}} R^{(b)} \alpha^{(b)} &= 0 \\ \alpha_{DG} \sum_{k=1}^n \alpha_k \sum_{b \in \mathbf{B}_k} R^{(b)} + \alpha_{DG} \sum_{b \in \mathbf{B}_{DG}} R^{(b)} \alpha^{(b)} &= 0 \end{aligned} \quad (6.27)$$

$$\text{where } \mathbf{B}'_k = \{\mathbf{B}_k \cap \overline{\mathbf{B}_{DG}}\}$$

From $\Delta XY = X\Delta Y + Y\Delta X$, (6.27) becomes

$$\begin{aligned} \alpha_{DG} \left(\sum_{k=1}^n \Delta \alpha_k \sum_{b \in \mathbf{B}'_k} R^{(b)} \right) + \left(\sum_{k=1}^n \alpha_k \sum_{b \in \mathbf{B}'_k} R^{(b)} \right) \Delta \alpha_{DG} + \dots \\ \alpha_{DG} \left(\sum_{b \in \mathbf{B}_{DG}} R^{(b)} \Delta \alpha^{(b)} \right) + \left(\sum_{b \in \mathbf{B}_{DG}} R^{(b)} \alpha^{(b)} \right) \Delta \alpha_{DG} = 0 \end{aligned} \quad (6.28)$$

Consider $\sum_{k=1}^n \alpha_k \sum_{b \in \mathbf{B}_k} R^{(b)}$ and $\sum_{b \in \mathbf{B}_{DG}} R^{(b)} \alpha^{(b)}$ in (6.28), the first term can be expanded as follows.

$$\begin{aligned} \sum_{k=1}^n \alpha_k \sum_{b \in \mathbf{B}_k} R^{(b)} &= \alpha_1 R_1 + \alpha_2 (R_1 + R_2) + \dots + \alpha_{DG} (R_1 + R_2 + \dots + R_{DG}) + \\ &\quad \alpha_{DG+1} (R_1 + R_2 + \dots + R_{DG}) + \dots + \alpha_n (R_1 + R_2 + \dots + R_{DG}) \end{aligned}$$

Rearrange the above equation will result in

$$\begin{aligned}
&(\alpha_1 + \alpha_2 + \dots + \alpha_n)R_1 + (\alpha_2 + \alpha_3 + \dots + \alpha_n)R_2 + \\
&(\alpha_3 + \alpha_4 + \dots + \alpha_n)R_3 + \dots + (\alpha_{DG} + \dots + \alpha_n)R_{DG} = \sum_{b \in \mathbf{B}_{DG}} R^{(b)} \alpha^{(b)}
\end{aligned}$$

Therefore,

$$\sum_{k=1}^n \alpha_k \sum_{b \in \mathbf{B}'_k} R^{(b)} = \sum_{b \in \mathbf{B}_{DG}} R^{(b)} \alpha^{(b)} \quad (6.29)$$

From (6.29), we can write (6.28) as follows:

$$\begin{aligned}
2 \times \Delta \alpha_{DG} \times \left\{ \sum_{b \in \mathbf{B}_{DG}} R^{(b)} \alpha^{(b)} \right\} &= -2 \times \left\{ \sum_{k=1}^n \Delta \alpha_k \sum_{b \in \mathbf{B}'_k} R^{(b)} \right\} \alpha_{DG} \\
\Delta \alpha_{DG} &= - \left[\sum_{k=1}^n \Delta \alpha_k \sum_{b \in \mathbf{B}'_k} R^{(b)} \right] \frac{\alpha_{DG}}{W_{DG}} \quad (6.30)
\end{aligned}$$

6.4.4 General Formula and Calculation Procedure

The general form of the formula in determining appropriate DG output power according to load variation can be expressed as (6.31).

$$\Delta \alpha_k = - \left\{ \sum_{i=k}^n \Delta \alpha_i \cdot \left(\sum_{b \in \mathbf{B}'_k} R^{(b)} \right) \right\} \frac{\alpha_{DG}}{W_{DG}} \quad (6.31)$$

Where k is the node that DG is installed, n is the total of supplied node, and $\mathbf{B}'_k = \{\mathbf{B}_k \cap \mathbf{B}_{DG}\}$. The detailed proof of the formula is provided in the following subsection.

According to (6.31), for the supplied nodes located behind the DG location, B will be limited to only node k . This can be seen from the example in (6.24), i.e. for

$\Delta\alpha_3$, the multiplier is only $(R_1 + R_2)$. The procedure in obtaining an appropriate DG output power based on the proposed method can be illustrated by Figure 6.5.

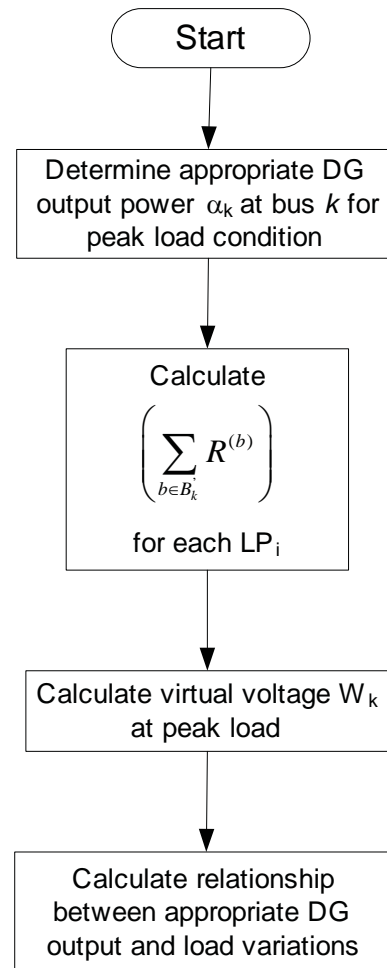


Figure 6.5 Procedure in determining load and DG output power relationship

From Figure 6.5, the appropriate DG output power is firstly determined at peak load to obtain α_k . Then, $\sum_{b \in B_k} R^{(b)}$ in (6.31) is calculated to obtain a coefficient for $\Delta\alpha_i$ at each Load Point (LP). Next, the virtual voltage W_k at peak load condition is calculated using (5.10). Then, substitute all the obtained parameters in (6.31) to determine the formula of the appropriate DG output and the load variation. As a result, for any given load conditions, the appropriate DG output power can be determined accordingly.

For example, at a considered interval, if demand is 30% of peak load, it means that $\Delta\alpha_i$ is 70%, i.e. 100%-30%. Substituting all $\Delta\alpha_i$ of every load point into the established relationship, the change in appropriate DG output power, $\Delta\alpha_k$ can be determined. Then, the new DG output power is calculated by adding up $\Delta\alpha_k$ to the appropriate DG output power at peak load, i.e. α_k .

6.5 Summary

From the analyses of DG impact on protection system coordination in Section 3.4, this section proposed the method for determining the maximum allowable DG capacity which does not result in protection mis-coordination. The problem is formulated as an optimization problem with an objective function (6.1) and a set of constraints (6.2) – (6.8) comprising of voltage, loss, and protection coordination, by which the procedure shown in Figure 6.1 will be applied. Regarding the protection coordination constraint, it will be selected based on DG and fault location as shown in Table 6.1. In addition, the process for applying the proposed method in the case that there is more than one DG connection is presented in Figure 6.2.

Since the existing protection coordination is a limit for the maximum allowable DG capacity, the protection adjustment method is proposed to allow higher penetration of DG. The methods comprise resetting protective devices, directional recloser application, and replacement of fuse with recloser.

From the impacts of DG on system service quality demonstrated in Section 4.4, the method for determining reliability index, i.e. SAIFI and SAIDI, in the presence of DG by which its capacity is larger than the maximum allowable is proposed. The PMA for three types of protection mis-coordination, i.e. back-feed current, fuse saving scheme problem, and fuse-fuse coordination will be determined and applied to calculate for PMI using (6.13) – (6.14) and update for SAIFI and SAIDI using (6.15) – (6.17). Furthermore, if a DG capacity is less than the maximum allowable, which also means SAIFI and SAIDI remains unchanged, the method for determining an improvement on SARFI-X and SARFI-Curve is developed.

From the analyses of DG output power and power loss with customer load profile consideration in Section 5.2 – 5.4, this section proposed the method for determining appropriate DG output power which does not increase system loss. The methods are consisted of direct search and approximation method. The first method formulates the problem as an optimization problem with an objective function (5.2) and loss constraint (6.3). The appropriate DG output power is then determined for each different load level. To simplify the problem and reduce computational time, the application of BCDLA is proposed to establish the relationship between a change of customer demand and appropriate DG output power from the procedure in Figure 6.5. The output from both methods is the appropriate DG output power profile.

All proposed methods comprising of the determination of maximum allowable DG capacity with protection coordination consideration, the determination of appropriate DG output power with customer load profile consideration, protection adjustment method for higher penetration of DG, and system service quality evaluation, will be applied next to analyze the test system in Chapter 7.

CHAPTER VII

SIMULATION RESULTS

All the proposed method will be tested with a modified RBTS Bus 2 [32-33]. The first subsection illustrates the obtained maximum allowable DG capacity which does not cause protection coordination failure. Next, the proposed protection adjustment method is applied to increase the maximum allowable capacity. Then, service quality of the test system is evaluated for two cases, i.e. when DG capacity is larger than the maximum allowable and when it is less. Finally, an appropriate DG output which does not increase system loss and take into account customer load profiles is determined. The obtained results are then applied to establish appropriate DG output profile for a dispatchable DG unit.

7.1 Maximum Allowable DG Capacity with Protection Consideration

This section presents all the results obtained from the proposed method. The analysis is divided into 3 cases according to constraint considerations, i.e.

- (a) Line loss constraint,
- (b) Protection coordination constraint, and
- (c) Protection coordination and line loss constraints.

Additionally, examples of the determination of maximum allowable DG capacity under multiple DG connections are also provided.

7.1.1 Simulation Results

The results of the maximum allowable capacity of the DG at each location of the test system are shown in Table 7.1. In addition, the percentage of the line loss reduction compared to the base case with no DG is also included.

From the results in Table 7.1, protection coordination clearly has impact in determining the maximum allowable capacity. If the protection coordination is

ignored, i.e. only system voltage and line loss are considered, the results of the maximum allowable DG capacity will become larger. For example, considering Feeder 3 without protection coordination constraint as of Case (a), the maximum allowable capacity of a DG at node 3D is 6.54 MW, which may, however, cause protection coordination failure. In Case (c), if the protection coordination is taken into account, the maximum allowable capacity of a DG at node 3D reduces to 2.74 MW.

Table 7.1 Maximum allowable DG capacity at each location

Feeder	DG location	In front of / behind Recloser	Maximum allowable DG size capacity (MW) / Loss reduction (%)		
			Case (a)	Case (b)	Case (c)
1	1A	In front	10.00 / 6.44%	10.00 / 6.44%	10.00 / 6.44%
	1B	In front	10.00 / 2.77%	10.00 / 2.77%	10.00 / 2.77%
	1C	Behind	8.62 / 0.00%	2.56 / 13.14%	2.56 / 13.14%
	1D	Behind	7.10 / 0.00%	2.63 / 12.62%	2.63 / 12.62%
2	2A	In front	7.22 / 0.00%	10.00 / -7.17%	7.22 / 0.00%
	2B	In front	5.70 / 0.00%	10.00 / -19.74%	5.70 / 0.00%
3	3A	In front	10.00 / 1.59%	10.00 / 1.59%	10.00 / 1.59%
	3B	In front	9.56 / 0.00%	8.51 / 4.88%	8.51 / 4.88%
	3C	Behind	8.33 / 0.00%	2.64 / 12.05%	2.64 / 12.05%
	3D	Behind	6.54 / 0.00%	2.74 / 11.26%	2.74 / 11.26%
4	4A	In front	10.00 / 4.53%	10.00 / 4.53%	10.00 / 4.53%
	4B	In front	10.00 / 0.07%	10.00 / 0.07%	10.00 / 0.07%
	4C	Behind	8.44 / 0.00%	2.66 / 13.29%	2.66 / 13.29%
	4D	Behind	7.37 / 0.00%	2.74 / 13.90%	2.74 / 13.90%

Figure 7.1 depicts the comparison of the obtained results with and without protection coordination consideration of Feeder 3. It is obviously seen that the maximum allowable DG capacity is reduce with a consideration of protection coordination. This also implies that protection coordination constraint presents a significant impact to the allowable DG capacity in the system. This result emphasizes

the necessity of protection consideration when determining for maximum allowable DG capacity. Otherwise, with only power loss consideration, the installed DG capacity may cause problem to the protection coordination.

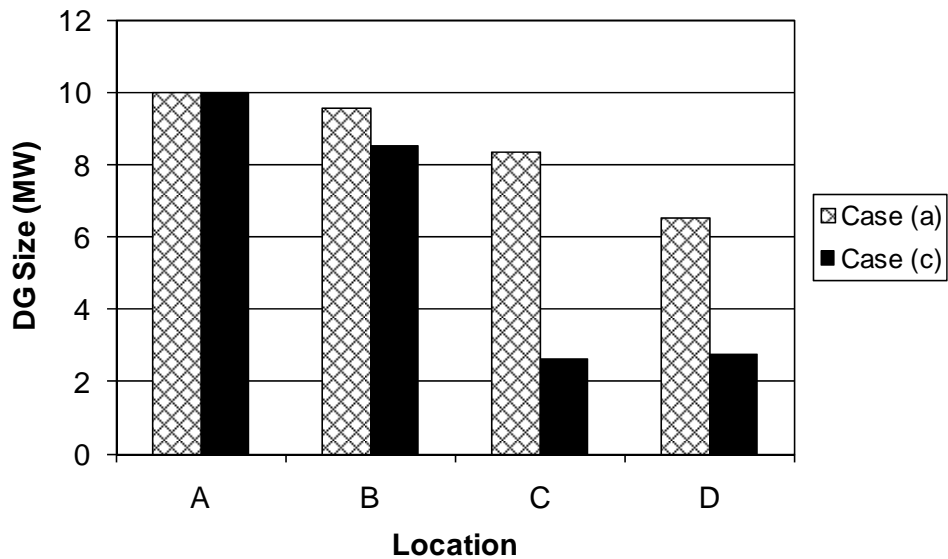


Figure 7.1 Comparison of maximum allowable DG capacity of Feeder 3 of Case (a) and Case (c)

In some situations, utility may not concern with power loss. In case of neglecting the line loss constraint, it may result in a higher allowable capacity. As an example, the maximum allowable DG capacity at node 2B is 5.70 MW as of Case (c). However, it increases to 10 MW when the loss constraint is neglected as of Case (b) with the increase of system loss by 19.74%.

In addition, it can be noticed that the maximum allowable size of DGs located in front of the recloser is larger than that those of located behind the recloser. Considering Feeder 1, which has a mid-line recloser and with all constraints being applied as in Case (c), the results in Table 7.1 show that the maximum capacity located in front of recloser, i.e. nodes 1A and 1B, is 10 MW. In contrast, the maximum allowable capacity of a DG located behind the recloser of Feeder 1, i.e. nodes 1C and 1D, are in the range of 2.5-2.6 MW. Similar results can be seen with

Feeders 3 and 4. Figure 7.2 summarizes the maximum allowable capacity of the DG located in front of and behind recloser for each feeder.

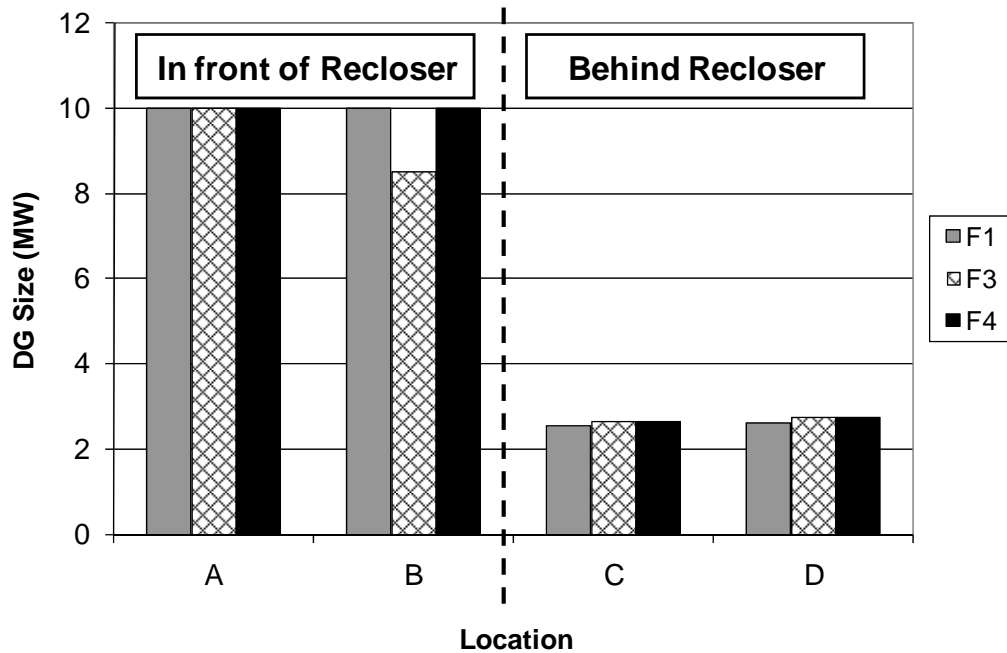


Figure 7.2 Comparison among the maximum allowable capacities of DGs located in front and behind the recloser of each feeder

Figure 7.3 illustrates maximum allowable capacity of a DG for each location of Feeder 1 and its associated loss reduction of Case (c). The figure shows that although the maximum allowable capacity of the DG behind the recloser is rather small, however the percentage of loss reduction is high, to an approximated value of 13%. In contrast, even though the maximum allowable capacity of the DG in front of recloser is high, its impact on the loss reduction is rather low, approximately 3-6%. Similar results can be found for Feeders 3 and 4.

Figure 7.4 graphically presents the results of Case (c). The maximum allowable capacity of a DG at each location along the main line is presented by a circle with its value. The size of the circle is related to capacity of a DG. It should be noted that a single DG connection is assumed in the figure.

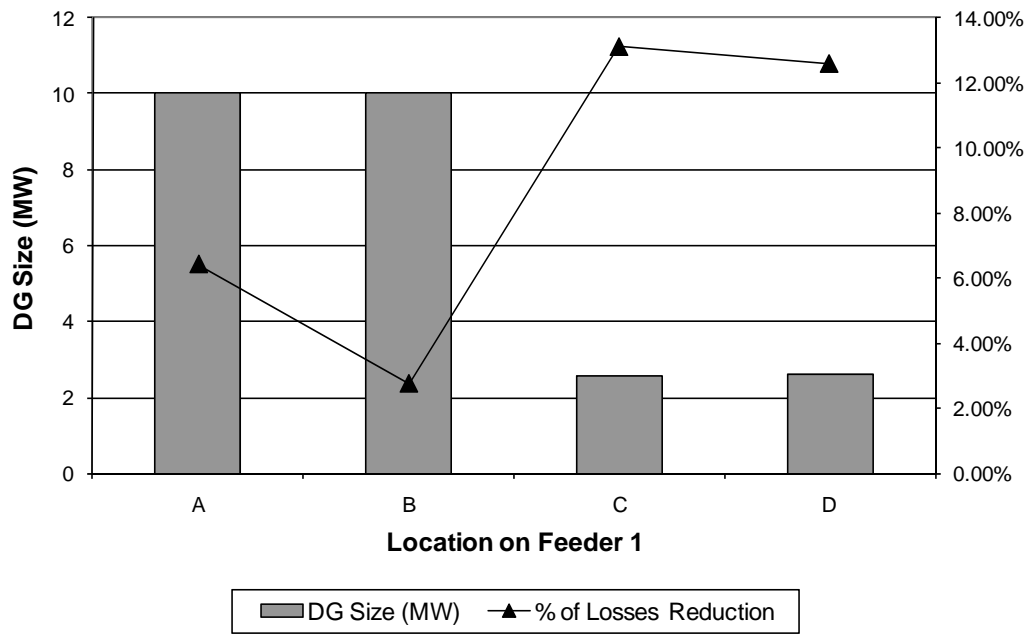


Figure 7.3 Maximum allowable capacity and its associated % loss reduction

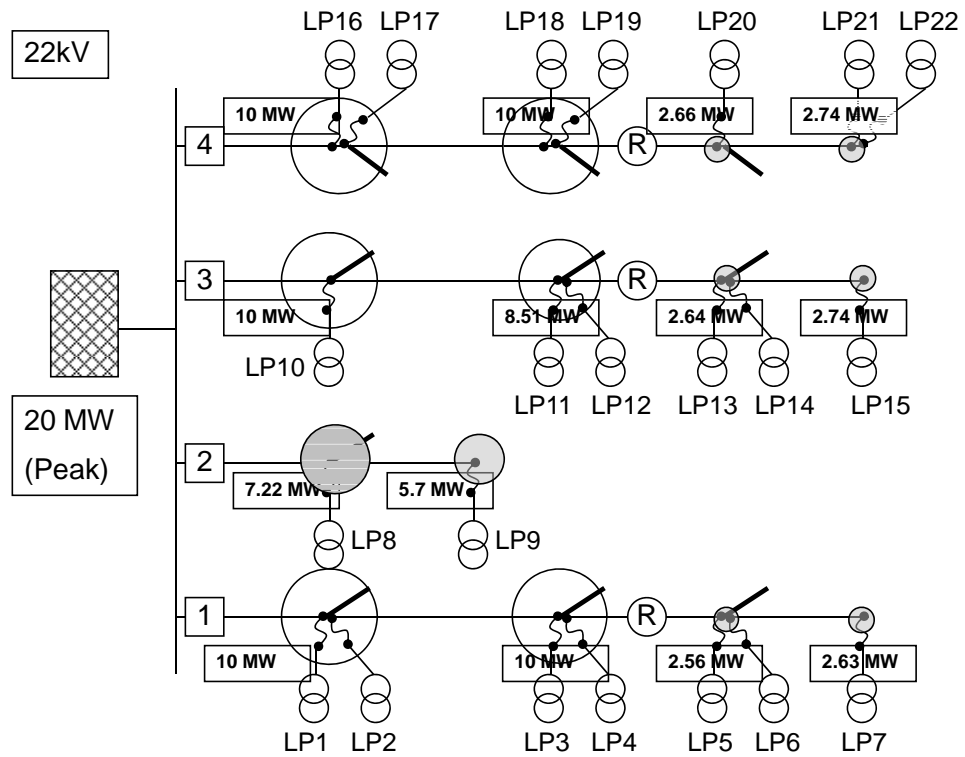


Figure 7.4 Maximum allowable capacity of a DG at each location with protection and losses consideration

At location 1A, 1B, 3A, 4A, and 4B, the maximum allowable DG capacity is 10 MW. This implies that the DG capacity for these locations reaches the upper limit of maximum DG capacity defined in subsection 6.1.1.

It is clearly shown that the developed method is a tool for distribution system engineers. A utility officer can quickly calculate the capability of allowing a DG connected to the existing system. This will help the utility officer screen the applied DG projects. For example, Figure 7.4 shows that if there is a DG request for its connection at node 2B, the desired maximum allowable capacity from the utility perspective will be 5.70 MW. If the DG is of less capacity, the utility officer will know that such a DG will not cause problem to the existing network in terms of loss, voltage profile, and protection coordination. Nonetheless, a larger capacity of the DG implies that the existing system needs to be modified or upgraded.

7.1.2 More than One DG Connection Application

In this section, the proposed method will be further tested with the test system for the case of having more than one DG connection. The procedure in Figure 6.2 will be applied to simulate for the results. Two examples are provided comprising the second DG unit, and multiple DG units cases.

In the first example, the maximum allowable DG capacity is determined for a system with a DG capacity of 5 or 10 MW connected to location 1A. The obtained results are shown in Table 7.2. The value in each parenthesis presents a percentage change of the maximum allowable DG capacity from that of the base case where there is no DG connection.

Based on the results, it is clearly seen that a DG connection at 1A does impact on the maximum allowable DG capacity in the system. At the same location, the maximum allowable is reduced from 10 MW to 7.45 MW and 2.45 MW after a connection of 5 MW and 10 MW DG respectively. In fact, the maximum allowable DG capacity at this location is 12.45 MW by which it is limited by loss constraint. Nevertheless, the maximum allowable DG capacity of the base case is 10 MW since it

is the upper limit for the solution. It can be seen that the new maximum allowable can be calculated directly by subtracting the installed capacity from 12.45 MW.

However, this is not true for other locations. For example, at location 1B, the maximum allowable DG capacity is reduced from 10 MW to 7.90 MW and 3.82 MW after a connection of 5 MW and 10 MW DG at 1A respectively, whereas at location 1C, the results remain unchanged. This implies that for other locations, the new maximum allowable cannot be calculated from a direct subtract and has to be determined using the proposed method.

Table 7.2 The maximum allowable DG capacity of the system with a DG connected to location 1A

Feeder	Location	Maximum allowable DG capacity (MW)		
		Base case	5MW at 1A	10MW at 1A
1	1A	10.00	7.45 (-26%)	2.45 (-76%)
	1B	10.00	7.90 (-21%)	3.82 (-62%)
	1C	2.56	2.56 (0%)	2.56 (0%)
	1D	2.63	2.63 (0%)	2.63 (0%)
2	2A	7.22	7.22 (0%)	7.22 (0%)
	2B	5.70	5.70 (0%)	5.70 (0%)
3	3A	10.00	10.00 (0%)	10.00 (0%)
	3B	8.51	7.82 (-8%)	7.29 (-14%)
	3C	2.64	2.64 (0%)	2.64 (0%)
	3D	2.74	2.74 (0%)	2.74 (0%)
4	4A	10.00	10.00 (0%)	10.00 (0%)
	4B	10.00	10.00 (0%)	9.91 (-1%)
	4C	2.66	2.66 (0%)	2.66 (0%)
	4D	2.74	2.74 (0%)	2.74 (0%)

In the second example, two DGs with capacity of 5MW each are assumed to be connected at locations 1A and 2B, and another DG of 2.5MW at location 3C. Applying the same method, the remaining maximum allowable DG capacity can be calculated and shown in Table 7.3. Figure 7.5 also depicts the obtained results when comparing with the base case. The figure graphically shows a reduction in the maximum allowable DG capacity.

Table 7.3 Maximum allowable DG capacity for a multiple DG case

Feeder	Location	Current DG connection (MW)	Maximum allowable DG capacity (MW)	
			Base case	DG at 1A, 2B, 3C
1	1A	5.00	10.00	7.45 (-26%)
	1B	-	10.00	7.42 (-26%)
	1C	-	2.56	2.56 (0%)
	1D	-	2.63	2.63 (0%)
2	2A	-	7.22	1.48 (-80%)
	2B	5.00	5.70	0.70 (-88%)
3	3A	-	10.00	7.23 (-28%)
	3B	-	8.51	3.09 (-64%)
	3C	2.5	2.64	0.14 (-95%)
	3D	-	2.74	0.14 (-95%)
4	4A	-	10.00	10.00 (0%)
	4B	-	10.00	9.59 (-4%)
	4C	-	2.66	2.66 (0%)
	4D	-	2.74	2.74 (0%)

7.1.3 Summary

The methodology in determining the maximum allowable capacity of a DG taking into account voltage, loss, and protection coordination constraints is presented

and demonstrated in this section. In obtaining the results, a direct search method is applied with a proper set of constraints related to the DG and the fault locations.

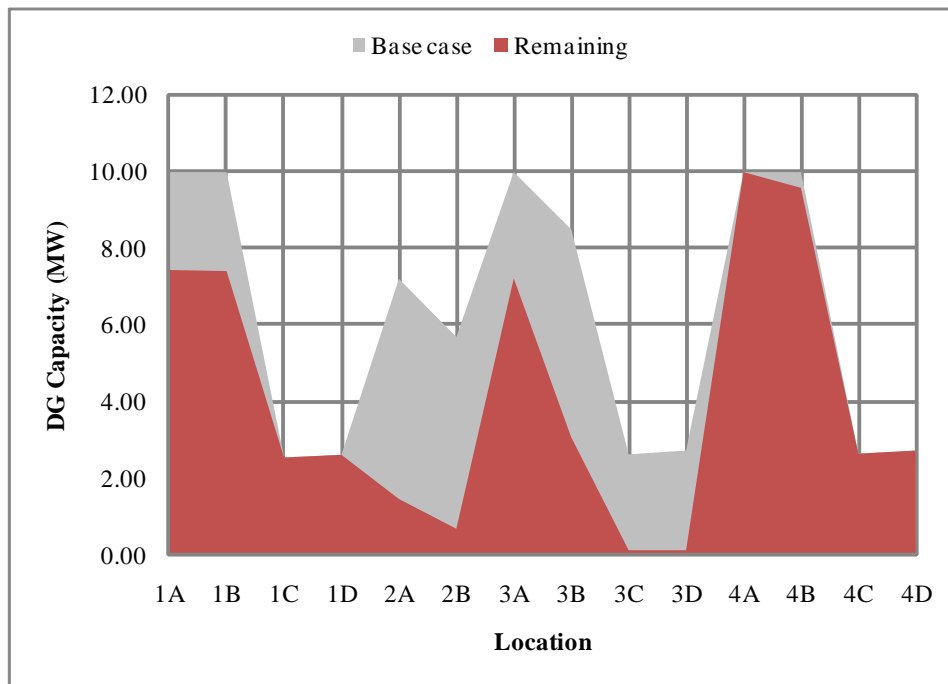


Figure 7.5 The maximum allowable DG capacity after DG connections at 1A and 2B of 5 MW and 3C of 2.5 MW

Impacts between loss and protection coordination constraints on the allowable DG capacity were analyzed. The obtained results in Table 7.1 show that protection coordination constraint dominates the line loss constraint. If the protection coordination is not considered, the maximum allowable capacity will be larger, but may cause protection coordination failure.

The results also show that maximum allowable DG capacity tends to be of a smaller size for a DG located behind the recloser, compared to the DG connected in front of the same recloser. Nonetheless, the smaller size of the DG behind the recloser, which is generally located closer to the end of the feeder, tends to have higher impact on system loss reduction than the DG connected in front of the recloser.

Additionally, the proposed method can be applied to the system which has more than one DG connection and calculate for the maximum allowable DG capacity. It is found that the results can be calculated by subtracting the installed DG capacity from that of the base case at the same location where there is no DG connection. However, for other locations, a direct subtract is not possible and the proposed method has to be applied. Nevertheless, the application considers the request for DG connection on the basis of first-come-first-serve.

7.2 Protection Adjustment Method for Higher Penetration of DG

This section illustrates the application of the proposed protection adjustment methods on the Modified RBTS Bus 2 to increase the maximum allowable DG capacity of the system. These methods, i.e. protective device resetting, directional recloser application, and replacement of fuse with recloser, which are presented in Section 6.2 will be presented. The obtained results will then be compared with the results in Section 7.1 to realize the improvement.

7.2.1 Protective Device Resetting

In this case, feeder 1 is selected for illustration. Based on the proposed algorithm, it needs following calculation steps.

Step 0: Fault currents at circuit breaker and recloser are calculated as 5,248.6 and 2,209 A respectively.

Step 1: Suppose that the line capacity is 500 A, then raise circuit breaker pick-up setting from 411 to 500 A, by (6.10).

Step 2: It is assumed that the setting of the incoming circuit breaker is

- Curve = SI, $I_{pickup} = 820\text{A}$, $TM = 0.25$;

where SI is Standard Inverse, TM is time multiplier

(The incoming circuit breaker is set to 125% of 25 MVA transformer rating, with operating time of 1.0s for the maximum fault current).

From the above settings, the operating time of the incoming for fault at the circuit breaker is determined to be 0.93s using (3.1)

Step 3: Assuming that t_{margin} is 0.3s, TM setting of the circuit breaker can be raised from 0.1 to 0.21 (the operating time of new setting for fault at the circuit breaker is 0.63s).

Step 4: Suppose that K is equal to 0.8 in (6.11), new $I_{R,Pick-up}$ is 400 A.

Step 5: The new protection coordination can be plotted as Figure 7.6.

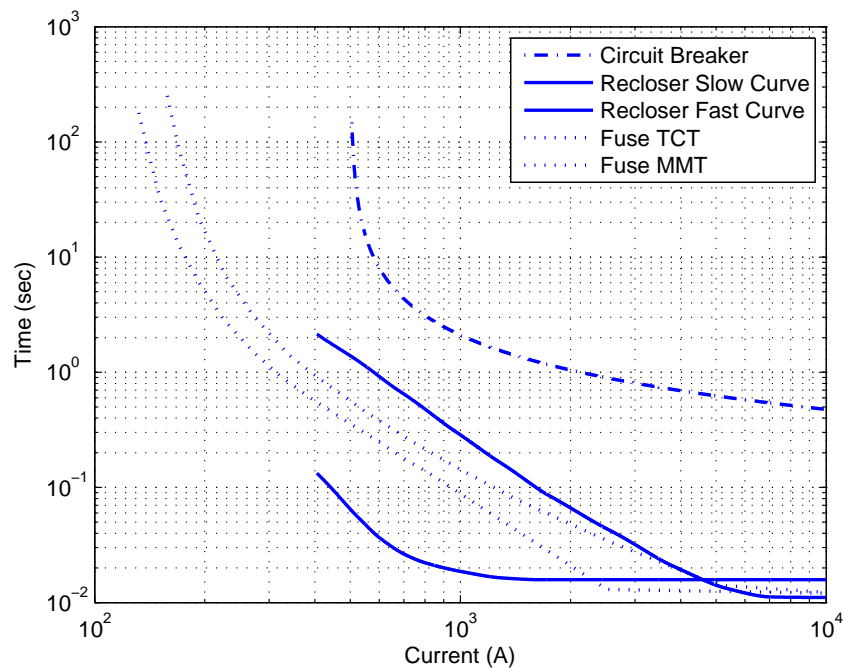


Figure 7.6 Protection coordination after resetting

The above process will be repeated for Feeders 3 and 4 to complete the protection resetting in every feeder. The setting in Feeder 2 remains unchanged since there is no mid-line recloser, i.e. constraints based on (6.8) are not applied.

In this case, it shows that the new setting values of Feeders 3 and 4 are equivalent to that of Feeder 1. In other cases, the settings can be different due to feeder capacity. The protection resetting of the test system can be summarized in Table 7.4.

Table 7.4 Summary of protection resettings

Feeder	Circuit Breaker		Recloser	
	Before	After	Before	After
1	$I_{pickup}=411A,$ $TM=0.1$	$I_{pickup}=500A,$ $TM=0.21$	$I_{R,Pickup}=260A$	$I_{R,Pickup}=400$
3	$I_{pickup}=349A,$ $TM=0.15$	$I_{pickup}=500A,$ $TM=0.21$	$I_{R,Pickup}=270A$	$I_{R,Pickup}=400$
4	$I_{pickup}=383A,$ $TM=0.1$	$I_{pickup}=500A,$ $TM=0.21$	$I_{R,Pickup}=270A$	$I_{R,Pickup}=400$

After resetting the devices, the maximum allowable DG capacity is recalculated. The new results are shown in Table 7.5. Since the proposed method has an effect only on the DG located behind the recloser, only those locations will be shown and compared to the original system.

From the table, it can be seen the maximum allowable DG capacity of a system for those locations behind recloser can be increased from 2.6 – 2.7 MW to approximately 4 MW.

7.2.2 Directional Recloser Application

Next, the existing recloser is replaced by a directional recloser. In addition, new devices will be set to respond for the fault only in a forward direction. Again, the maximum allowable DG capacity is recalculated. Similar to the protective device resetting, only the capacity of the DG located behind the recloser will be affected. The obtained results are shown in Table 7.6. From the Table, the maximum allowable DG

capacity can be increased significantly to 5 – 6 MW compared to the results in Table 7.5.

Table 7.5 Maximum allowable DG capacity after protection resetting

Feeder	Location	DG capacity (MW)	
		Base case	New Results
1	1C	2.56	4.00
	1D	2.63	4.18
3	3C	2.64	3.97
	3D	2.74	4.18
4	4C	2.66	4.00
	4D	2.74	4.18

Table 7.6 Maximum allowable capacity of a DG after directional recloser application

Feeder	Location	DG capacity (MW)	
		Base case	New Results
1	1C	2.56	5.85
	1D	2.63	6.18
3	3C	2.64	5.32
	3D	2.74	5.66
4	4C	2.66	6.11
	4D	2.74	6.47

7.2.3 Replacement of Fuse with Recloser

It is assumed that lateral fuses behind the mid-line recloser of Feeder 1 are changed to an auto-reclose device, e.g. recloser, drop-out recloser. Then, the fast operation of the mid-line recloser is turned off whereas those of the new lateral devices are turned on. The new maximum allowable DG capacity can be re-calculated as shown in Table 7.7. In this case, the proposed method can help improve the results

for those DGs located in front of a mid-line recloser as it resolves the problem of fault level constraints on fuse saving scheme, which is clearly seen from the results at location 3B. It can be seen that this methodology allows the highest DG penetration compared to the other two previous methods.

Table 7.7 Maximum allowable capacity with replacement of fuse by recloser

Feeder	Location	DG capacity (MW)	
		Base case	New Results
1	1A	10.00	10.00
	1B	10.00	10.00
	1C	2.56	8.62*
	1D	2.63	7.10*
2	2A	7.22*	7.22*
	2B	5.70*	5.70*
3	3A	10.00	10.00
	3B	8.51	9.56*
	3C	2.64	8.33*
	3D	2.74	6.54*
4	4A	10.00	10.00
	4B	10.00	10.00
	4C	2.66	8.44*
	4D	2.74	7.37*

7.2.4 Summary

The results show that the proposed protection adjustment methods can help increase maximum allowable DG capacity. Nevertheless, each method has its own characteristics.

Protection resetting and directional recloser application methods can help increase the capacity for those DGs located behind the mid-line recloser. The obtained

results from the application of a directional recloser tend to be greater than those of the protection resetting since it completely eliminates the mis-operation of the mid-line recloser from a back-feed fault current. The protection resetting can help alleviate the back feed problem, however it depends on the level of existing pick-up current which can be increased. In addition, the raise of setting will result in longer system fault clearing time.

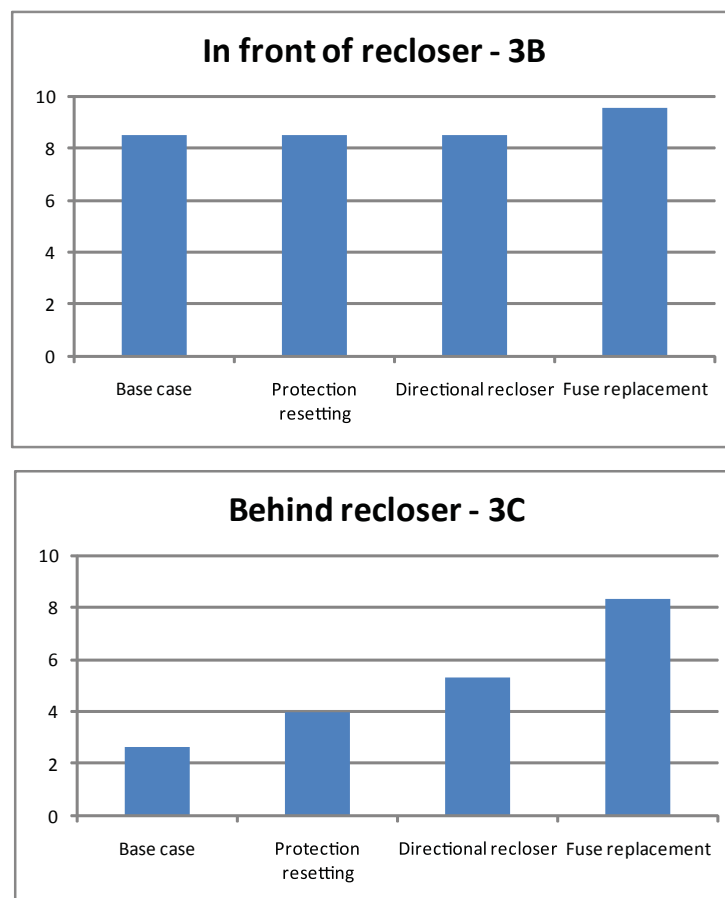


Figure 7.7 The comparison of all protection adjustment methods

Replacement of fuse with recloser method can solve both the back-feed current problem and the fault current constraint on the fuse saving scheme. It should be noticed that only this method can improve the results for the DGs located in front of the mid-line recloser. As a result, this method allows highest DG penetration improvement. Figure 7.7 compares the results of all methods based on the same DG locations, i.e. 3B and 3C representing in front and behind the recloser, which clearly

shows that the fuse replacement method is the most promising one to allow more DG penetration than the base case, especially for the DG located behind the recloser. Nevertheless, the method will increase system fault clearing time especially for those faults on the main line behind the recloser since the fast operation is turned-off.

Table 7.8 summarizes the characteristics of each protection adjustment method. From the Table, the protection adjustment method can be selected in accordance with system conditions and utility requirement. For example, using the test system for illustration, if a DG capacity of 3 MW is requested for a connection at location 1C, utility may consider resetting protective devices method with acceptance of longer fault clearing time. However, if a DG capacity of 5 MW requests for connection, utility may apply a directional recloser method since it will be less costly than the replacement of fuse with recloser. However, for a proper justification, a pre-study of each method should be conducted to realize current status and potential increase of maximum allowable DG capacity.

Table 7.8 Summary of characteristic of each protection adjustment method

	Protection Resetting	Directional Recloser	Replacement of Fuse with Recloser
Effectiveness	DG behind recloser	DG behind recloser	DG behind and in front of recloser
Implementation consideration	No cost of new equipment but with longer fault clearing time	Installation of one directional recloser	Replace all lateral fuse behind recloser by recloser/dropout recloser with longer fault clearing time

7.3 System Service Quality Index Evaluation

The developed method is illustrated with the Modified RBTS Bus 2 shown in Appendix A with its reliability information in Appendix D. The section starts with the

application of the method on system reliability evaluation in the situation that the connected DG is larger than the maximum allowable. Then, the application of the method on system voltage sag evaluation in a presence of DG is presented. The benefit of the DG to system voltage sag performance can then be quantified.

7.3.1 Results of System Reliability

Feeder 3 of the Modified RBTS Bus 2 system shown in Figure 4.3 is applied for the illustration.

Based on the results in Section 7.1.1, Table 7.1, the maximum allowable of a DG with protection coordination consideration at location 3C is 2.64 MW. This implies that if a DG project of less capacity than 2.64 MW is applied for this location, it will not cause problem to the protection system coordination and thus will not degrade system reliability. However, if it is assumed in this case that the DG capacity to be connected at this location is 6 MW. The proposed method will be used to evaluate reliability performance and level of protection mis-coordination. Base on the procedure in Section 6.3, the PMA for the back feed problem is firstly determined.

Step 0: From Table 3.2, the recloser on Feeder 3 has a pick-up current setting of 270 A. Searching on the main line, it is found that every point along the line results in back-feed current greater than 270 A. Therefore, $PMA_{back-feed,m}$ is equal to 7.75 km.

Step 1: Searching on the lateral in front of the mid-line recloser, it is also determined that every point is resulted in back-feed current greater than 270 A. Therefore, $\Sigma PMA_{back-feed,l}$ is equal to 10.75 km.

The above PMA can be illustrated as shown in Figure 7.8.

Then, PMA for fuse saving scheme is determined as described below.

Step 0: According the selection of fuse size shown in Table 3.2 and the coordination plot in Figure 3.7, the maximum fault current design for fuse saving scheme between recloser fast curve and fuse 65K is approximately 2,300 A.

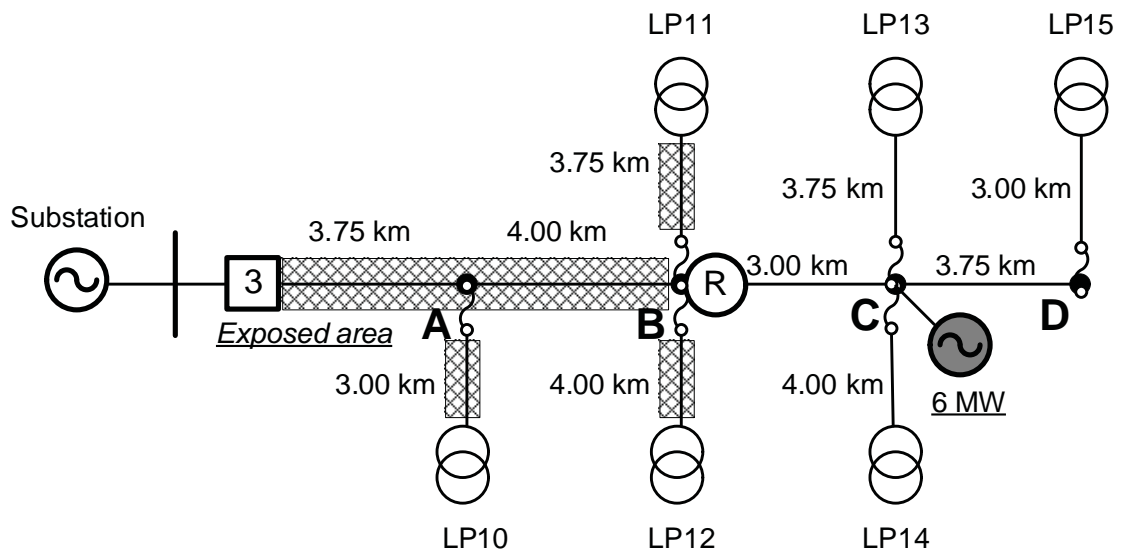


Figure 7.8 $PMA_{back-feed}$ in main and lateral feeders

Step 1: Searching on the lateral behind the mid-line recloser, it is determined that the lateral supplying LP13 and LP14 has PMA of 0.29 km each. Therefore, $\Sigma PMA_{fuse-save,l}$ is equal to 0.58 km.

The above PMA can be illustrated as shown in Figure 7.9.

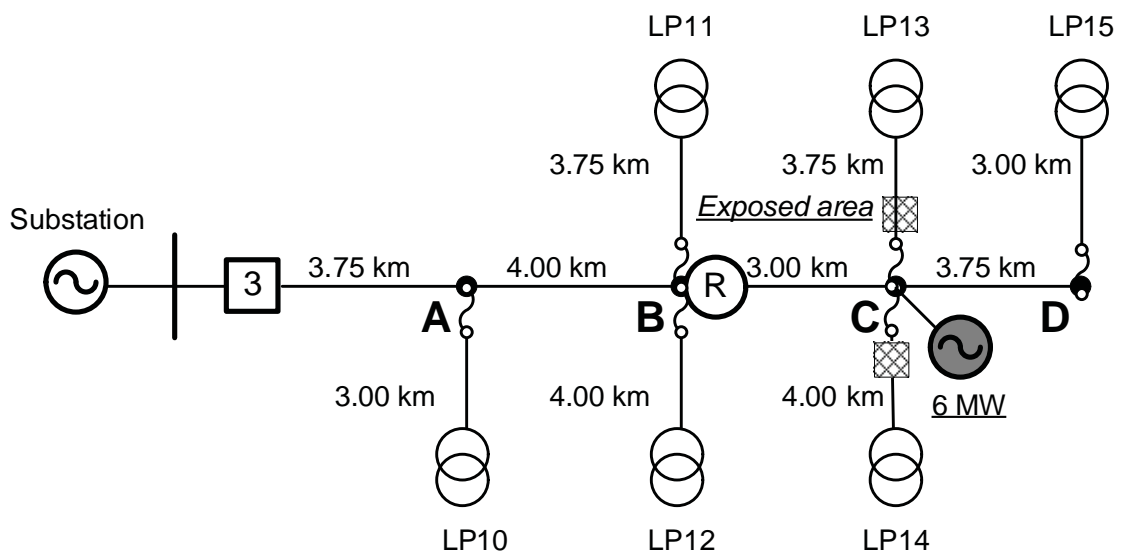


Figure 7.9 $PMA_{fuse-save}$ in lateral feeders

Since fuse-fuse coordination does not exist in the system, $PMA_{fuse-fuse}$ is equal to zero value.

After obtaining the value of PMA, the PMI can be calculated according to (6.13) as follows:

$$\begin{aligned}
 PMI &= 7.75(0.060) + 10.75(0.060 + 0.046) + 0.58(0.060) \\
 &= 1.6393
 \end{aligned}
 \tag{7.1}$$

From the above calculation, PMI is determined to be 1.6393 times/year. This implies that the connection of 6 MW DG at location 3C will result in protection mis-coordination event in the system for 1.6393 times/year. Nevertheless, if the anti-islanding protection of the DG works perfectly as previously described in Section 4.4, the PMA for back-feed problem will be zero and the PMI is recalculated as 0.0348 time/year.

The new SAIFI and SAIDI value can be determined in the similar way as illustrated in Section 4.3 but with the update of λ_i and r_i according to (6.16) – (6.17). Table 7.9 presents the updated value of λ_i and r_i from the PMA above. New SAIFI and SAIDI are presented in Table 7.10.

Table 7.9 Update of λ_i and r_i from PMA for all load point in Feeder 3

LP	PMA (km)			λ_i (times/year)	r_i (min)
	back-feed,m	Σ back-feed,l	fuse-save,l		
LP10	0	0	0	0.6745	383.93
LP11	0	0	0	0.7540	372.57
LP12	0	0	0	0.7805	369.30
LP13	7.75	10.75	0.29	2.2889	224.91
LP14	7.75	10.75	0.29	2.3004	226.18
LP15	7.75	10.75	0	2.4095	240.27

Table 7.10 SAIFI and SAIDI value of Feeder 3 after DG connection

	Base case	DG 6 MW at 3C	% Change
SAIFI (times/year)	0.7365	0.7670	4.14%
SAIDI (min)	277.74	281.40	1.32%

In this example, λ_i and r_i are changed only for those location behind a mid-line recloser. The obtained results show that a large DG can reduce system reliability by increasing both SAIFI and SAIDI. In this example, the SAIFI is increased by 4.14% and SAIDI by 1.32%. Again, if PMA for back-feed problem is zero, the SAIFI and SAIDI will be slightly increased to 0.7366 and 277.75 respectively. However, the change depends largely on the system configuration and number of customer at each location.

7.3.2 Results of System Voltage Sag

In this section, the proposed method for system voltage sag evaluation is demonstrated with the modified RBTS Bus 2. In this case, it is assumed that a DG of 6 MW is installed at location 3B, by which its capacity is less than the maximum allowable according to Table 7.1. Therefore, the benefit from DG to the system service quality will be of interest.

From the procedure in Section 6.3, the SARFI-X can be calculated and is shown in Table 7.11.

Based on the results, it is obvious that the connection of DG in the system can improve system voltage sag performance. In this example, an increase in fault level on the system from the DG can help improve the system voltage sag performance by almost 10%. The most effective area in this example is in the range of 50-70% voltage sag.

Table 7.11 SARFI-X improvement after 6 MW DG connection at location 3B

Voltage sag (p.u.)	SARFI-X (times/year)		% Improvement
	Base case	DG 6 MW at 3B	
0.9	13.8405	13.8405	0.00%
0.8	13.7265	13.1345	4.31%
0.7	8.6841	7.7496	10.76%
0.6	4.8039	4.2809	10.89%
0.5	2.6332	2.2848	13.23%
0.4	1.4076	1.3092	6.99%
0.3	0.9136	0.8500	6.96%
0.2	0.5384	0.5003	7.08%
0.1	0.2416	0.2242	7.20%

As for SARFI-Curve, the proposed procedure in Section 6.3 will be applied to the same system. The obtained results are shown in Table 7.12. It can be seen that in this example, SARFI-SEMI F47 gets improve by approximately 7%, where as a bigger improvement can be found in SARFI-ITIC, which is increased by almost 20%.

Table 7.12 SARFI-Curve improvement after 6 MW DG connection at location 3B

Curve	SARFI-Curve (time/year)		% Improvement
	Base case	DG 6 MW at 3B	
SEMI F47	3.0257	2.8025	7.38%
ITIC	6.7519	5.4244	19.66%

From the above simulation results, it can be concluded that the DG can improve system voltage sag performance if the installed capacity is less than the maximum allowable DG capacity. In addition, the improvement can be quantified and realized by the proposed method.

7.3.3 Summary

The proposed method has been used to evaluate system service quality with the presence of DG.

The reliability evaluation is performed through the concept of PMA by which the frequency of protection mis-coordination for a considered period of time can be quantified. Additionally, PMA can be applied to calculate for a new SAIFI and SAIDI. It is clearly seen from the result that a larger penetration of DG than maximum allowable will result in system reliability degradation.

Nevertheless, if the installed DG capacity is less than the maximum allowable, the proposed approximation method can be applied to calculate for the improvement on system voltage sag indices, i.e. SARFI-X and SARFI-Curve. Based on the results, it has been shown that the benefit from the DG on the system voltage sag performance can be quantified. In addition, it is implied that the proposed method is advantageous to the simple and exact equation method since it can be applied to complicated systems including those having a DG connection, and to estimate for SARFI-Curve indices

7.4 Appropriate DG Output Power with Loss and Customer Load Profile Consideration

In this section, it is supposed that an existing DG capacity is already known. The proposed methodology in Section 6.4 will be applied to the test system to calculate for appropriate DG output power with loss and customer load profile consideration. Again, the Modified RBTS Bus 2 will be used for the illustration. The connected DG unit is assumed to be connected at location B. The obtained results from the proposed method will then be compared with the results from direct search method.

7.4.1 Simulation Results Using Direct Search Method

To illustrate for determination of appropriate DG output power using direct

search method, it is assumed that the DG is installed at location B of Feeder 1 as shown in Figure 5.1. Based on information of customer type location and load profile presented in Appendix, a single feeder load profile can be established by aggregating customer load profile of all load points. Consequently, the feeder load profile of Feeder 1 can be established and divided into 7 time intervals as presented in Table 7.13.

Table 7.13 Aggregated feeder load pattern

No.	Time	Type of customer (percent of peak load)			Total load	
		R	S	C	P (MW)	Q (MVAR)
1	22:00-05:00	25%	30%	30%	1.65	1.32
2	05:00-08:00	50%	30%	30%	2.30	1.84
3	08:00-10:00	35%	100%	30%	3.19	2.55
4	10:00-16:00	35%	100%	100%	4.24	3.39
5	16:00-18:00	60%	30%	100%	3.61	2.89
6	18:00-21:00	100%	30%	80%	4.35	3.48
7	21:00-22:00	60%	30%	30%	2.56	2.05

Table 7.14 Appropriate output of the DG according to load variation

No.	Time	DG Output Power (MW)
1	22:00-05:00	2.90
2	05:00-08:00	3.78
3	08:00-10:00	5.92
4	10:00-16:00	8.18
5	16:00-18:00	6.35
6	18:00-21:00	7.14
7	21:00-22:00	4.13

After obtaining feeder load profile, a direct search method is applied at each time interval. The obtained simulation results are shown in Table 7.14, from which an appropriate output DG profile can be calculated and shown in Figure 7.10. It implies that, if appropriate DG output powers are within this output profile, it will certainly benefit the system in term of system loss reduction. Otherwise, the DG is likely to increase the system loss.

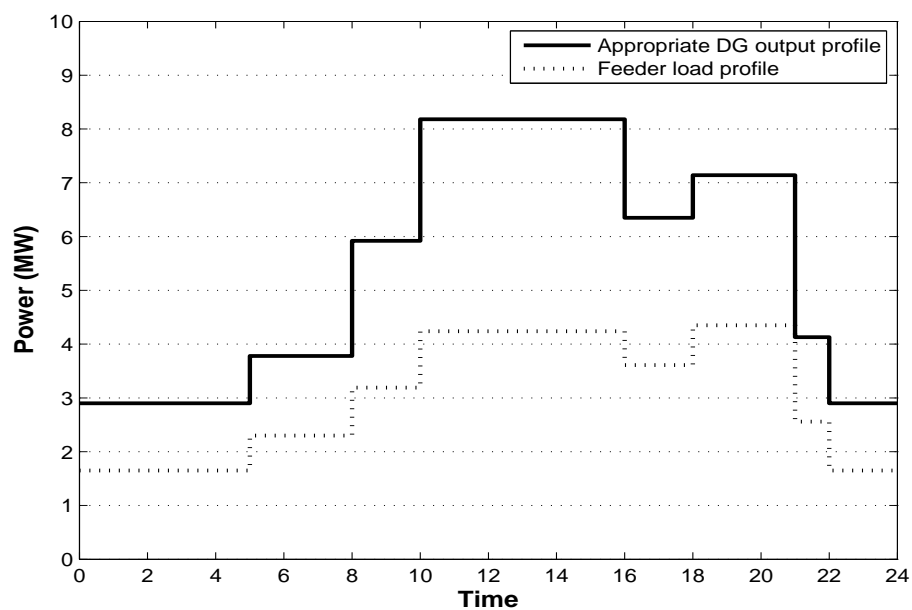


Figure 7.10 Appropriate DG output at location B and feeder load profile

7.4.2 Simulation Results Using Approximation Method

From Table 5.1 in Section 5.2, appropriate output power of the DG determined at peak load or α_B is 10.54 MW. By using (5.10), the virtual voltage (W_b) can be determined as shown below.

$$\begin{aligned}
 W_B &= 0.7912 \times (4.4662) + 0.7912 \times (6.1998) \\
 &= 8.4394
 \end{aligned}
 \tag{7.2}$$

Consequently, by applying (6.31), the relationship between appropriate DG

output and load variation can be established as follows:

$$\Delta\alpha_B = -\left(\sum_{i=1}^7 \Delta\alpha_i \times A_i\right) \times \frac{10.54}{8.4394} \quad (7.3)$$

Where i is load point number, $\Delta\alpha_i$ is percent change from maximum load at load point i , i.e., if load factor is 25%, percent change from maximum load or $\Delta\alpha$ is 75%, and the values of A_i for each load point are as shown below.

$$A_i = \begin{cases} 0.7912, & i = 1, 2 \\ 1.5825, & i = 3, 4, 5, 6, 7 \end{cases} \quad (7.4)$$

After obtaining a value of $\Delta\alpha_B$, a new appropriate DG output can be calculated from (7.5).

$$\alpha_B' = 10.54 + \Delta\alpha_B \quad (7.5)$$

Based on (7.3) – (7.5), an appropriate DG output power according to system demand in Table 7.13 can be calculated. The obtained results are presented in Table 7.15 and compared with the results from the direct search method.

According to Table 7.15, it can be seen that the relationship between load variation and appropriate DG output provides a fair accuracy compared to the direct search method. However, the problem becomes a simple linear equation. Consequently, the method is suitable for the applications which require less calculation time, while small error can be allowed.

Based on the above results, it can be found that the proposed method provides the appropriate outputs with error ranging from 2-16 % when compared to the results from direct search method. The cause of the error mainly comes from the fact that the proposed method is developed based on the assumption that voltage at every bus is

equal to 1.0 p.u. Therefore, if the original feeder voltage is well regulated, it is anticipated that the error will be less than the ones shown in the Table 7.15. Table 7.16 demonstrates the average system bus voltage deviation if a DG with capacity of 10.54 MW is connected at point B for the whole study period. It can be found that when the deviation of system bus voltage magnitude and angle from the assumed 1.0 p.u. is high, the percent errors according to Table 7.15 are correspondingly increased.

Table 7.15 Appropriate output power of a DG at location B

No.	Time	DG output (MW)			Percent Difference (1), (2)
		Peak Load	Direct Search(1)	Proposed Method(2)	
1	22:00-05:00	10.54	2.90	3.36	16%
2	05:00-08:00	10.54	3.78	4.22	12%
3	08:00-10:00	10.54	5.92	6.24	5%
4	10:00-16:00	10.54	8.18	8.31	2%
5	16:00-18:00	10.54	6.35	6.63	4%
6	18:00-21:00	10.54	7.14	7.41	4%
7	21:00-22:00	10.54	4.13	4.56	10%

Table 7.16 Average system bus voltage at different load level when DG of 10.54 MW is connected at location B

No.	Time	Total load		Average voltage deviation (p.u.)
		P (MW)	Q (MVAR)	
1	22:00-05:00	1.65	1.32	0.0498
2	05:00-08:00	2.30	1.84	0.0477
3	08:00-10:00	3.19	2.55	0.0431
4	10:00-16:00	4.24	3.39	0.0399
5	16:00-18:00	3.61	2.89	0.0420
6	18:00-21:00	4.35	3.48	0.0411
7	21:00-22:00	2.56	2.05	0.0469

Table 7.17 presents total power loss and energy loss as the results of the DG output power for each load level shown in Table 7.15. It can be seen that the total power loss and energy loss for the case of having no DG and the output power level from the direct search method are the same, i.e. loss does not increase. The results from the proposed method are slightly higher than that of both cases. In term of energy loss, the result from the proposed method is 8% higher. This is due to the node voltage assumption of 1.0 p.u. by the proposed method. However, if the DG is operated as a must-run unit for a single output power level, calculated from only peak demand, the total power loss increases significantly and the energy loss is almost four times to that of the proposed allowable output power of the DG. With these results, it is clear that if we can keep the DG output within the allowable levels, there will be a high chance of feeder loss reduction.

Table 7.17 Power and energy losses

No.	Time	Total Power Loss (MW)			
		Peak Load	Direct Search	Proposed Method	No DG
1	22:00-05:00	0.2682	0.0149	0.0200	0.0149
2	05:00-08:00	0.2513	0.0255	0.0317	0.0255
3	08:00-10:00	0.2195	0.0626	0.0692	0.0626
4	10:00-16:00	0.2066	0.1248	0.1285	0.1248
5	16:00-18:00	0.2196	0.0765	0.0828	0.0765
6	18:00-21:00	0.2122	0.0955	0.1021	0.0955
7	21:00-22:00	0.2455	0.0309	0.0373	0.0309
Energy Loss (kWh)		5630.6	1525.5	1653.1	1525.5

With the application of the direct search or the proposed method, appropriate DG output according to customer daily load profiles can be established. Consequently, providing that the DG is a dispatchable unit, the utility can control an appropriate DG output in such a way that it will not increase total system loss.

However, if the DG is a non-dispatchable unit and its output is kept constant, e.g. at 6 MW, it will increase system loss during off peak period whereas it only help decrease system loss during peak period.

7.4.3 Summary

This section has illustrated the impact of load variation to an appropriate DG output power which will not increase total system loss. The study shows that when load decreases, the DG output power should be reduced accordingly. Otherwise, the DG may increase total system loss.

An appropriate DG output power according to system demand can be determined from the direct search method. In addition, the BCDLA is employed to quickly estimate appropriate DG output power.

Based on the proposed method, an appropriate DG output profile for a considered day can be established. The result assures that the DG being dispatched with the obtained output profile is likely not to result in the loss increase.

CHAPTER VIII

APPLICATIONS ON ACTUAL SYSTEM

This section demonstrates the application of the proposed method in this thesis on a practical test system based on PEA data referred as PEA test system. The data of the system and its protection system are described in Appendix E [46].

In general, the PEA test system is similar to the Modified RBTS Bus 2 for system configuration and protection design. In addition, the system contains the fuse-fuse coordination. As a result, this test system is a good and practical example for testing the method proposed in this thesis.

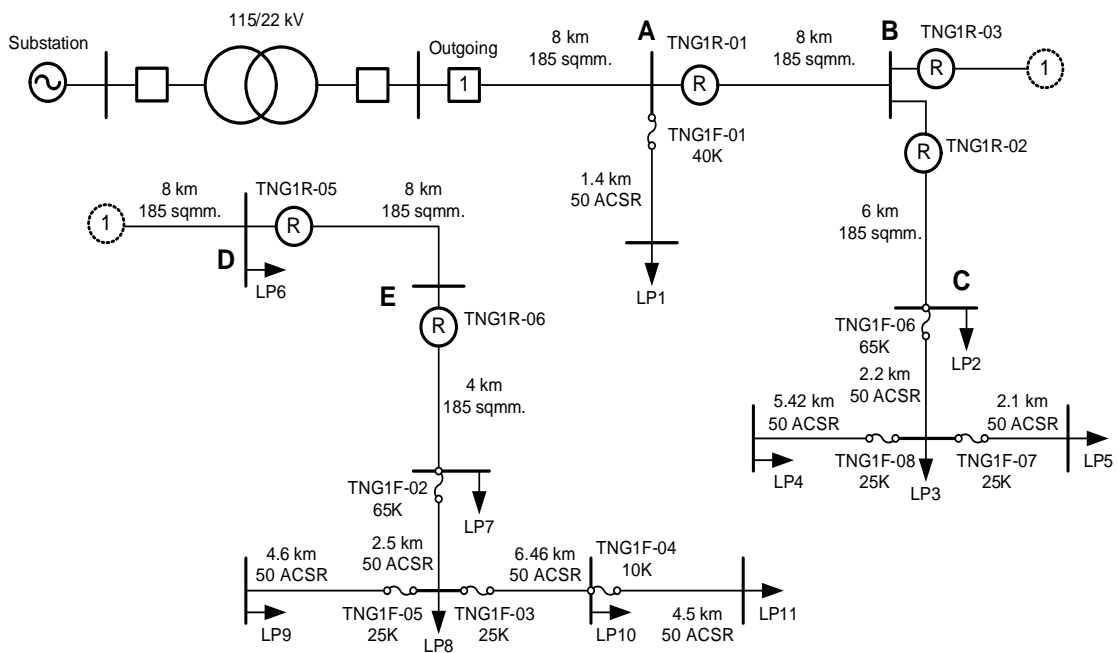


Figure 8.1 PEA test system and potential locations for DG connection

Determination of maximum allowable DG capacity with protection coordination consideration

To begin with, it is assumed that the potential locations for DG connection on the test system are marked by a capital letter as shown in Figure 8.1. Similarly to the Modified RBTS Bus 2 case, the locations are restricted to the main line only.

Accordingly, the maximum allowable DG capacity with protection coordination consideration is determined and presented in Table 8.1.

Table 8.1 Maximum allowable DG capacity of PEA test system

Feeder	Location	Maximum allowable DG capacity (MW)
1	A	6.9694*
	B	3.4915
	C	1.9677
	D	2.8360
	E	2.5150

* The result is limited by loss constraint instead of protection coordination.

It can be seen that the results in all location are less than the maximum allowable DG capacity of 8 MW specified in PEA regulation for a 22 kV system by which the number is determined primarily from feeder capacity [3].

Service quality evaluation

Since the connected DG of 3 MW capacity is within the maximum allowable study results according to Table 8.1, the presence of DG will not impact on protection system coordination. As a result, system reliability measured by SAIFI and SAIDI remains unchanged.

For the voltage sag event, the benefit from a presence of DG through an improvement on SARFI-X and SARFI-Curve index can be presented in Table 8.2 and 8.3 respectively.

Appropriate DG output power profile with customer load profile consideration

Next, it is assumed that the DG capacity of 3 MW is to be connected at location B. With customer types according to Appendix E, Table E.2, an appropriate

DG output power profile which does not increase system loss can be determined. First, the direct search method is applied as follows.

Step 0: The feeder load profile is established as shown in Table 8.4.

Step 1: At each interval, the direct search method is applied to determined appropriate DG output power which will not increase system loss. The obtained results are shown in Table 8.5. Figure 8.2 presents a plot of the results and the feeder load profile.

Table 8.2 SARFI-X improvement after 3 MW DG connection at location B

Voltage sag (p.u.)	SARFI-X (times/year)		% Improvement
	Base case	DG 3 MW at B	
0.9	6.3160	6.0314	4.51%
0.8	3.3136	3.1074	6.22%
0.7	1.6059	1.6059	0.00%
0.6	0.9975	0.9922	0.53%
0.5	0.6402	0.6402	0.00%
0.4	0.4320	0.4320	0.00%
0.3	0.2809	0.2809	0.00%
0.2	0.1659	0.1659	0.00%
0.1	0.0742	0.0742	0.00%

Table 8.3 SARFI-Curve improvement after 3 MW DG connection at location B

Curve	SARFI-Curve (time/year)		% Improvement
	Base case	DG 3 MW at B	
SEMI F47	0.8475	0.8474	0.01%
ITIC	1.2502	1.1426	8.61%

Table 8.4 Feeder load pattern of PEA test system

No.	Time	Type of customer (percent of peak load)			Total load	
		R	S	C	P (MW)	Q (MVAR)
1	22:00-05:00	25%	30%	30%	0.8700	0.6525
2	05:00-08:00	50%	30%	30%	1.4700	1.1025
3	08:00-10:00	35%	100%	30%	1.3900	1.0425
4	10:00-16:00	35%	100%	100%	1.7400	1.3050
5	16:00-18:00	60%	30%	100%	2.0600	1.5450
6	18:00-21:00	100%	30%	80%	2.9200	2.1900
7	21:00-22:00	60%	30%	30%	1.7100	1.2825

R: Residential, S: State Agency, and C: Commercial

Table 8.5 Appropriate output of the DG at location B according to load variation

No.	Time	DG Output Power (MW)
1	22:00-05:00	1.5079
2	05:00-08:00	2.4863
3	08:00-10:00	2.4783
4	10:00-16:00	3.0000
5	16:00-18:00	3.0000
6	18:00-21:00	3.0000
7	21:00-22:00	2.8818

From Table 8.5, it should be noticed that for the time interval from 10:00 to 21:00, appropriate DG output powers are determined to be 3.2211, 3.6295, and 5.0378 respectively. Since these results are greater than the maximum output power of the connected DG, the output power for these time intervals are therefore trimmed down to 3 MW.

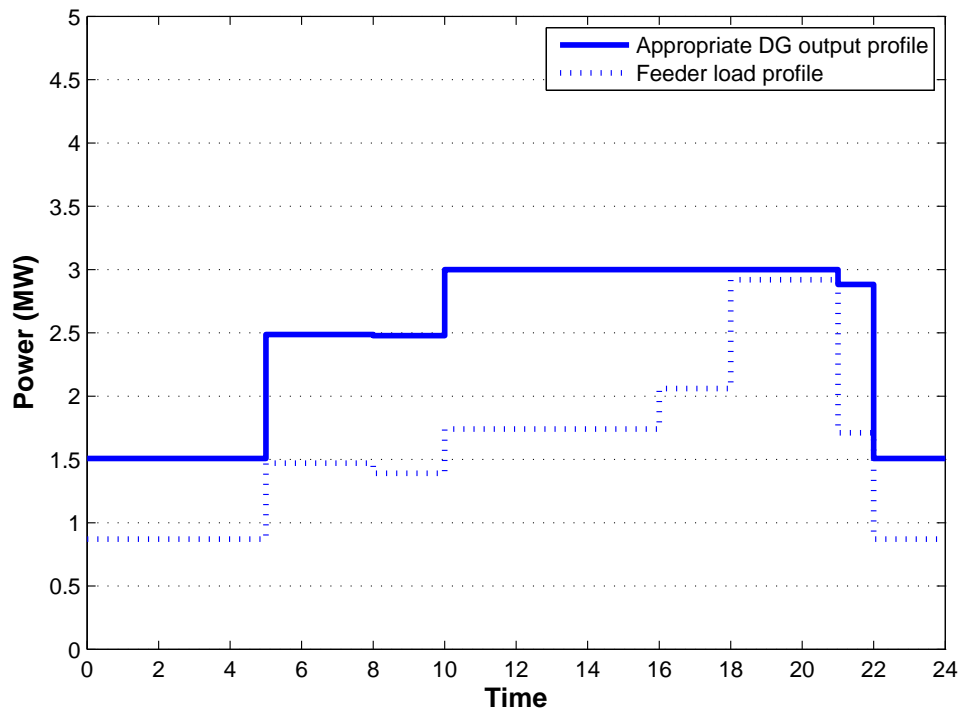


Figure 8.2 Appropriate DG output at location B and feeder load profile

Secondly, the approximation method for establishing the relationship between appropriate DG output power and customer load profiles is illustrated below.

Step 0: By applying the method in Section 5.2, the maximum allowable output power of the DG at peak load or α_B is determined to be 5.8748 MW. Using (5.10), the virtual voltage (W_B) can be determined as shown below.

$$\begin{aligned}
 W_B &= 0.29043 \times (2.5748) + 0.29043 \times (3.5748) \\
 &= 1.78606
 \end{aligned}
 \tag{8.1}$$

Step 1: Applying (6.31), the relationship between appropriate DG output and load variation can be established as follows.

$$\Delta\alpha_B = -\left(\sum_{i=1}^{11} \Delta\alpha_i \times A_i\right) \times \frac{5.8748}{1.78606} \quad (8.2)$$

Where i is load point number and the value of A_i for each load point are shown below.

$$A_i = \begin{cases} 0.29043, & i = 1 \\ 0.58087, & i = 2-11 \end{cases} \quad (8.3)$$

Step 2: From (8.2) and (8.3), an approximated DG output power profile can be calculated as follows.

Table 8.6 Appropriate output power of a DG at location B

No.	Time	DG output (MW)			Percent Difference (1), (2)
		Peak Load	Direct Search(1)	Proposed Method(2)	
1	22:00-05:00	5.8748	1.5079	1.9485	29%
2	05:00-08:00	5.8748	2.4863	2.8560	15%
3	08:00-10:00	5.8748	2.4783	2.8465	15%
4	10:00-16:00	5.8748	3.2211	3.5152	9%
5	16:00-18:00	5.8748	3.6295	3.8877	7%
6	18:00-21:00	5.8748	5.0378	5.1488	2%
7	21:00-22:00	5.8748	2.8818	3.2190	12%

Energy loss evaluation of an option on DG output power profiles

From Table 8.6, the resulted energy loss from the operation of DG according each output power profile can be evaluated. Again, since the connected DG is of 3 MW, those results of output power which exceeds this number are therefore adjusted

to 3 MW. In addition, in this example, the obtained results will be compared with the results from DG capacity of 8 MW based on PEA regulation. The evaluation results are presented in Table 8.7.

Table 8.7 Power and energy losses

No.	Time	Total Power Loss (MW)			
		8 MW DG	Direct Search	Proposed Method	No DG
1	22:00-05:00	1.8625	0.0521	0.0838	0.0521
2	05:00-08:00	0.7273	0.0606	0.0773	0.0606
3	08:00-10:00	0.4846	0.0396	0.0507	0.0396
4	10:00-16:00	1.3762	0.1894	0.1894	0.1894
5	16:00-18:00	0.4464	0.0689	0.0689	0.0892
6	18:00-21:00	0.6238	0.1539	0.1539	0.2541
7	21:00-22:00	0.2345	0.0272	0.0329	0.0272
Energy Loss (kWh)		5755.25	591.74	656.95	712.15
Percent of Energy Loss		808.15%	83.09%	92.25%	100.00%

It can be seen that operating DG with appropriate output profiles from both direct search and proposed method will not result in system loss increase, while running DG output power constantly at 8 MW will increase system loss by eight times approximately.

Discussions

From the analyses of the PEA test system in Figure 8.1, the maximum allowable DG capacity with protection coordination consideration is determined as shown in Table 8.1. For example, at location B, it is determined to be 3.49 MW. As a result, a request for DG connection of 3 MW at this location can be approved.

It is supposed that a DG of 3 MW capacity is installed at location B. The benefit from the DG on system voltage sag performance can be realized from the results in Table 8.2 and 8.3. It can be seen that SARFI-X is improved for a voltage sag of 0.6, 0.8, and 0.9 p.u., whereas the biggest improvement is found from SARFI-ITIC.

From the proposed method, the DG should be dispatched according to the appropriate DG output profile in Figure 8.2 as not to increase system loss. The dispatch according to the result from BCDLA method in Table 8.6, though contains some errors, is also possible since the analyses in Table 8.7 shows that it will not increase system loss.

CHAPTER IX

CONCLUSIONS

This thesis has explored the pattern of protection mis-coordination which may be caused by the presence of DG in a distribution feeder. Based on the obtained classification of protection mis-coordination, the DG capacity which does not cause protection coordination failure can be formulated. Accordingly, a methodology to identify maximum allowable DG capacity has been developed. The method also takes into account other system operating constraints, e.g. voltage regulation, power loss. It is also capable of determining maximum DG capacity taking into account existing DG units. With the limitation imposed by the existing protection system, this thesis has also investigated protection adjustment method in order to allow a higher penetration of DG.

In addition, this thesis has developed a method and proposed new service index, i.e. PMI, to calculate the impact of DG on system service quality. An increase in SAIFI and SAIDI resulting from the protection mis-coordination due to a larger DG unit can be calculated. Moreover, an improvement on system voltage sag, i.e. SARFI-X and SARFI-Curve from a present of DG in the system can be evaluated

Besides system reliability, power loss is another important issue. Too large output power from the connected DG can increase power loss significantly. Moreover, demand variation during a day or customer load profile is another important factor for determining appropriate DG output power. Accordingly, this thesis has proposed the methodology for determining DG output power profile, i.e. direct search and approximation method such that power loss will not increase. In addition, the energy loss calculation has been demonstrated to evaluate the impact of DG to the system loss.

In conclusion, the key contributions from this thesis are as follows:

- (a) Classification of protection mis-coordination from the presence of DG,

- (b) Methodology for determining maximum allowable DG capacity with protection coordination consideration,
- (c) Protection adjustment procedure to allow a larger DG capacity,
- (d) Methodology for evaluating system service quality, and
- (e) Methodology for determining appropriate DG output power with power loss and customer load profile consideration.

The proposed methodology can help utility fasten the screening process of a request for DG connection. As a result, the DG will not create problem to the protection system coordination. Unless there is a request for a large DG connection, the proposed methods can also be applied to determine a level of impact from the DG to the system protection. In addition, the protection adjustment method can also be applied for a higher DG penetration.

Regarding power loss, a dispatch of DG output power according to the proposed appropriate output profile can help utilities control their system loss not to significantly increase, which is beneficial to utility cost. Furthermore, the proposed method can help utility evaluate the benefit from the DG to the improvement on system voltage sag performance, by which it can be used to compare among several DG sites or to select a good location for a DG.

The test with two systems, i.e. modified RBTS Bus 2 and PEA test system have shown promising results by which all the proposed method can be exploited for several future research areas, e.g. distributed generation, protection, reliability and possibly smart grids, including a wide range of practical application for the distribution utility.

References

- [1] Farret, F. A., and Simões, M. G. Integration of Alternative Sources of Energy. New Jersey: John Wiley & Sons, Inc., 2006.
- [2] Jenkins, N., Allan, R., Crossley, P., Kirschen, D., and Strbac, G. Embedded Generation. London: The Institution of Electrical Engineers, 2000.
- [3] PEA, MEA Regulations for the Purchase of Power from Very Small Renewable Energy Power Producers, 2006.
- [4] EPPO Report on VSPP Status based on Fuel Types, 2011.
- [5] Barker, P. P., Mello, R. W. D. Determining the impact of distributed generation on power system: Part 1 – radial distribution systems. IEEE Power Engineering Society Summer Meeting 3 (2000): 1645-1656.
- [6] Doyle, M.T. Reviewing the Impacts of Distributed Generation on Distribution System Protection. IEEE Power Engineering Society Summer Meeting 1 (July 2002): 103-105.
- [7] Junlakarn, S., and Hoonchareon, N. Optimal Sizing of Distributed Generators in Consideration of Impacts on Protection Coordination Using Genetic Algorithms. Proceedings of the 30th Electrical Engineering Conference (EECON) 1 (October 2007): 109-112.
- [8] Chaitusaney, S., and Yokoyama, A. Impact of Protection Coordination on Sizes of Several Distributed Generation Sources. The 7th International Power Engineering Conference (IPEC) 2 (December 2005): 669-674.
- [9] California Electric Rule No. 21 (2005)
- [10] IEEE Standard 1547-2003 IEEE Standard for Interconnecting Distributed Resources with Electric Power Systems, 2003

- [11] Borges, C., Falcao, D. Optimal distributed generation allocation for reliability, losses, and voltage improvement. International Journal of Electrical Power and Energy Systems 28 (2006): 413-420.
- [12] Singh, D., Singh, D., Verma, K. Multi-objective optimization for DG planning with load models. IEEE Transactions on Power Systems 24, 1 (2009): 427-436.
- [13] Ayres, H.M., Freitas, W., De Almeida, M.C., and Da Silva, L.C.P. Method for determining the maximum allowable penetration level of distributed generation without steady-state voltage violations. IET Generation, Transmission & Distribution, 4, 4 (2010): 495-508.
- [14] Con Edison Distributed Generation - Process Guide. http://www.coned.com/dg/process_guide/processGuide.asp, accessed 2010.
- [15] Wang, D. Y. and Lee, W. J. Distributed Generation Policy of Con Edison. IEEE Power and Energy Society General Meeting (2008)
- [16] Public Utility Commission of Texas Distributed Generation Interconnection Manual, 2002.
- [17] Samotyj, M. Service Quality Index – Example Application. California: EPRI, 2006.
- [18] Bollen, M. H. J. Understanding Power Quality Problems – Voltage Sags and Interruptions. New York: The Institute of Electrical and Electronics Engineers, Inc., 2000.
- [19] Billinton, R., Allan, R. N. Reliability Evaluation of Power Systems. 2nd edn. New York: Plenum Press, 1996.

- [20] Carpaneto, E., Chicco, G., Akilimali, J. S. Branch current decomposition method for loss allocation in radial distribution systems with distributed generation. IEEE Transactions on Power Systems 21, 3 (2006): 1170-1179.
- [21] Keller, J. and Kroposki, B. Understanding Fault Characteristics of Inverter-Based Distributed Energy Resources. NREL, 2010.
- [22] Kasikci, I. Short Circuits in Power Systems: A Practical Guide to IEC 60909. Wiley-VCH, 2002.
- [23] Saadat, H. Power System Analysis. McGraw-Hill, 1999.
- [24] Boutsika, T. N., Papathanassiou, S. A. Short-circuit calculation in networks with distributed generation. Electric Power Systems Research 78 (2008): 1181-1191.
- [25] Gers, J., and Holmes, E. Protection of Electricity Distribution Networks. 2nd edn. Institution of Engineering and Technology, 2004.
- [26] Alstom Network Protection and Automation Guide, 2002.
- [27] Power Systems Division, McGraw-Edison Company Distribution System Protection Manual, 1971.
- [28] Blackburn, J. L., Domin, T. J. Protective Relaying Principles and Applications. 3rd edn. CRC Press Taylor & Francis Group, 2007.
- [29] IEC Standard 60255 Electrical Relays, 1988.
- [30] Cooper Power Systems Recloser: Electrical Apparatus 280-91, 1995.
- [31] S&C Electric Company Positrol Fuse Links: Time-current characteristic curves, S&C "K" speed, 1986.

- [32] Allan, R. N., Billinton, R., Sjarief, I., Goel, L., So, K. S. A reliability test system for educational purposes – basic distribution system data and results. IEEE Transactions on Power Systems 6 (1991): 813-820.
- [33] Saksornchai, T., Eua-Arporn, B. Determination of allowable capacity of distributed generation with protection coordination consideration. Engineering Journal 13, 3 (2009): 29-44.
- [34] ITIC ITI(CBEMA) Curve, 2000.
- [35] SEMI F47-0200 Specification for Semiconductor Processing Equipment Voltage Sag Immunity. SEMI, 2000.
- [36] Bollen, M. H. J. Method of critical distances for stochastic assessment of voltage sags. Proceedings of Institute Electrical Engineering, Generation, Transmission & Distribution 145, 1 (January 1998): 70-76.
- [37] Borges, C. L. T. and Falcão, D. M. Impact of distributed generation allocation and sizing on reliability, losses and voltage profile. IEEE Power Tech Conference Proceedings 2 (2003): 1-5.
- [38] Atwa, Y. M. and El-Saadany, E. F. Reliability evaluation for distribution system with renewable distributed generation during islanded mode of operation. IEEE Transactions on Power Systems 24, 2 (May 2009): 572-581.
- [39] Conejo, A. J., Galiana, F. D., and Kockar, I. Z-Bus loss allocation. IEEE Transactions on Power System 16, 1 (2000): 105-109.
- [40] Fang, W. L. and Ngan, H. W. Succinct method for allocation of network losses. Proceedings of Institute Electrical Engineering, Generation, Transmission & Distribution 149, 2 (2002): 171-174.

- [41] Mutale, J., Strbac, G., Curcic, S. and Jenkins, N. Allocation of losses in distribution systems with embedded generation. Proceedings of Institute Electrical Engineering, Generation, Transmission & Distribution 147, 1 (2000): 7-14.
- [42] Zimmerman, R. D., Murillo-Sanchez, C. E. and Gan, D. MATPOWER: A MATLAB Power System Simulation Package. <http://www.pserc.cornell.edu/matpower>, accessed 2009.
- [43] Carlson, N. and Asgeirsson, H. A smart recloser for the smart grid. T&D World, 2008.
- [44] Mozina, C. The Impact of Distributed Generation. PAC World 5 (2008): 19-25.
- [45] Junlakarn, S. Optimal sizing of distributed generators in consideration of impacts on protection coordination using genetic algorithms. Master's Thesis, Department of Electrical Engineering, Faculty of Engineering, Chulalongkorn University, 2006.
- [46] Khundee, C. Radial distribution protection coordination analysis using an expert system. Master's Thesis, Department of Electrical Engineering, Faculty of Engineering, Chulalongkorn University, 2001.

APPENDICES

APPENDIX A

MODIFIED RBTS BUS 2

A modified RBTS BUS 2 [32-33] shown in Figure A.1 is used as the test system in this thesis. A 200 MVA fault level is assumed at the station bus (25 MVA transformer with impedance voltage 12.5% or 2.42 Ohm). In this test system, the line length is assumed to be increased by five times of the original data whereas the operating voltage is modified from 11 to 22 kV to be comparable with a typical characteristic of a distribution feeder of the Provincial Electricity Authority of Thailand.

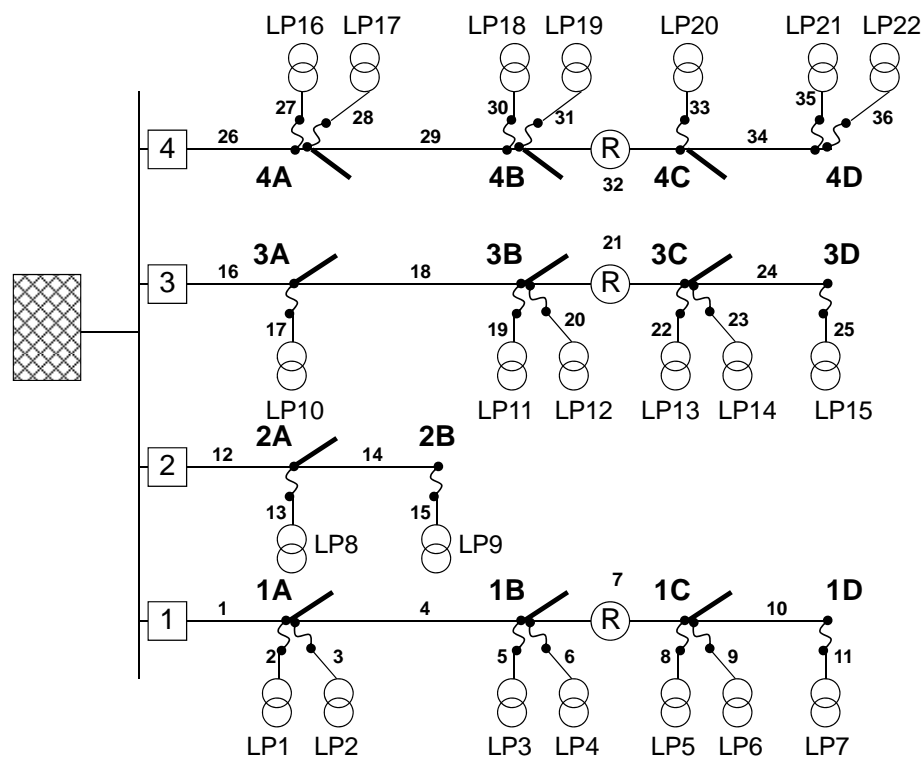


Figure A.1 Test System RBTS Bus 2

In Figure A.1, LP is represented for load point, and “R” is for a mid-line recloser. The number followed by capitalized letter indicates possible DG locations on

each feeder. As an example, “2B” represents the possible DG location is at point B in Feeder 2. In this study, the possible location for DG will be restricted to the main feeder. All necessary parameters, e.g. impedance, line length, and load are shown in Tables A.1-A.4. It was found from the base case analysis that the total system loss with no presence of DG is of 0.6094 MW.

Table A.1 Modified RBTS Bus 2 Feeder length data

No.	Feeder length (km)	Branch no.
1	3.0	2, 6, 10, 14, 17, 21, 25, 28, 30, 34
2	3.75	1, 4, 7, 9, 12, 16, 19, 22, 24, 27, 29, 32, 35
3	4.0	3, 5, 8, 11, 13, 15, 18, 20, 23, 26, 31, 33, 36

Table A.2 Modified RBTS Bus 2 Feeder impedance (Ohm/km)

Type	Impedance (Ohm/km)	
	Complex	Absolute
Main Feeder	$0.211 + 0.414j$	0.465
Lateral Feeder	$0.341 + 0.456j$	0.569

Table A.3 Modified RBTS Bus 2 Load information

Load Point (LP)	Customer type	Peak demand	
		Real power (MW)	Reactive power (MVAR)
1-3, 10, 11	Residential	0.8668	0.6934
12, 17-19	Residential	0.7291	0.5833
8	Medium Industry	1.6279	1.3023
9	Medium Industry	1.8721	1.4977
4, 5, 13, 14, 20, 21	State agency	0.9167	0.7334
6, 7, 15, 16, 22	Commercial	0.7500	0.6000
Total		20.0006	16.0006

Table A.4 Modified RBTS Bus 2 Load summary per feeder

Feeder	Load Point (LP)	Peak Demand	
		Real power (MW)	Reactive power (MVAR)
1	1-7	5.9338	4.747
2	8-9	3.5000	2.8000
3	10-15	5.0461	4.0369
4	16-22	5.5207	4.4167
Total		20.0006	16.0006

APPENDIX B

CUSTOMER LOAD PROFILE

In order to investigate the impact of load variation on an appropriate DG output level, customer load profile or load curve information is required. In this study, it is assumed that there are three types of customer, i.e. residential, state agency, and commercial in accordance with Table A.3. The daily load profile of each customer type for typical working days is assumed to be as shown in Figure B.1. It can be seen that the hourly load profile is presented in the percentage of its peak load.

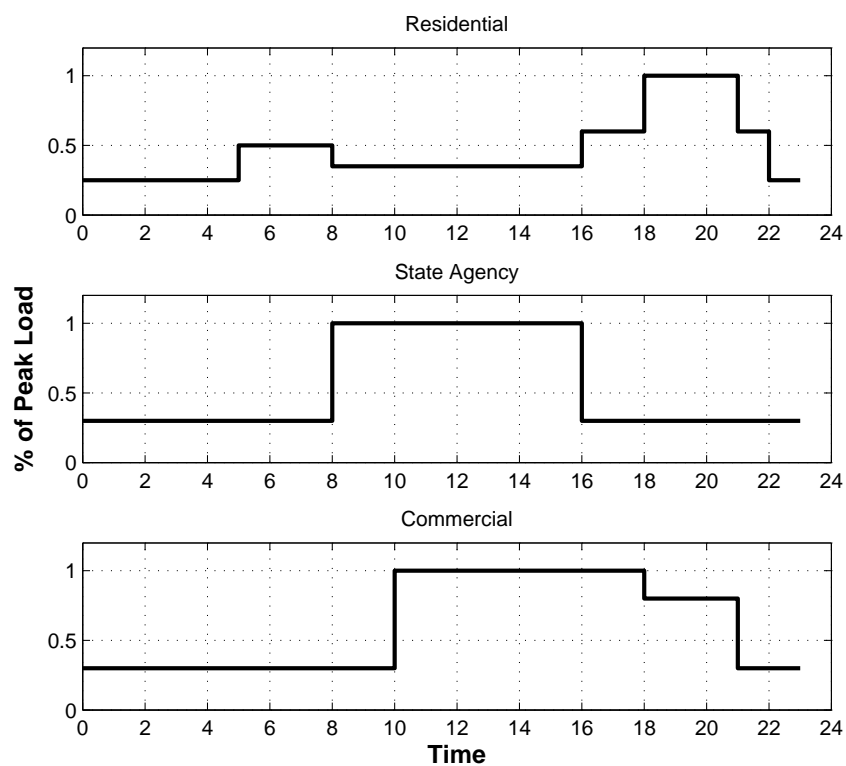


Figure B.1 Load profile of each customer type

APPENDIX C

PARAMETER OF DG

For fault analysis, the total sub-transient reactance including step-up transformer of the DG is assumed to be 0.25 per unit based on a typical value [24, 26]. Therefore, the DG will be modeled as a voltage source in series with a reactance of 0.25 per unit value connecting to the grid at PCC.

APPENDIX D

RELIABILITY DATA

This section provides a reliability data of the Modified RBTS Bus2 system based on the original RBTS Bus2 system [32]. The failure rate and repair time are presented in Table D.1.

Table D.1 Failure rate and repair time of the equipment in test system

No.	Item	Description	Value
1	λ_p	Failure rate (permanent fault)	0.046 times/year/km
2	λ_t	Failure rate (temporary fault)	0.060 times/year/km
3	r_p	Repair time (for permanent fault)	480 min (8 hr)
4	r_s	Switching time (for fuse replacement)	120 min (2 hr)

The type and number of customer at each load point in the test system is presented in Table D.2.

Table D.2 Type and number of customer at each load point

Feeder	LP	Type	Number
1	1	Residential	210
	2	Residential	210
	3	Residential	210
	4	State agency	1
	5	State agency	1
	6	Commercial	10
	7	Commercial	10
2	8	Medium industry	1
	9	Medium industry	1
3	10	Residential	210
	11	Residential	210
	12	Residential	200
	13	State agency	1
	14	State agency	1
	15	Commercial	10
4	16	Commercial	10
	17	Residential	200
	18	Residential	200
	19	Residential	200
	20	State agency	1
	21	State agency	1
	22	Commercial	10

APPENDIX E

PEA TEST SYSTEM

An outgoing Feeder 1 of Thoeng substation as shown in Figure E.1 [46] is applied as Provincial Electricity Authority (PEA) test system. A 200 MVA fault level is assumed at the station bus. The system operating voltage is at 22 kV. Besides system configuration, the figure shows protective devices location, i.e. circuit breaker, recloser, fuse and its size which is of K-Type. It also provides information of line type and line length where as LP represents a customer load point. Other related information, i.e. Line impedance, Customer data and Protection setting are presented in Table E.1 – E.3.

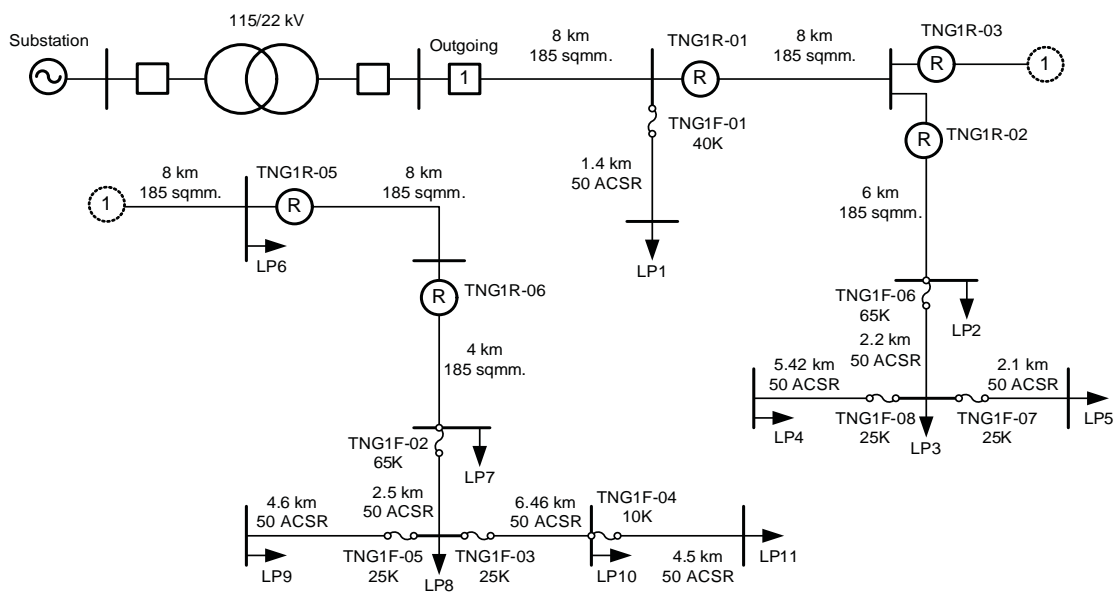


Figure E.1 PEA test system

Table E.1 Equipment impedance of PEA test system

Type	Impedance (Ohm)
185A(S) (1 km)	$0.175713+0.334439j$
50ACSR(S) (1 km)	$0.666638+0.376216j$

Table E.2 Customer data for PEA test system

Load Point (LP)	Customer Type	Peak Demand	
		Real Power (MW)	Reactive Power (MVAR)
1	Residential	1.0000	0.7500
2	Residential	0.4000	0.3000
3	Commercial	0.2000	0.1500
4	Residential	0.2000	0.1500
5	Residential	0.2000	0.1500
6	State agency	0.2000	0.1500
7	Commercial	0.1000	0.0750
8	State agency	0.2000	0.1500
9	Residential	0.4000	0.3000
10	Commercial	0.2000	0.1500
11	Residential	0.2000	0.1500
Total		3.1000	2.3250

Table E.3 Protection setting of PEA test system

Device	Setting
Circuit Breaker	Curve=SI, $I_{pickup}=420A$, $TM=0.2$
Recloser (1R-01)	Fast curve=101, Slow curve=116, $I_{R,Pickup}=340A$
Recloser (1R-02)	Fast curve=101, Slow curve=116, $I_{R,Pickup}=200A$
Recloser (1R-03)	Fast curve=101, Slow curve=116, $I_{R,Pickup}=280A$
Recloser (1R-05)	Fast curve=101, Slow curve=116, $I_{R,Pickup}=250A$
Recloser (1R-06)	Fast curve=101, Slow curve=116, $I_{R,Pickup}=200A$

Biography

Titti Saksornchai was born in Bangkok, Thailand, on April 11, 1978. He received B.Eng from Chulalongkorn University and M.S. degree from the University of Texas at Arlington, in 2000 and 2003, respectively. He joined Protection and Relay Division, Provincial Electricity Authority (PEA) since Dec 2006. Currently, he is Assistant Chief of Energy Research Section, Research Division, Power System R&D Department, PEA and working towards a Ph.D. in electrical engineering at Chulalongkorn University. His current research interests include electric power system analysis, power system protection, distributed generation planning, and smart grids.